

REACTIONS OF OXYGEN CONTAINING LIGANDS IN
THE COORDINATION SPHERE OF PERMETHYLHAFNOCENE
AND PERMETHYLANTALOCENE

Thesis by
Allan van Asselt

In Partial Fulfillment of the Requirements
for the Degree of
Doctor of Philosophy

California Institute of Technology
Pasadena, California, U.S.A., Earth

1987

(Submitted June 8, 1987)

Acknowledgements

I guess it is time to finish some twenty odd years of formal education. The past five and a half years at Caltech have been very special and many people have made the experience enjoyable. At the top of the list are members of the Bercaw group, both past and present. Nancy and Jimmy showed me the ropes on Bercaw vacuum lines. DMR, Greg Hillhouse, Larry Fong and Jaun Manriquez exemplified different approaches for entering alternate space. Eric and Paul both played the tuba, and I enjoyed the years playing with them in the Caltech wind ensemble and jazz band. Don, along with the Grubbs group, gave me my first introduction to rock climbing at Caltech. Facilities for water sports on second floor Noyes, were kindly provided by Chris.

Tippy Thompson, soon to be a professor at Princeton, has shown me that anything is possible if you catch the right wave. He was also a great housemate and friend. So are Marty and Cindy, who understand my need for rainbows. Lura Street will live on in my heart.

Rocco has provided hours and hours and hours of conversation, and has loaned me a few books, although I never seem to finish them. Ray is the only man in the Bercaw group I ever wanted and couldn't have. I thank Barb for the birthday cakes and the wonderful aerobics tights. I pray for Ramsey.

It wouldn't do to forget our slimy brit postdocs, Vern, the perfect English gentleman, Dai, proof positive that Britain sent all of her gallant young men overseas, and Ged, the heyokah.

I'm glad Trim was part of the lunch crew, otherwise I might never have heard him talk. Emilio, who works over lunch, makes me feel guilty. Pam won't have me to chase into men's restrooms anymore, I suggest it may be time to pick on Ray. I'm sorry to leave LeRoy without a hackysack partner, but I'm happy to leave him with the vacuum line and Janet, before she starts doing sulfur chemistry. And our visiting prof, John Moss, is, after all, John Moss.

Claudia, the newest member of the Bercaw group, has been a magic friend. I love you all.

While at Caltech, I ended up in a group that not only does fun science, but goes on skiing and backpacking trips together. Back in the old days, we even used to go out drinking together. Thank you, John, for making it all possible.

Others at Caltech have been special friends as well. Leon Gelles always defined that sense of cultured bitterness, so necessary at times. The Space Weapons Study Group has been alot of fun over the years, and I've had the chance to work with some wonderful people on projects other than science.

My family is always with me.

DuPont and Shell helped support my habits of living under a roof and eating every day. For this, I am grateful.

Abstract: A series of *tert*-butylperoxide complexes of hafnium, $\text{Cp}^*_2\text{Hf}(\text{R})(\text{OOCMe}_3)$ ($\text{Cp}^* = (\eta^5\text{-C}_5\text{Me}_5)$; $\text{R} = \text{Cl}, \text{H}, \text{CH}_3, \text{CH}_2\text{CH}_3, \text{CH}_2\text{CH}_2\text{CH}_3, \text{CH}_2\text{CH}_2\text{CH}_2\text{CH}_3, \text{CH}_2\text{CHMe}_2, \text{CH}=\text{CHCMe}_3, \text{C}_6\text{H}_5, \text{meta-C}_6\text{H}_3(\text{CH}_3)_2$) and $\text{Cp}^*(\eta^5\text{-C}_5(\text{CH}_3)_4\text{CH}_2\text{CH}_2\text{CH}_2)\text{Hf}(\text{OOCMe}_3)$, has been synthesized. One example has been structurally characterized. $\text{Cp}^*_2\text{Hf}(\text{OOCMe}_3)\text{CH}_2\text{CH}_3$ crystallizes in space group $\text{P}2_1/\text{c}$, with $a = 19.890(7)\text{\AA}$, $b = 8.746(4)\text{\AA}$, $c = 17.532(6)\text{\AA}$, $\beta = 124.987(24)^\circ$, $V = 2498(2)\text{\AA}^3$, $Z = 4$ and $R_F = 0.054$ (2222 reflections, $I > 0$). Despite the coordinative unsaturation of the hafnium center, the *tert*-butylperoxide ligand is coordinated in a mono-dentate ligand. The mode of decomposition of these species is highly dependent on the substituent R. For $\text{R} = \text{H}, \text{CH}_2\text{CH}_3, \text{CH}_2\text{CH}_2\text{CH}_3, \text{CH}_2\text{CH}_2\text{CH}_2\text{CH}_3, \text{CH}_2\text{CHMe}_2$ a clean first order conversion to $\text{Cp}^*_2\text{Hf}(\text{OCMe}_3)(\text{OR})$ is observed (for $\text{R} = \text{CH}_2\text{CH}_3$, $\Delta H^\ddagger = 19.6 \text{ kcal}\cdot\text{mol}^{-1}$, $\Delta S^\ddagger = -13 \text{ e.u.}$). These results are discussed in terms of a two step mechanism involving η^2 -coordination of the *tert*-butylperoxide ligand. Homolytic O–O bond cleavage is observed upon heating of $\text{Cp}^*_2\text{Hf}(\text{OOCMe}_3)\text{R}$ ($\text{R} = \text{C}_6\text{H}_6, \text{meta-C}_6\text{H}_3(\text{CH}_3)_2$). In the presence of excess 9,10-dihydroanthracene thermolysis of $\text{Cp}^*_2\text{Hf}(\text{OOCMe}_3)\text{C}_6\text{H}_6$ cleanly affords $\text{Cp}^*_2\text{Hf}(\text{C}_6\text{H}_6)\text{OH}$ and HOCMe_3 ($\Delta H^\ddagger = 22.6 \text{ kcal}\cdot\text{mol}^{-1}$, $\Delta S^\ddagger = -9 \text{ e.u.}$). The O–O bond strength in these complexes is thus estimated to be 22 kcal mol^{-1} .

$\text{Cp}^*_2\text{Ta}(\text{CH}_2)\text{H}$, $\text{Cp}^*_2\text{Ta}(\text{CHC}_6\text{H}_5)\text{H}$, $\text{Cp}^*_2\text{Ta}(\text{C}_6\text{H}_4)\text{H}$, $\text{Cp}^*_2\text{Ta}(\text{CH}_2=\text{CH}_2)\text{H}$ and $\text{Cp}^*_2\text{Ta}(\text{CH}_2=\text{CHMe})\text{H}$ react, presumably through $\text{Cp}^*_2\text{Ta-R}$ intermediates, with H_2O to give $\text{Cp}^*_2\text{Ta}(\text{O})\text{H}$ and alkane.

$\text{Cp}^*_2\text{Ta}(\text{O})\text{H}$ was structurally characterized: space group $\text{P}2_1/\text{n}$, $a = 13.073(3)\text{\AA}$, $b = 19.337(4)\text{\AA}$, $c = 16.002(3)\text{\AA}$, $\beta = 108.66(2)^\circ$, $V = 3832(1)\text{\AA}^3$, $Z = 8$ and $R_F = 0.0672$ (6730 reflections). Reaction of *tert*-butylhydroperoxide with these same starting materials ultimately yields $\text{Cp}^*_2\text{Ta}(\text{O})\text{R}$ and HOCMe_3 .

$\text{Cp}^*_2\text{Ta}(\text{CH}_2=\text{CHR})\text{OH}$ species are proposed as intermediates in the olefin hydride reactions.

$\text{Cp}^*_2\text{Ta}(\text{O}_2)\text{R}$ species can be generated from the reaction of the same starting materials and O_2 . Lewis acids have been shown to promote oxygen insertion in these complexes.

Table of Contents

Acknowledgements	ii
Abstract	iii
An Introductory Statement	v
Chapter 1: Metal Based Oxidation Systems	1
Chapter 2: <i>tert</i> -Butyl Peroxide Complexes of Permethylhafnocene, Cp* ₂ Hf(R)(OOCMe ₃)	21
Chapter 3: Oxygen Derivatives of Permethyltantallocene	55

An Introductory Statement

When lightning struck the forest, sending flames leaping into the air, an awareness of the awesome power of oxidation chemistry was forced on humankind. After a time, it became possible to generate and preserve fire and apply its power to chemically modify food stuffs. Technology advanced, and torches were developed to give light where none was available before. The exploitation of controlled oxidation processes had begun. The study of combustion has drawn chemists like moths to a flame, and, consequently, the field has evolved quite a bit since the early days. Even so, much remains to be understood concerning the fundamental processes of oxidation. What follows is but a minor contribution to this vast and historic field of enquiry and, in the end, it may not be as interesting as sitting in front of a campfire in the mountains. But they don't fund too much research in that area, and you do what you can to get by.

CHAPTER 1

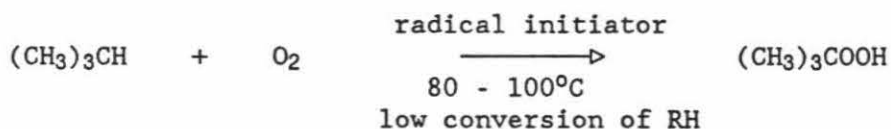
Metal Based Oxidation Systems

Introduction

The selective transfer of oxygen is a process of fundamental importance. Oxygen breathing organisms are literally kinetically controlled oxidation systems, harnessing the exothermicity of oxidation reactions to drive all other processes. On the molecular level, biological systems perform extremely selective oxygen transfer to carry out chemical synthesis. For industry, the oxygenation of petroleum derived feed stocks is often the first step in converting these materials to more useful chemicals. The synthesis of complex organic molecules often requires sources which will deliver oxygen with extreme regio-, stereo- and enantio- selectivity.

All of the above processes are complicated by the nature of the dioxygen molecule, which in its ground state contains two unpaired electrons. Most substrates, by contrast, have singlet ground states and no unpaired electrons. Direct reaction of triplet ground state O_2 with singlet ground state substrates is a spin forbidden process and generally involves one electron processes with large activation energies. The subsequent radical chain reactions often lead to multiple products. This limits the usefulness of direct reaction with O_2 for reactions when selective oxygen transfer is desired.

Radical chain reactions are not always nonselective, as can be observed in the controlled autoxidation of isobutane.¹ The product, *tert*-butylhydroperoxide (TBHP), still contains active oxidizing equivalents and is a singlet ground state molecule.



This suggests, along with the processes observed in biological systems, that one might be able to use derivatives of the O_2 molecule to circumvent the problems encountered during

direct reaction with oxygen. This has, of course, proven to be a viable approach, and most oxidation chemists are occupied with the task of generating clean and selective sources of "preactivated" oxygen and studying their reactivity. These preactivated sources of oxygen have the additional advantage over O_2 that one can control the electronic and steric environment of the oxygen transfer step. Among these sources are: organic peracids, singlet oxygen, alkylhydroperoxides and hydrogen peroxide in conjunction with transition metal or main group templates, metal complexes which react directly with O_2 , metal oxo complexes and metal based systems, e.g., the Wacker process, which make indirect use of O_2 's oxidizing abilities to reoxidize the metal center. In general, the pursuit of selective oxidation systems has been highly empirical, with little understanding of the actual details of the chemical processes of oxygen transfer. A greater understanding of the mechanisms of oxygen transfer might allow the design of new oxidation systems and the improvement of existing ones.

Early Transition Metal Oxidation Systems

Our primary focus will be on metal based oxidation systems, most specifically on the reactions of early transition metal group IV and V complexes with alkylhydroperoxides and O_2 . Historically, metal based oxidation reactions have been poorly understood. The active oxygen transfer intermediate was often written as an ill defined metal adduct. More sophisticated speculation concerning metal based oxygen transfer mechanisms has appeared in recent years,¹ however, experimental evidence supporting these speculations is still relatively ambiguous. Clean systems for detailed study have been difficult to find. Well characterized model complexes for key proposed intermediates are few and far between. The permethyl- hafnocene and tantalocene systems have provided exceptionally nice examples of proposed intermediates, some new reactivity, and limited mechanistic information. These systems will be discussed in the following chapters. First, it may be

useful to examine related oxidation systems, key proposed intermediates and selected models for oxygen transfer.

Reactions of Alkylhydroperoxides with Transition Metals:

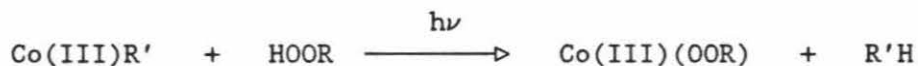
Alkylhydroperoxides, in conjunction with transition metal templates, have proven to be highly successful reagents for selective oxygen transfer to such substrates as olefins, allyl alcohols, sulphides and amines.¹ Transition metal alkylperoxide complexes are often proposed as key intermediates for these reactions. In other systems, metal hydroxide and metal oxo complexes are thought to be the key intermediates in olefin epoxidations and hydroxylation of alkenes, alkanes and arenes.

One can classify the most common reactions of alkylhydroperoxides with transition metals into three broad categories.

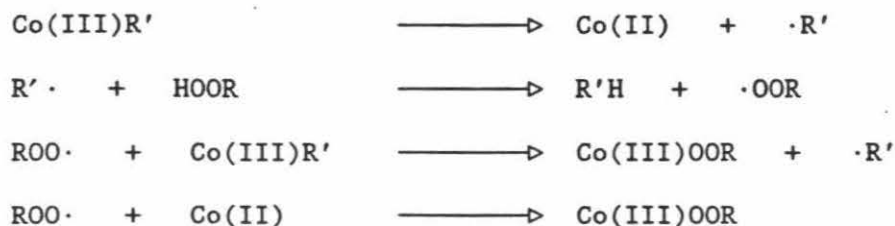
1) The first involves a formal protolytic attack of the alkylhydroperoxide ($H^+ \cdot OOR$) on the metal center ($M-X$) to give a $M-O-O-R$ complex and HX .² The oxidation state of the metal does not change, and these reactions only occur if HX is a reasonable leaving group.



The photochemical substitutions of cobalt(III) alkyls with alkylhydroperoxide have the same stoichiometries but probably proceed by a radical mechanism.³



The proposed mechanism is listed below.



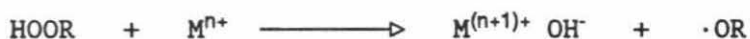
2) Category two reactions occur when the metal attacks the alkylhydroperoxide O-O bond as a nucleophile⁴ in a manner similar to the proposed mechanism for olefin epoxidations by peracids.⁵



(TPP = *meso*-tetraphenylporphyrinato)

These reactions proceed by H^+ transfer to the $\cdot\text{OR}$ group of the alkylhydroperoxide and generate metal oxo complexes and ROH. This reaction mode is favored when the metal can undergo a facile two electron oxidation and R is an electron withdrawing group (peracids, where $\text{R} = -\text{COR}'$, are an extreme example of this, and often carry out this type of reaction with greater facility than normal alkylperoxides).

3) In the third category are reactions which involve electron transfer (analogous to the Haber-Weiss mechanism for Fenton's reagent) from the metal to the alkylhydroperoxide.¹



These reactions have been proposed to initially generate metal hydroxide complexes and $\cdot\text{OR}$. Subsequent reactions can lead to the catalytic decomposition of alkylhydroperoxide¹ (above) or to metal alkylperoxide complexes⁶ (below). In some cases added substrates can be oxidized by the intermediate alkylperoxy radicals. It has also been suggested that the reaction of metal salts with trace amounts of alkylperoxides is the initiation step for metal catalyzed autoxidations.



The initially formed metal hydroxide, oxo and alkylperoxide complexes are commonly highly reactive and it is often difficult to determine in which mode the initial reaction of metal complex plus alkylhydroperoxide takes place. In some systems, it is very likely that more than one mechanism is operative and, perhaps, more than one species transfers oxygen to substrate.

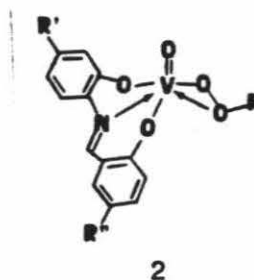
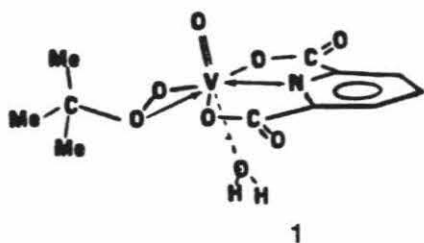
Metal Alkylperoxide Complexes:

The homogeneous molybdenum catalyzed "Halcon process" and the silica supported titanium catalyzed "Shell process" are proposed to operate through metal alkylperoxide species.¹ These processes are used commercially to convert propene to propylene oxide on a scale of billions of pounds per year. In the Sharpless titanium based asymmetric epoxidation system, metal alkylperoxide species are the proposed active oxygen transfer intermediates for allyl alcohol oxidation to form epoxides with very high enantiomeric excesses.⁷ In addition, alkylperoxide complexes are proposed as transient intermediates in the autoxidation of group IV and other metal alkyl species.⁸

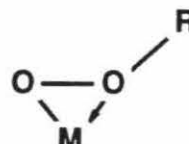
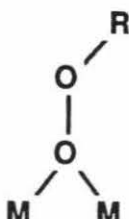
Relatively few examples of M-O-O-R species have been isolated and studied. Successful techniques of synthesis have included photochemical substitution,³ addition of RX to metal peroxide complexes⁹ and most commonly, metathesis of alkylhydroperoxides with metal hydroxide, alkoxide or carboxylate species.¹⁰ Although alkylhydroperoxides as oxygen transfer agents have found the greatest use with early transition metals, most of the examples studied, and all but one of the complexes structurally characterized, are found in the group VIII transition metals. These late transition metal complexes will generally oxidize substrates such as carbon monoxide, phosphines and, more rarely, olefins. Relatively minor changes in the ligand environment can have significant effects on the reactivity of these complexes. For example, as one varies the *trans* ligand of *trans*-(PPh₃)₂Pt(R)(OOCMe₃) from R = Ph, Ph-*o*-CN, to CF₃ in dichloroethane the yield of oxygenated 1-octene rises from 46 to 55 to 80 percent respectively.² The *cis* derivatives will not oxidize olefins at all.

The only examples of well characterized early transition metal alkylperoxide complexes, before the work reported in Chapter 2, have been prepared in recent years by Mimoun and coworkers. Again it is interesting to note that seemingly minor changes in ligand

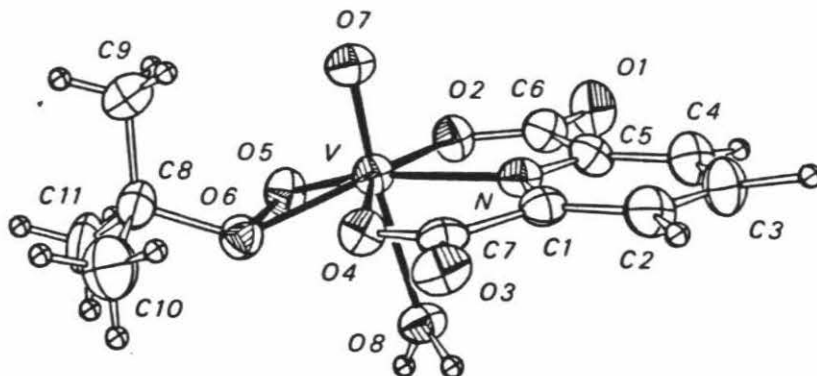
environment in these vanadium systems can cause considerable changes in the chemistry of the alkyl peroxide moiety. Two systems have been reported, both with Schiff bases as the primary ligand. With the tridentate Schiff base ligand 2,6-pyridinedicarboxylate (dipic) the complexes $(\text{dipic})\text{VO}(\text{OOR})(\text{L})$ (1) ($\text{R} = t\text{-Bu}, \text{CMe}_2\text{Ph}$; $\text{L} = \text{H}_2\text{O}, \text{HMPT}$), which oxidize olefins, alkanes and arenes by radical pathways, can be isolated.¹¹ When the base is changed to the N -(2-oxidophenyl)salicylideneaminato tridentate ligand ($\text{R}'\text{-OPhsal-R}''$) the free ligand L is no longer coordinated and the complex $(\text{R}'\text{-OPhsal-R}'')\text{VO}(\text{OOR})$ (2) oxidizes only olefins, probably via a heterolytic pathway.¹² Why some complexes react homolytically and others heterolytically remains an open question. This will be discussed a bit further in connection with the results presented in Chapter 2.



A small number of metal alkylperoxide complexes have been structurally characterized by x-ray diffraction.¹³ Three different binding modes of the alkylperoxide ligand, terminal,^{13a,b} bridging^{13c} and bidentate,^{13d} are found in these structures.



General agreement has been reached that bidentate coordination of the alkylperoxide ligand is a probable step in the heterolytic transfer of oxygen to substrate.¹⁴



1

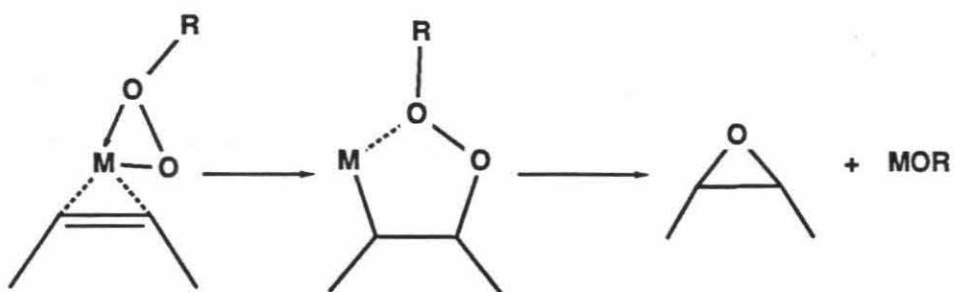
Although $(\text{dipic})\text{VO}(\text{OO}t\text{-Bu})(\text{L})$ (1) appears to react homolytically in solution, the bidentate *t*-butylperoxide ligand found in the solid state structure¹¹ (above) is the best experimental evidence for this commonly proposed mechanism. Consistent with this mechanism, all of the systems which cleanly transfer oxygen have open coordination sites for binding the alkoxy oxygen of the peroxide ligand. The first kinetic evidence indicating the likelihood of the bidentate binding step is discussed in Chapter 2.^{13e} Homolytic cleavage of the O-O bond will be discussed below.

For non-radical olefin epoxidation reactions, the numerous proposals concerning the nature of the actual oxygen transfer step can be encompassed by two different mechanisms.¹ The fundamental difference between these two interpretations lies in the still open question of whether it is necessary to coordinate olefin to the metal center before oxygen transfer takes place and what the nature of the alkylperoxide oxygen is (nucleophilic or electrophilic). Mimoun argues that olefin coordination is required to activate the olefin towards nucleophilic attack by the peroxide (mech A).¹⁵ Sharpless, in his proposed mechanism for early transition metal epoxidation systems, offers the

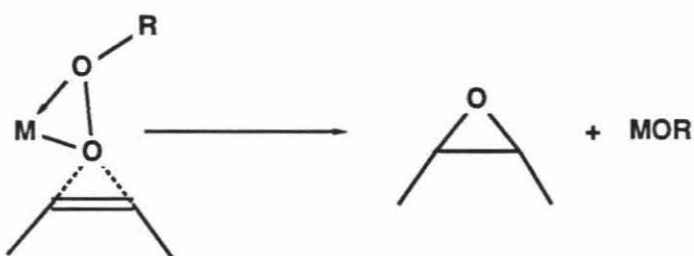
alternative of direct attack of the olefin on an electrophilic peroxide moiety (mech B).^{7,16}

The Sharpless mechanism is reminiscent of the proposed mechanism for peracid oxidations.⁵

Mechanism A

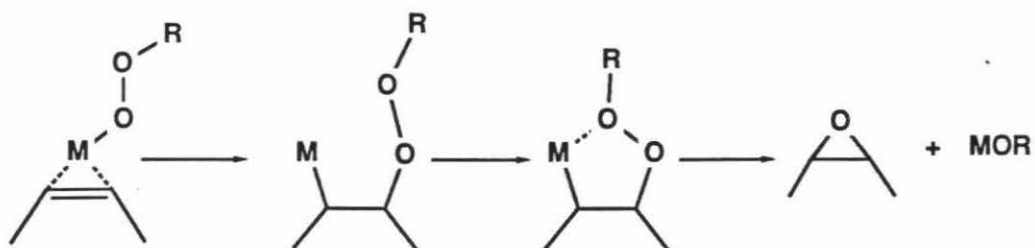


Mechanism B



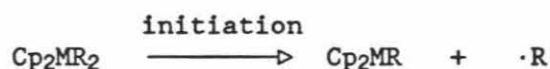
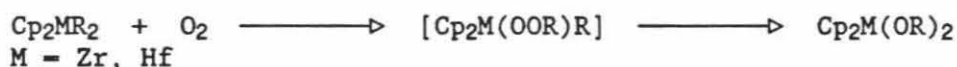
For the reactions of $(R^1\text{-OPhsal-R}^2)\text{VO(OOR)}$ with olefins, Mimoun has recently offered the first kinetic evidence for olefin coordination in an a metal alkylperoxide oxidation (mech C).¹² He has altered the above mechanism to suggest olefin insertion into an η^1 -alkylperoxide followed by (or simultaneous with) η^2 -coordination of the alkoxide oxygen. Several recent reports of olefin insertion into metal oxygen bonds support the possibility of this type of mechanism.¹⁷

Mechanism C



It seems quite probable that all three of these various mechanisms function in different systems. Olefin coordination in some systems may be necessary, in part, to simply bring the reactants together (metal template effect). For the Sharpless allyl alcohol epoxidations, formation of the metal allyl alkoxide presumably performs the same function and olefin coordination may not be necessary.

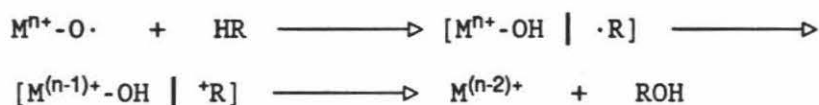
As mentioned earlier group IV metal alkylperoxide species have been invoked as intermediates in the autoxidation of metal alkyls. Blackburn, Labinger, and Schwartz were the first to explore the interaction of $\text{Cp}_2\text{ZrR}(\text{Cl})$ with O_2 .¹⁸ They suggested metal alkylperoxide complexes as intermediates and reported the synthesis of the first isolated Group IV alkylperoxide complex, $\text{Cp}_2\text{Zr}(\text{OO}t\text{-Bu})\text{Cl}$, from Cp_2ZrCl_2 and $\text{NaOO}t\text{-Bu}$. No characterization of the compound was reported. In 1981, Scotton and Brindley reported the isolation of bisalkoxide species from the radical chain reaction of O_2 with Cp_2MR_2 ($\text{M} = \text{Zr, Hf}$; $\text{Cp} = \eta^5\text{-C}_5\text{H}_5$; $\text{R} = \text{Me, benzyl}$), and suggested the bisalkoxides resulted from the decomposition of alkylperoxide alkyl intermediates.¹⁹ Their suggested mechanism for the autoxidation is shown below.



Similar transformations have been recently reported by Wolczanski and Lubben for the reaction of $(\text{triox})_2\text{MMe}_2$ ($\text{triox} = ((\text{CH}_3)_3\text{C})_3\text{CO}$; $\text{M} = \text{Ti, Zr}$) with O_2 to yield $(\text{triox})_2\text{M}(\text{OMe})_2$.⁸

Metal Oxo Complexes:

Homolytic cleavage of metal alkylperoxides leads to $M^{n+}-O\cdot$ and $\cdot OR$. Writing $M^{n+}-O\cdot$ is only reasonable if the metal cannot undergo further oxidation to $M^{(n+1)+}=O$ or $M^{(n+1)+}-O\cdot$, e.g., when starting from a d^0 metal alkylperoxide complex. As the first step in hydroxylation reactions, intermediates of the type $M-O\cdot$ have been invoked to explain hydrogen abstraction from alkanes and the allyl positions of alkenes. A plausible mechanism is shown below.¹



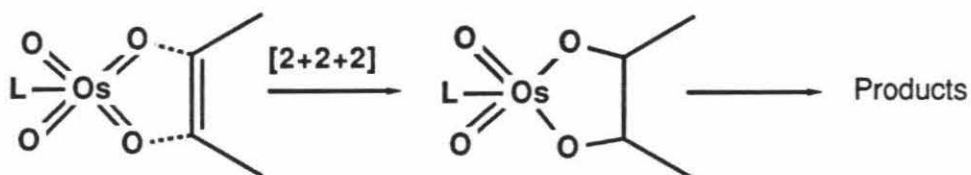
$M-O\cdot$ has also been proposed to undergo electrophilic attack on arenes as the first step in arene hydroxylations.

Metal oxo species can also be generated directly from alkylhydroperoxides without the intermediate step of forming metal alkylperoxide complexes (*vide supra*).

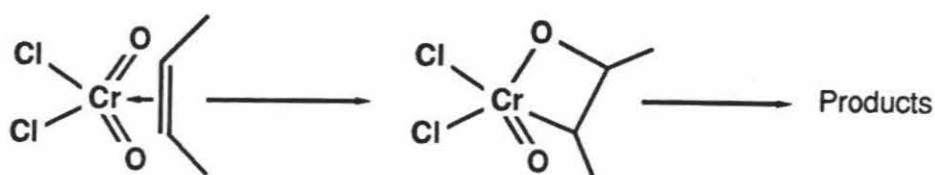
Alkylhydroperoxides have been used as oxygen sources to generate proposed metal oxo or hydroxo species for cytochrome P-450 model studies.⁴ They can also be used as oxygen sources to regenerate oxo reagents such as OsO_4 or SeO_2 for catalytic oxidations.

One of the traditional mechanisms for oxidation with metal oxo reagents involves initial electron transfer from the substrate to the metal center. The substrate radical cation subsequently reacts with the metal oxo or hydroxo species to give products.

Another possibility has been suggested for the reaction of olefins with OsO_4 : an allowed [2+2+2] direct attack of the olefin on the *cis* metal oxo ligands (below).



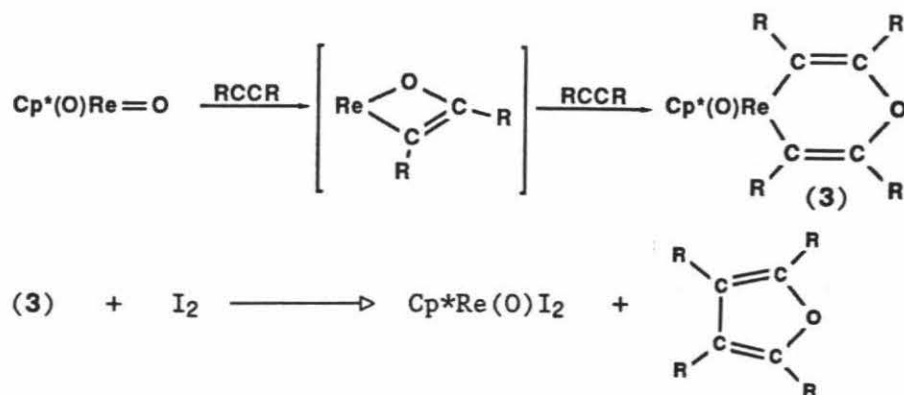
In 1977, Sharpless proposed organometallic species as intermediates in the oxidation of olefins by high valent metal oxo species.²⁰ He reasoned that the Lewis acid, d^0 metal center is the likely site of initial olefin coordination and helps explain the apparent electrophilic nature of many of these reactions. Oxygenation takes place with olefin migration to the oxo ligand, possibly forming metallaoxetane intermediates.



This mechanism offers a reasonable explanation for the product stereochemistries of low temperature CrO_2Cl_2 oxidation of olefins. It also is consistent with asymmetric induction observed when oxidizing prochiral olefins with OsO_4 and a chiral amine ligand.²¹ Non-radical electrophilic attack by metal oxo complexes on C–H bonds has also been proposed for alkane activation.

Evidence has accumulated to support the proposition that organometallic species are viable intermediates in these oxidations. However, the number of relevant model compounds, *e.g.*, metal oxo olefin and metal oxo alkyl complexes, remains small and kinetic and stereochemical evidence is still ambiguous. It seems likely that the proposed mechanisms simply represent extremes and that many reactions are intermediate in character or proceed by more than one pathway. The limited evidence in support of organometallic intermediates is discussed below.

Some of the best evidence comes from a recent report by de Boer.²² At short reaction times, Cp^*ReO_3 ($\text{Cp}^* = \eta^5\text{-C}_5\text{Me}_5$) reacts with phosphine in alkyne solution to yield $\text{Cp}^*\text{Re}(\text{O})(\text{RCCR})$. When the reaction is allowed to run longer, species of the stoichiometry $\text{Cp}^*\text{Re}(\text{O})((\text{RCCR})_2\text{O})$ (**3**) are isolated. Starting with the phosphine reduced complex $[\text{Cp}^*\text{Re}(\text{O})_2]$, De Boer's mechanism for the formation of these species is shown below. These species, when reacted with I_2 , yield $\text{Cp}^*\text{Re}(\text{O})\text{I}_2$ and substituted furans.



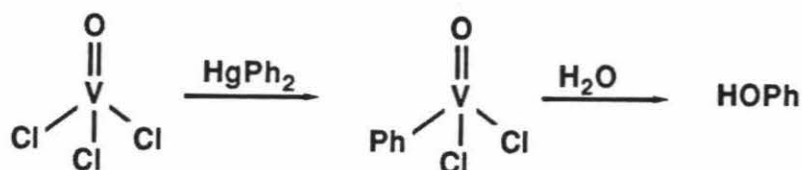
Mayer and coworkers have reported a series of interesting tungsten complexes which contain oxo ligands and coordinated olefin, $\text{W}(\text{O})(\text{PMePh}_2)_2(\text{Cl})_2(\text{H}_2\text{C}=\text{CHR})$ ($\text{R} = \text{H}, \text{Me}, \text{CHCH}_2$).²³ $\text{W}(\text{O})(\text{PMePh}_2)_2(\text{Cl})_2(\text{H}_2\text{C}=\text{CH}_2)$ can be obtained from the addition of ethylene oxide to $\text{W}(\text{PMePh}_2)_4\text{Cl}_2$,²⁴ providing evidence that the reverse of the olefin oxo complex to epoxide conversion can take place. Earlier Mayer reported a Re oxo alkyne complex.²⁵ Although interesting as model complexes for organometallic intermediates, these compounds as of yet have not shown any tendency to undergo further reactions of the type proposed for oxygen transfer.

Collman and coworkers have recently advanced kinetics and shape selectivity arguments for reversibly formed olefin intermediates in olefin epoxidation studies with $\text{Mn}(\text{TPP})\text{Cl}$ (TPP = *meso*-tetraphenylporphyrinato) or $\text{Mn}(\text{TMP})\text{Cl}$ (TMP = *meso*-tetramesitylporphyrinato) and lithium hypochlorite.²⁶ In further cytochrome P-450 model studies they have also reported

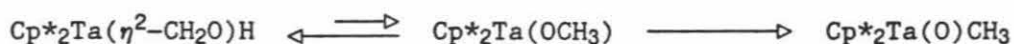
similar results for olefin oxidation with Fe(PFP)Cl (PFP = pentafluorophenylporphyrinato) and F₅PhIO.²⁷ The proposed intermediates in these systems are metallaoxetanes.

Groves and Watanabe have reported spectroscopic evidence for an intermediate in the low temperature epoxidation of olefins with Fe(TMP)Cl and *m*-chloroperbenzoic acid.²⁸ They suggest either an olefin oxo complex or a metallaoxetane species as the intermediate formed.

Examples of organometallic species containing both oxo and alkyl ligands on the metal are more prevalent than species with olefin and oxo ligands.²⁹ However, none of the examples yet reported have shown carbon oxygen bond formation, one of the key steps for the oxidation mechanism proposed by Sharpless. Indirect evidence for this type of rearrangement is provided by the V(O)Cl₃ reaction with Ph₂Hg.³⁰ Hydrolytic workup of the product of this reaction gives phenol. Presumably a vanadium oxo phenyl complex is initially generated and the phenyl group subsequently migrates to the vanadium oxo group.



A model for the reverse reaction, the migration of alkyl group from an alkoxy ligand to form a metal oxo alkyl species, is found in the rearrangement of Cp*₂TaH(η²-CH₂O).³¹ Barbara Burger has shown that the production of Cp*Ta(O)Me upon heating Cp*₂TaH(η²-CH₂O) probably involves the unobserved intermediate Cp*₂Ta(OMe). This intermediate, which is subject to rapid β-hydride elimination to return to Cp*₂Ta(η²-CH₂O)H, occasionally rearranges by migration of the methyl group from oxygen to the metal center.



Metal Dioxygen Complexes:

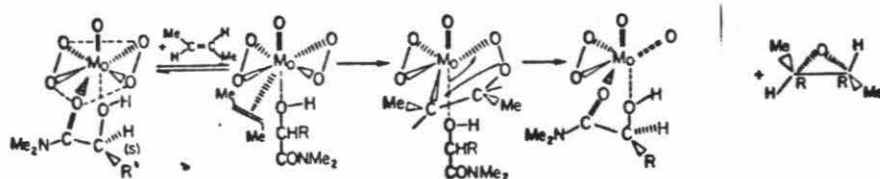
Biological systems are required to use the O₂ molecule as their primary source of oxygen. Nature makes use of metal centers in specialized environments to activate oxygen as the first step in carrying out the various functions required to keep the system operational; oxygen transport, synthesis, energy conversion, *etc.* This has prompted a great deal of interest among chemists in modeling these types of reactions. There are a large number of late transition metal model complexes which react cleanly with O₂ to form peroxide (or dioxygen) species.³² One finds very few examples of early transition metal complexes which react similarly.¹



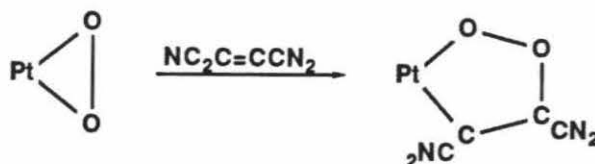
(TPP)Ti(O₂) can also be generated from H₂O₂.



It is, in fact, much more common with early metals to generate these species from the metathesis reactions of metal complexes with hydrogen peroxide. The late transition metal peroxide complexes in general react as nucleophiles with external substrates. By contrast, most early transition metal peroxo complexes are in their highest oxidation states and tend to react as electrophiles. Others react as radical sources. The electrophilic nature of these reagents may be due again to initially formed organometallic species. Mimoun's proposed mechanism for M(O)(O₂)₂ oxidation of olefins with a chiral coligand is presented below.³³



The supporting evidence for organometallic intermediates in these systems is still thin. No early metal complexes containing both peroxo ligands and olefins or alkyls ligands have been reported. The only example of this type of proposed intermediate is $\text{Ir}(\text{PPh}_3)_2(\text{C}_2\text{H}_4)(\text{O}_2)\text{Cl}$ and there is no evidence to indicate its rearrangement to give epoxide.³⁴ Palladium and platinum peroxide complexes react with carbonyl compounds and activated olefins to give metallacyclic structures of the type proposed by Mimoun.³⁵ These species do not, however, decompose to give epoxides.



The first examples of isolated metal peroxide complexes with alkyl ligands will be reported in Chapter 3.

- 1) Sheldon, R.A.; Kochi, J.K. "Metal-Catalyzed Oxidations of Organic Compounds" Academic Press, New York, 1981.
- 2) Strukul, G.; Michelin, R.A.; Orbell, J.D.; Randaccio, L. *Inorg. Chem.* **1983**, *22*, 3706.
- 3) Giannotti, C.; Fontaine, C.; Chiaroni, A.; Riche, C. *J. Organomet. Chem.* **1976**, *113*, 57.
- 4) Yaun, L.C.; Bruice, T.C. *J. Am. Chem. Soc.* **1986**, *108*, 1643 and references therein.
- 5) Curci, R.; Edwards, J.O. in "Organic Peroxides" Vol. 1, 199, (Ed. Swern, D.) Wiley-Interscience, New York, 1970.
- 6) Saussine, L.; Brazi, R.; Robine, A.; Mimoun, H.; Fischer, J.; Weiss, R. *J. Am. Chem. Soc.* **1985**, *107*, 3534.
- 7) Sharpless, K.B.; Woodard, S.S.; Finn, M.G. *Pure Appl. Chem.* **1983**, *55*, 1823.
- 8) Lubben, T.; Wolczanski, P.T. *J. Am. Chem. Soc.* **1987**, *109*, 424.
- 9) Tatsuno, Y.; Otsuka, S. *J. Am. Chem. Soc.* **1981**, *103*, 5832.
- 10) a) ref. 2 b) Strukul, G.; Ros, R.; Michelin, R.A. *Inorg. Chem.* **1982**, *21*, 495 c) Mimoun, H.; Charpentier, R.; Mitschler, A.; Fischer, J.; Weiss, R. *J. Am. Chem. Soc.* **1980**, *102*, 1047.
- 11) Mimoun, H.; Chaumette, P.; Mignard, M.; Saussine, L.; Fischer, J.; Weiss, R. *Nouv. J. Chim.* **1983**, *7*, 467.
- 12) Mimoun, H.; Mignard, M.; Brechot, P.; Saussine, L. *J. Am. Chem. Soc.* **1986**, *108*, 3711.
- 13) a) ref. 2 b) ref. 3 c) ref. 10c d) ref. 11 e) van Asselt, A.; Santarsiero, B.; Bercaw, J.E. *J. Am. Chem. Soc.* **1986**, *108*, 8291.
- 14) Sharpless, K.B.; Verhoeven, T.R. *Aldrichimica Acta* **1979**, *12*, 63.
- 15) a) Mimoun, H. *J. Mol. Cat.* **1980**, *7*, 1 b) ref. 12.
- 16) Bach, R.D.; Wolber, G.J.; Coddens, B.A. *J. Am. Chem. Soc.* **1984**, *106*, 6098.

- 17) a) Bryndza, H.E. *Organometallics* 1985, 4, 406. b) Jensen, C.M.; Trogler, W.C. *Science* 1986, 233, 1069.
- 18) Blackburn, R.F.; Labinger, J.A.; Schwartz, J. *Tet. Lett.* 1975, 34, 3041.
- 19) Brindley, P.B.; Scotton, M.J. *J. Chem. Soc. Perkins II* 1981, 419.
- 20) Sharpless, K.B.; Teranishi, A.Y.; Baeckvall, J.-E. *J. Am. Chem. Soc.* 1977, 99, 3120.
- 21) Hentges, S.G.; Sharpless, K.B. *J. Am. Chem. Soc.* 1980, 102, 4263.
- 22) de Boer, E.J.M.; de With, J.; Orpen, A.G. *J. Am. Chem. Soc.* 1986, 108, 8271.
- 23) Su, F.-M.; Cooper, C.; Geib, S.J.; Rheingold, A.L.; Mayer, J.M. *J. Am. Chem. Soc.* 1986, 108, 3545.
- 24) Mayer, J.M.; Su, F.M.; Bryan, J.C.; Geib, S.J.; Rheingold, A.L. Amer. Chem. Soc., 192nd National Meeting, Anaheim, September 1986.
- 25) Mayer, J.M.; Thorn, D.L.; Tulip, T.H. *J. Am. Chem. Soc.* 1985, 107, 7454.
- 26) Collman, J.P.; Brauman, J.I.; Meunier, B.; Hayashi, T.; Kodadek, T.; Raybuck, S.A. *J. Am. Chem. Soc.* 1985, 107, 2000.
- 27) Collman, J.P.; Kodadek, T.; Raybuck, S.A.; Papzian, L.M. *J. Am. Chem. Soc.* 1985, 107, 4343.
- 28) Groves, J.T.; Watanabe, Y. *J. Am. Chem. Soc.* 1986, 108, 507.
- 29) a) Herrmann, W.A.; Serrano, R.; Kusthardt, U.; Ziegler, M.L.; Guggolz, E.; Zahn, T., *Angew. Chem.Int. Ed. Engl.*, 1984, 23, 515-517; b) Legzdins, P.; Rettig, S.J.; Sanchez, L., *Organometallics*, 1985, 4, 1470-1471; c) Feinstein-Jaffe, I.; Gibson, D.; Lippard, S.J.; Schrock, R.R.; Spool, A., *J. Am. Chem. Soc.*, 1984, 106, 6305; d) Schrauzer, G.N.; Hughes, L.A.; Strampach, N.; Robinson, P.R.; Schlemper, E.O., *Organometallics* 1982, 1, 44; e) Schrauzer, G.N.; Hughes, L.A.; Strampach, N.; Ross, F.; Ross, D.; Schlemper, E.O., *Organometallics*, 1983, 2, 481-485; f) Schrauzer, G.N.; Hughes, L.A.; Schlemper, E.O.; Ross, F.; Ross, D., *Organometallics*, 1983, 2, 1163-1166; g) Alves, A.S.; Moore, D.S.; Andersen, R.A.;

- Wilkinson, G., *J. Organomet. Chem.*, **1969**, *19*, 387; h) Mowat, W.; Shortland, A.; Yagupsky, G.; Hill, N.J.; Yagupsky, M.; Wilkinson, G., *J. Chem. Soc. Dalton Trans.*, **1972**, 533; i) Mertis, K.; Williamson, D. H.; Wilkinson, G., *J. Chem. Soc. Dalton Trans.*, **1975**, 607; j) Middleton, A. R.; Wilkinson, G. *J. Chem. Soc. Dalton Trans.* **1980**, 1888; k) Santini-Scampucci, C.; Riess, J.G. *J. Chem. Soc. Dalton Trans.* **1974**, 1433; l) Beattie, I.R.; Jones, P.J., *Inorg. Chem.* **1979**, *18*, 2318.
- 30) a) ref. 19 b) Thiele, K.-H.; Schumann, W.; Wagner, S.; Brueser, W. *Z. Anorg. Allg. Chem.* **1972**, *390*, 280 c) Reichle, W.T.; Carrick, W.L. *J. Organomet. Chem.* **1970**, *24*, 419.
- 31) van Asselt, A.; Burger, B.J.; Gibson, V.C.; Bercaw, J.E. *J. Am. Chem. Soc.* **1986**, *108*, 5347.
- 32) a) Vaska, L. *Accts. Chem. Res.* **1976**, *9*, 175 b) Valentine, J.S. *Chem. Rev.* **1973**, *73*, 235.
- 33) Mimoun, H.; Seree de Roch, I.; Sajus, L. *Tetrahedron* **1970**, *26*, 37
- 34) a) van der Ent, A.; Onderdelinden, A.L. *Inorg. Chim. Acta* **1973**, *7*, 203 b) Brown, J.M.; John, R.A.; Lucy, A.R. *J. Organomet. Chem.* **1985**, *279*, 245.
- 35) a) Sheldon, R.A.; van Doorn, J.A. *J. Organomet. Chem.* **1975**, *94*, 115 b) Zanderighi, G.M.; Ugo, R.; Fusi, A.; Ben Taarit, Y. *Inorg. Nucl. Chem. Lett.* **1976**, *12*, 729.

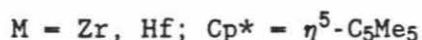
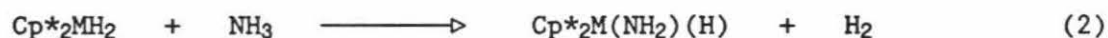
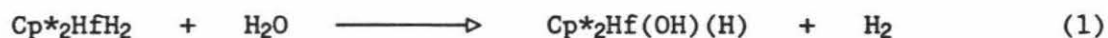
CHAPTER 2

tert-Butyl Peroxide Complexes of Permethylhafnocene, Cp*₂Hf(R)(OOCMe₃)

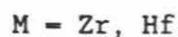
Abstract: A series of *tert*-butylperoxide complexes of hafnium, Cp*₂Hf(R)(OOCMe₃) (Cp* = ((η⁵-C₅Me₅); R = Cl, H, CH₃, CH₂CH₃, CH₂CH₂CH₃, CH₂CH₂CH₂CH₃, CH₂CHMe₂, CH=CHCMe₃, C₆H₅, *meta*-C₆H₃(CH₃)₂) and Cp*(η⁵-C₅(CH₃)₄(CH₂)₃)Hf(OOCMe₃), has been synthesized. One example has been structurally characterized. Cp*₂Hf(OOCMe₃)CH₂CH₃ crystallizes in space group P2₁/c, with a = 19.890(7)Å, b = 8.746(4)Å, c = 17.532(6)Å, β = 124.987(24)°, V = 2498(2)Å³, Z = 4 and R_F = 0.054 (2222 reflections, I > 0). Despite the coordinative unsaturation of the hafnium center, the *tert*-butylperoxide ligand is coordinated in a mono-dentate ligand. The mode of decomposition of these species is highly dependent on the substituent R. For R = H, CH₂CH₃, CH₂CH₂CH₃, CH₂CH₂CH₂CH₃, CH₂CHMe₂ a clean first order conversion to Cp*₂Hf(OCMe₃)(OR) is observed (for R = CH₂CH₃, ΔH[‡] = 19.6 kcal·mol⁻¹, ΔS[‡] = -13 e.u.). These results are discussed in terms of a two step mechanism involving η²-coordination of the *tert*-butylperoxide ligand. Homolytic O-O bond cleavage is observed upon heating of Cp*₂Hf(OOCMe₃)R (R = C₆H₆, *meta*-C₆H₃(CH₃)₂). In the presence of excess 9,10-dihydroanthracene thermolysis of Cp*₂Hf(OOCMe₃)C₆H₆ cleanly affords Cp*₂Hf(C₆H₆)OH and HOCMe₃ (ΔH[‡] = 22.6 kcal·mol⁻¹, ΔS[‡] = -9 e.u.). The O-O bond strength in these complexes is thus estimated to be 22 kcal mol⁻¹.

Introduction

The sterically demanding ligand environment of permethylzirconocene and permethylhafnocene fragments has allowed the isolation of a large number of monomeric hydride complexes. Unlike most late transition metal hydrides, which often react as acids (H^+),¹ zirconium and hafnium hydrides consistently react as hydrides (H^-).^{2,3} Greg Hillhouse investigated the reaction chemistry of water and ammonia with these complexes (eq 1,2).² Even these relatively weak acids protonate the metal hydride bond to generate H_2 . Water reacts cleanly with $Cp^*_2HfH_2$ ($Cp^* = \eta^5-C_5Me_5$) in several steps. Initially, $Cp^*_2Hf(OH)H$ is formed. In the presence of excess $Cp^*_2HfH_2$, $Cp^*_2Hf(OH)H$ reacts to yield the bridging oxo hydride dimer, $Cp^*_2Hf(H)-O-(H)HfCp^*_2$. Additional H_2O drives the reaction to $Cp^*_2Hf(OH)_2$. Ammonia reacts only once to generate $Cp^*_2M(NH_2)H$ and H_2 .



The reactivity exhibited by these hydride complexes with water stimulated our interest in synthesizing alkylperoxide derivatives by a similar method (eq 3).

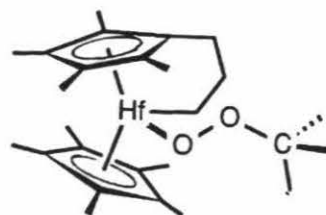
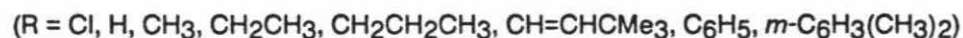


This chapter discusses the synthesis and reactivity of a series of hafnium *t*-butylperoxide complexes. This series provides the first well characterized examples of group IV alkylperoxide complexes.

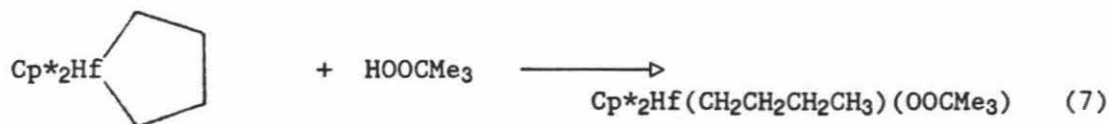
Results and Discussion

Synthesis: The room temperature addition of *t*-butylhydroperoxide (TBHP) to $\text{Cp}^*_2\text{MH}_2^3$ ($\text{M} = \text{Zr}, \text{Hf}$) yields $\text{Cp}^*_2\text{M}(\text{O}t\text{-Bu})(\text{OH})$ and H_2 . Low temperature addition (-50°C) of TBHP to $\text{Cp}^*_2\text{HfH}_2$ gives a complex which, based on ^1H nmr spectroscopic evidence, is $\text{Cp}^*_2\text{Hf}(\text{OO}t\text{-Bu})(\text{H})$. The decomposition of the zirconium analogue, $\text{Cp}^*_2\text{Zr}(\text{OO}t\text{-Bu})(\text{H})$, is too fast to allow its observation even at low temperature. The first moderately stable complex we observed was $\text{Cp}^*_2\text{Hf}(\text{OO}t\text{-Bu})\text{Cl}$, synthesized from the reaction of $\text{Cp}^*_2\text{Hf}(\text{Cl})(\text{H})$ with TBHP. The analogous zirconium derivative is observed at low temperature, but decomposes upon warming to room temperature. The instability of the zirconium species led us to concentrate on preparing hafnium derivatives.

A series of hafnium *t*-butylperoxide complexes were synthesized by protolytic cleavage of Hf-H bonds with 1.1 equivalents of *t*-butylhydroperoxide (eq 4,5): $\text{Cp}^*_2\text{Hf}(\text{R})(\text{OOCMe}_3)$ ($\text{Cp}^* = (\eta^5\text{-C}_5\text{Me}_5)$; $\text{R} = \text{Cl}, \text{H}, \text{CH}_3, \text{CH}_2\text{CH}_3, \text{CH}_2\text{CH}_2\text{CH}_3, \text{CH}=\text{CHCMe}_3, \text{C}_6\text{H}_5, \textit{meta}\text{-C}_6\text{H}_3(\text{CH}_3)_2$ and $\text{Cp}^*(\eta^5, \eta^1\text{-C}_5(\text{CH}_3)_4(\text{CH}_2)_3)\text{Hf}(\text{OOCMe}_3)$). $\text{Cp}^*_2\text{Hf}(\text{H})(\text{OOCMe}_3)$ was not isolated.

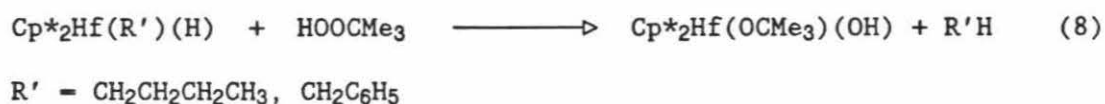


The ring opening cleavage of hafnium metallacycles with excess TBHP has provided a second synthesis pathway to give two derivatives not accessible by the first route ($R = \text{CH}_2\text{CH}_2\text{CH}_2\text{CH}_3, \text{CH}_2\text{CHMe}_2$) (eq 6,7).



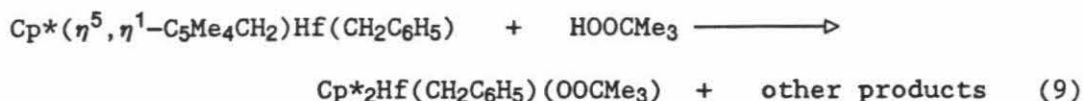
The reactions are carried out at room temperature or 0°C depending on the stability of the product (*vide infra*). These compounds are extremely soluble in alkane and arene solvents. Isolation of the compounds was considerably facilitated by the fortuitous discovery, while washing glassware, that these complexes are relatively insoluble in acetone. Reactions are carried out in petroleum ether (many of the starting materials react with acetone) and the products are isolated from acetone. The isolated complexes are stable for months when stored at low temperature. Analytical, ^1H nmr, and IR ($\nu(\text{O}-\text{O}) = 835 - 850 \text{ cm}^{-1}$) data support the above formulations.

We were not able to synthesize several other derivatives of interest. When the alkyl ligand (R') of $\text{Cp}^*_2\text{Hf}(R')(\text{H})$ is larger than propyl, the addition of TBHP results in loss of alkane and the formation of $\text{Cp}^*_2\text{Hf}(\text{OCMe}_3)(\text{OH})$ (eq 8).

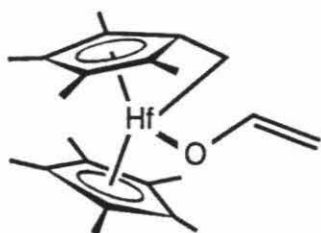


Several other approaches for synthesizing the benzyl derivative were attempted. The most successful involves the addition of TBHP to the ring-metallated benzyl compound, $\text{Cp}^*(\eta^5, \eta^1\text{-C}_5\text{Me}_4\text{CH}_2)\text{Hf}(\text{CH}_2\text{C}_6\text{H}_5)$ (eq 9). The reaction yields approximately 40% of the

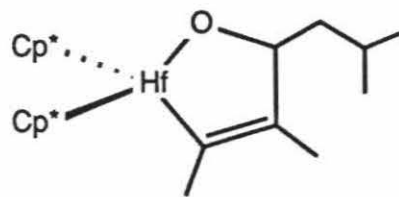
desired product, along with an intractable mixture of other products. No reaction was observed upon addition of TBHP to $\text{Cp}^*_2\text{Hf}(\text{CH}_2\text{C}_6\text{H}_5)_2$.



We were also unable to synthesize derivatives with alkoxides as the coligand. For example, attempts to generate a species similar to the proposed intermediate of the Sharpless epoxidation system,⁴ by reacting TBHP with the allyl alkoxide derivatives $\text{Cp}^*_2\text{Hf}(\text{OCH}_2\text{CH}=\text{CH}_2)(\text{H})$, $\text{Cp}^*(\eta^5, \eta^1\text{-C}_5\text{Me}_4\text{CH}_2)\text{Hf}(\text{OCH}_2\text{CH}=\text{CH}_2)$ (1) and $\text{Cp}^*_2\text{Hf}(\text{OCH}(\text{CH}_2\text{CHMe}_2)\text{C}(\text{CH}_3)=\text{C}(\text{CH}_3))$ (2), proved unsuccessful.



1



2

Crystallographic Results: Crystals were grown by slow cooling of an acetone solution of $\text{Cp}^*_2\text{Hf}(\text{OO}t\text{-Bu})(\text{Et})$. A skeletal view of the molecule with non-hydrogen atoms is given in Figure 1 and depicts the pseudotetrahedral coordination or "bent sandwich" configuration of ligands about the hafnium atom and gives selected bond angles and distances. Also included are the frontier orbitals of a bent metallocene fragment. Figure 2 gives the numbering scheme for the non-hydrogen atoms. The R-Hf-R (R = Cp* ring centroid) angle of 135.0° and range of Hf-C (Cp*) distances, 2.528(14)-2.572(14) Å are unexceptional when compared to other bispentamethylcyclopentadienyl-hafnium complexes, *cf.*, $\text{Cp}^*_2\text{Hf}(\text{H})(\eta^3\text{-CH}_2\text{CHCH}_2)$, with average Hf-C(ring) distances of 2.55 Å and R-Hf-R angle of 130° .⁵ The inner-ring carbon atoms of the Cp* ligands are planar,

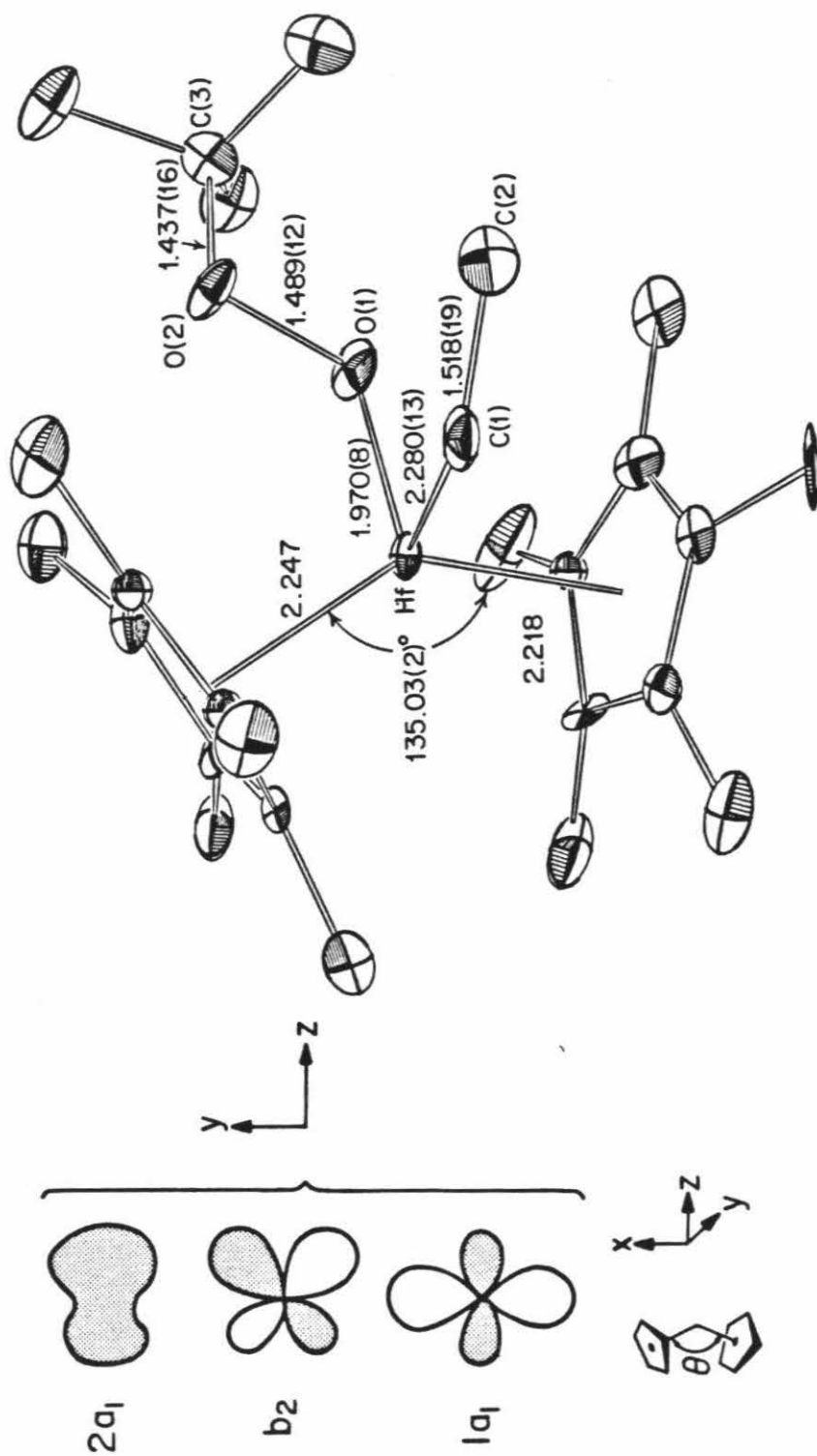


Figure 1. Selected bond angles and distances, $\text{Cp}^*_2\text{Hf}(\text{OOCMe}_3)\text{CH}_2\text{CH}_3$. Frontier orbitals for bent metallocenes.

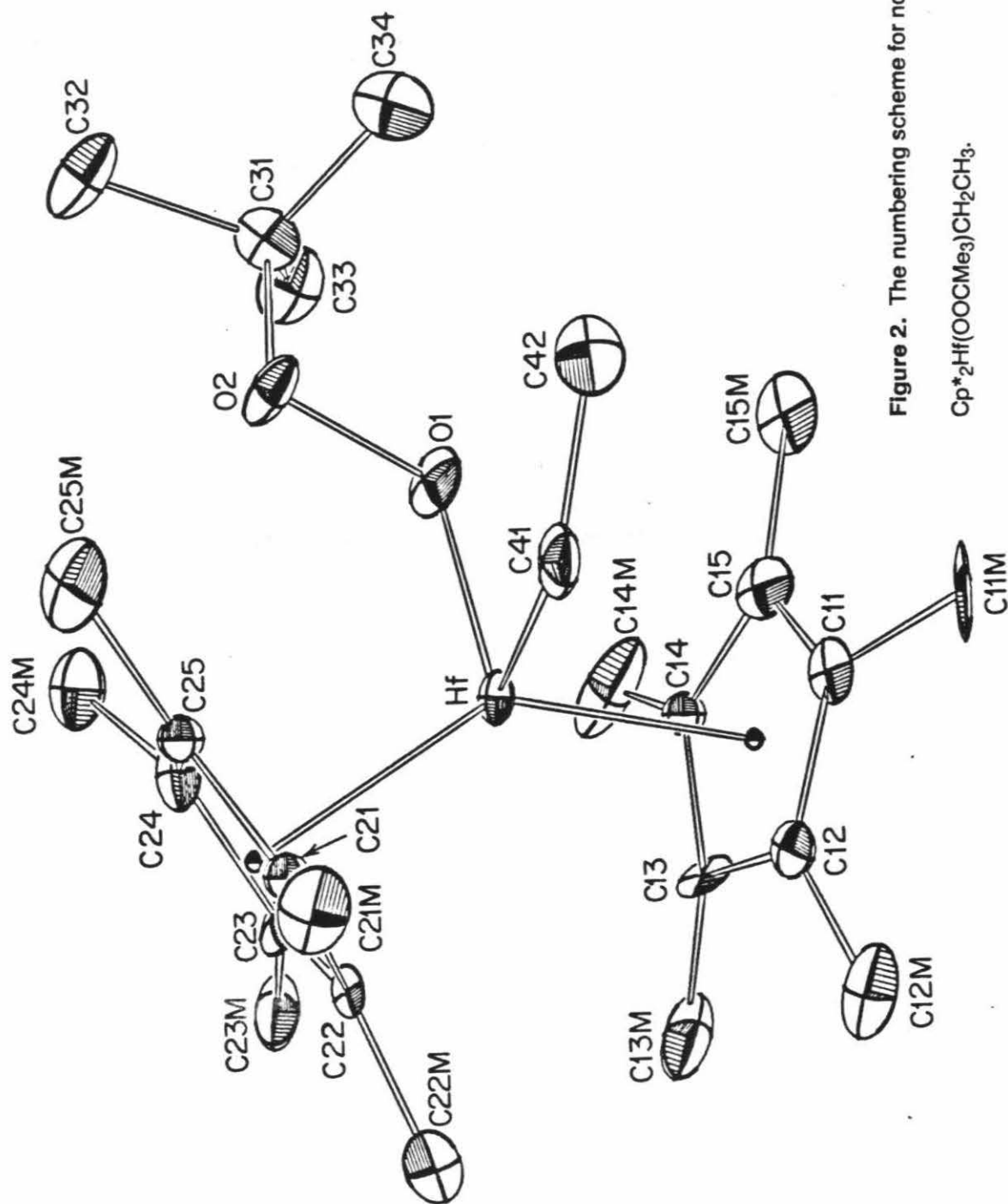


Figure 2. The numbering scheme for non-hydrogen atoms,



and the methyl groups are displaced from the ring and away from the Hf atom by 0.16 Å on average; the greatest deviations are by C12M and C13M on one ring and C23M on the other (the shortest CH₃ ···CH₃ non-bonding contact is C13M ···C23M at 3.31 Å). In addition, there are intimate contacts between the ring methyl groups and the ethyl group, C11M ···C41 3.18 Å and C11M ···C42 3.39 Å, and the ring methyl groups and the *t*-butylperoxide ligand, C15M ···O1 2.93 Å and C24M ···O2 2.95 Å. The Hf-C41 bond length of 2.280(13) Å is normal, *cf.*, 2.295(14) Å in (Cp₂HfMe)₂O.⁶

The Hf–O bond length of 1.970(8) Å indicates considerable π -donation from the lone pair orbitals on O1 into the empty (2a₁)⁷ orbital on hafnium; the predicted Hf–O single bond length is approximately 2.19 Å, *cf.*, Zr–O bond length in Zr(acac)₄, 2.20 Å and $r(\text{Zr}) - r(\text{Hf}) = 0.01$ Å.⁸ The C41-Hf-O1-O2 torsion angle is $-70.9(7)^\circ$, a geometry consistent with oxygen lone pair π -donation from O1 into Hf.

The O1-O2 bond length of 1.489(12) Å is like that reported for other transition metal alkylperoxide structures.⁹ The O2-C31 bond length of 1.437(16) Å is normal. The Hf-O1-O2 of $119.6(6)^\circ$ is larger than that reported for similar structures and is possibly a result of unfavorable steric interactions. The sterically demanding *t*-butoxide group is found tilted into the middle of the wedge between the two Cp* ligands.

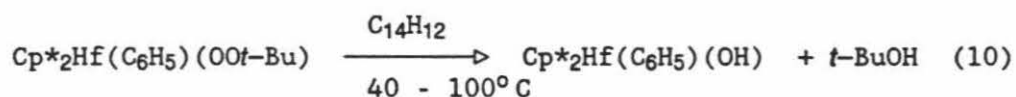
The most striking feature of the structure is the monodentate coordination of the *t*-butylperoxide ligand. As mentioned in the introductory chapter, the related structure of (dipic)VO(OO*t*-Bu)L contains an η^2 -*t*-butylperoxide ligand. For Cp*₂Hf(OOCMe₃)(Et), coordination of the alkoxy oxygen to Hf would satisfy the 18 electron rule. This is apparently precluded in the ground state structure by steric interactions of the *t*-butylperoxide oxygens with the ring methyls.

Indirect evidence that the ground state structure in solution is also monodentate is available from the ^1H nmr spectra of $\text{Cp}^*_2\text{Hf}(\text{OO}t\text{-Bu})(\text{H})$. An empirical trend in the hydride shifts of $\text{Cp}^*_2\text{Hf}(\text{X})(\text{H})$ has been noted.^{3b} The hydride signals of 16 electron $\text{Cp}^*_2\text{HfH}_2$ are found relatively far downfield at 15.6 ppm. The hydride resonances of the closed-shell, 18 electron complexes $\text{Cp}^*_2\text{Hf}(\text{H})(\eta^3\text{-CH}_2\text{CHCH}_2)$ 3.6 ppm and $\text{Cp}^*_2\text{Hf}(\text{H})_2(\text{CO})$ 2.7 ppm are shifted significantly upfield of the 16 electron complexes. Table 1 summarizes the chemical shifts for several $\text{Cp}^*_2\text{Hf}(\text{X})(\text{H})$ complexes and one can observe an apparent correlation between the hydride shift and the extent of π donation from X into the empty orbital ($2a_1$) on hafnium. The hydride shift of $\text{Cp}^*_2\text{Hf}(\text{OO}t\text{-Bu})(\text{H})$ at 10.7 ppm falls in the range of that reported for formally 16 electron, π -donating alkoxide derivatives. It is not consistent with the closed-shell, 18 electron configuration of an η^2 -*t*-butylperoxide ligand. It is possible, however, that an η^2 -coordinated intermediate is present in the reactions of these complexes (*vide infra*).

Table 1. ^1H NMR Chemical Shifts for the Hydride Resonance of $\text{Cp}^*_2\text{Hf}(\text{X})\text{H}$.

X	δ (ppm)
H	15.6
I	15.3
$\text{CH}_2\text{CH}(\text{CH}_3)_2$	13.6
Br	13.5
C_6H_5	13.1
CH_3	13.0
Cl	12.7
CH_2CH_3	12.2
$\text{NH}(\text{C}_6\text{H}_5)$	11.6
$\text{N}(\text{CH}_3)_2$	11.5
F	11.1
OOCMe_3	10.3
OH	10.2
OCH_3	9.9
$\eta^2\text{-HNNC}(\text{C}_6\text{H}_4\text{CH}_3)_2$	8.2
$\eta^3\text{-C}_3\text{H}_5$	3.6
$\text{H}(\text{CO})$	2.7

Reactivity: At least three modes of decomposition have been observed for the series $\text{Cp}^*_2\text{Hf}(\text{R})(\text{OO}t\text{-Bu})$. The preferred mode of decomposition is highly dependent on the nature of the R group. When R equals C_6H_5 or $m\text{-C}_6\text{H}_3(\text{CH}_3)_2$ one observes decomposition only upon heating above room temperature. In fact, $\text{Cp}^*_2\text{Hf}(\text{C}_6\text{H}_5)(\text{OO}t\text{-Bu})$, unlike the alkyl derivatives, is stable in the solid state at room temperature for over a year. Upon heating, products consistent with O-O bond homolysis and formation of *t*-butoxide radical are observed. In the presence of 5 - 16 equivalents of radical trap and hydrogen donor 9,10-dihydroanthracene, clean first order formation of $\text{Cp}^*_2\text{Hf}(\text{C}_6\text{H}_5)(\text{OH})$ and *t*-BuOH is observed (eq 10).

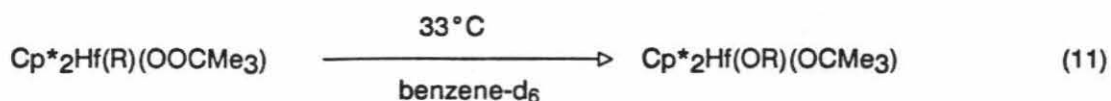


The activation parameters for the above reaction were calculated by measuring the kinetics of the reaction over the temperature range of 40 to 90°C ($\Delta H^\ddagger = 22.6$ kcal/mol, $\Delta S^\ddagger = -9.7$ e.u.). Replacing the two *meta*-hydrogens on the phenyl group with methyl groups, *i.e.*, $\text{Cp}^*_2\text{Hf}(m\text{-C}_6\text{H}_3(\text{CH}_3)_2)(\text{OO}t\text{-Bu})$, had no measurable effect on the kinetics of decomposition. From the activation parameters one can estimate a value of 22 kcal/mol for the O-O bond strength, considerably lower than those measured for normal dialkylperoxides (37 ± 1 kcal/mol).¹⁰

$\text{Cp}^*_2\text{Hf}(\text{Cl})(\text{OO}t\text{-Bu})$ decomposes slowly at room temperature in benzene solution to give an intractable mixture of products. This decomposition likely proceeds by more than one pathway and involves the apparent loss of at least one Cp^* ligand. Addition of PMe_3 , CO, cyclohexene or ethylene has no effect on the decomposition and one observes no oxidation of substrate. 9,10-Dihydroanthracene also has no effect on the decomposition.

The methyl and neohexenyl derivatives also decompose by more than one pathway to give rise to one major product and an intractable mixture of products similar to those of the chloride derivative's decomposition. For the methyl case we observe approximately 50% conversion to $\text{Cp}^*_2\text{Hf}(\text{OCH}_3)(\text{Ot-Bu})$. Observed in about 30% yield, the only identifiable product of the neohexenyl decomposition is $\text{Cp}^*_2\text{Hf}(\text{CH}=\text{CHCMe}_3)\text{OH}$.

When $\text{R} = \text{H}, \text{CH}_2\text{CH}_3, \text{CH}_2\text{CH}_2\text{CH}_3, \text{CH}_2\text{CH}_2\text{CH}_2\text{CH}_3, \text{CH}_2\text{CH}(\text{CH}_3)_2$ and for $\text{Cp}^*(\eta^5, \eta^1\text{-C}_5(\text{CH}_3)_4\text{CH}_2\text{CH}_2\text{CH}_2)\text{Hf}(\text{OOCMe}_3)$ we observe clean first order decomposition at room temperature or below to the corresponding alkoxy *t*-butoxide derivatives (eq 11, 12; Table 2).



($\text{R} = \text{CH}_3, \text{CH}_2\text{CH}_3, \text{CH}_2\text{CH}_2\text{CH}_3, \text{CH}_2\text{CH}_2\text{CH}_2\text{CH}_3, \text{CH}_2\text{CHMe}_2$)

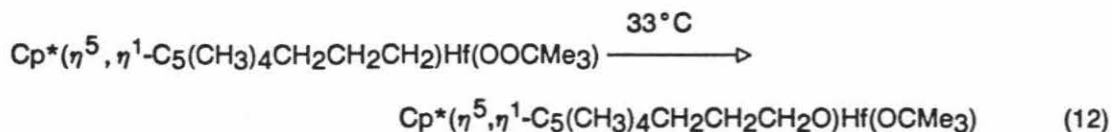


Table 2. Kinetics of oxygen insertion (benzene-*d*₆, 33 °C).

	k ($\times 10^5, \text{sec}^{-1}$)
$\text{Cp}^*_2\text{Hf}(\text{CH}_2\text{CH}_3)(\text{OOCMe}_3)$	9.5
$\text{Cp}^*_2\text{Hf}(\text{CH}_2\text{CH}_2\text{CH}_2\text{CH}_3)(\text{OOCMe}_3)$	10
$\text{Cp}^*_2\text{Hf}(\text{CH}_2\text{CH}_2\text{CH}_3)(\text{OOCMe}_3)$	15
$\text{Cp}^*(\eta^5, \eta^1\text{-C}_5(\text{CH}_3)_4\text{CH}_2\text{CH}_2\text{CH}_2)\text{Hf}(\text{OOCMe}_3)$	45
$\text{Cp}^*_2\text{Hf}(\text{CH}_2\text{CHMe}_2)(\text{OOCMe}_3)$	180

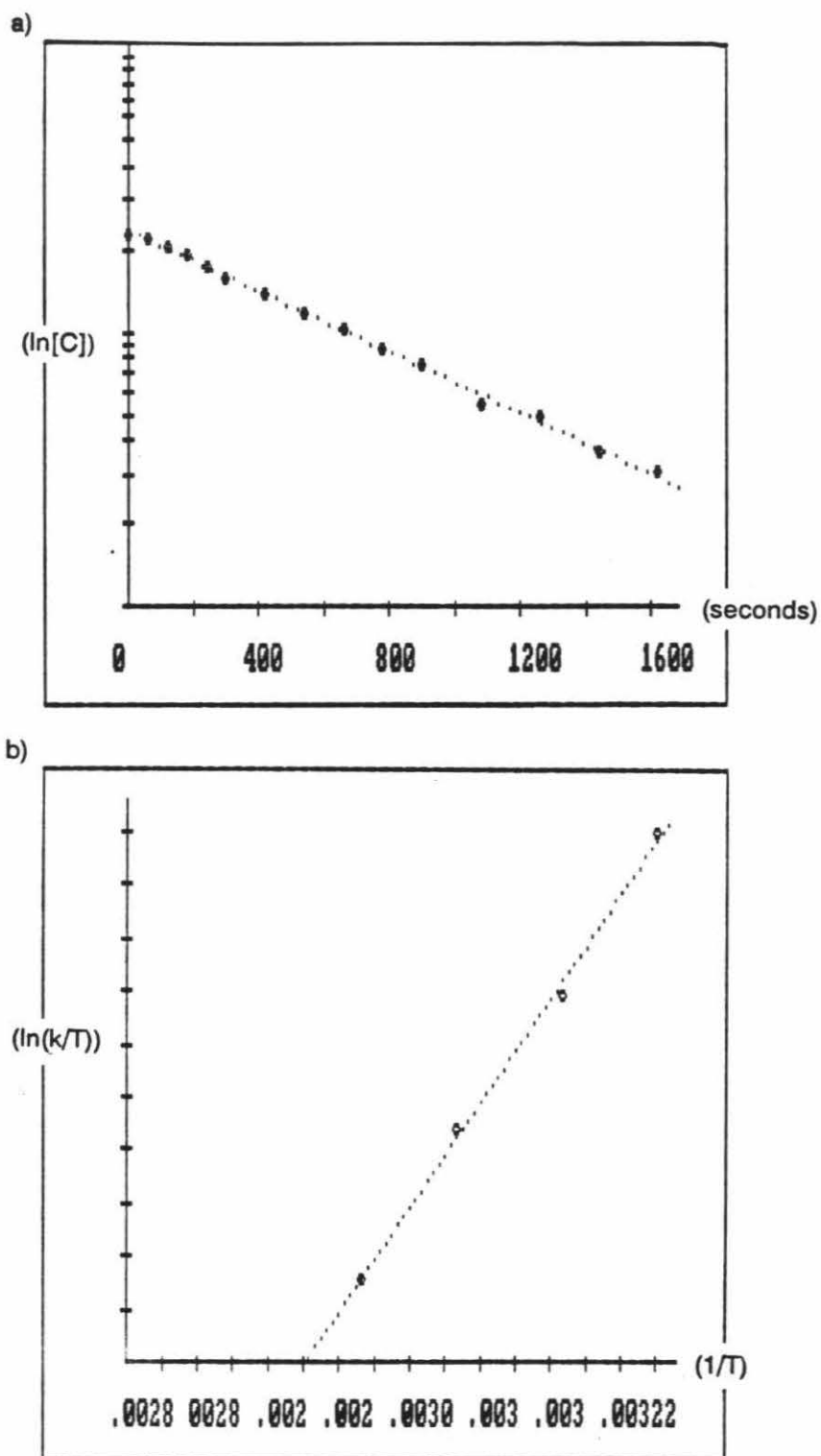
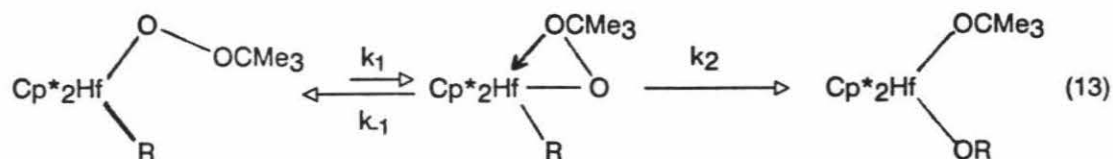


Figure 3. a) Kinetics at 60°C for the transformation of $\text{Cp}^*_2\text{Hf}(\text{CH}_2\text{CH}_3)(\text{OOCMe}_3)$ to $\text{Cp}^*_2\text{Hf}(\text{OCH}_2\text{CH}_3)(\text{OCMe}_3)$; $\ln[C]$ vs. $t(\text{sec})$, $k = 5.38 \times 10^{-4}$. b) Eyring Plot for the rearrangement of $\text{Cp}^*_2\text{Hf}(\text{CH}_2\text{CH}_3)(\text{OOCMe}_3)$ at 35°, 42°, 52° and 60°: $\ln(k/T)$ vs. $(1/T)$, $\Delta H^\ddagger = 19.6 \text{ kcal/mol}$ $\Delta S^\ddagger = -13 \text{ e.u.}$

Figure 3 shows a typical example of a kinetics run for $\text{Cp}^*_2\text{Hf}(\text{CH}_2\text{CH}_3)(\text{OOCMe}_3)$. The relative rates do not seem to follow any regular pattern and may reflect a multistep pathway for rearrangement (*vide infra*). Activation parameters for $\text{Cp}^*_2\text{Hf}(\text{CH}_2\text{CH}_3)(\text{OOCMe}_3)$ ($\Delta H^\ddagger = 19.6 \text{ kcal/mol}$, $\Delta S^\ddagger = -13 \text{ e.u.}$; Figure 3) were calculated from kinetics measurements over a temperature range of $35^\circ - 60^\circ \text{ C}$ and are consistent with an intramolecular rearrangement. Indirect evidence of the intramolecular nature of the rearrangement was obtained by carrying out the decomposition in the presence of $\text{Cp}^*_2\text{HfH}_2$. No formation of $\text{Cp}^*_2\text{Hf}(\text{H})(\text{OH})$ or related species was observed.² No measurable rate change was observed when the kinetics of $\text{Cp}^*_2\text{Hf}(\text{CH}_2\text{CH}_3)(\text{OOCMe}_3)$ decomposition were followed in more polar solvents; CD_2Cl_2 , $\text{THF-}d_8$ and acetonitrile- d_3 /benzene- d_6 (40:60). One observes slower further decomposition of the bis(alkoxides) in coordinating solvents to give Cp^*H and unknown metal containing species.

Mechanism: As mentioned in Chapter 1, a likely first step in oxygen transfer reactions from metal alkylperoxide complexes is η^2 -coordination of the alkylperoxide ligand. We have not observed a $\eta^2\text{-OOCMe}_3$ intermediate in this system. The complex rate dependence on the sterics of the alkyl ligand, however, can be interpreted as consistent with a stepwise process as shown in equation 13.



One would expect the preequilibrium step (k_1) to respond primarily to steric factors. Particularly noteworthy is the over 10-fold increase in rate observed for the sterically demanding isobutyl complex vs. the n-alkyl derivatives.

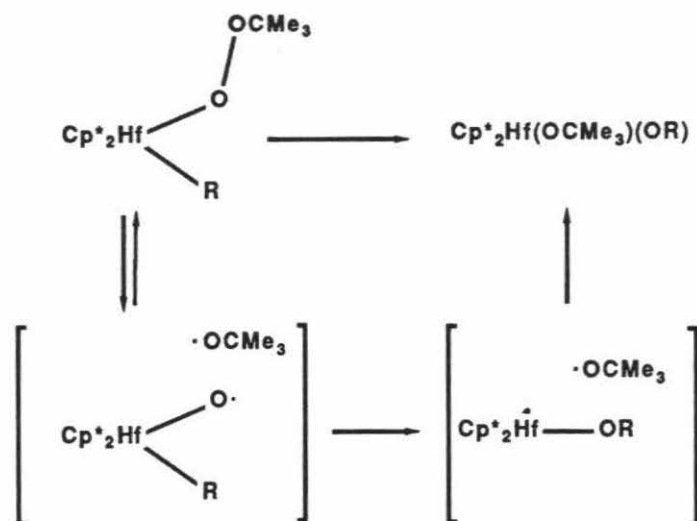
We are not able to draw many conclusions concerning the actual oxygen transfer step (k_2), which should be sensitive to electronic and steric changes in R. Empirical trends, noted for $\text{Cp}^*_2\text{Hf}(\text{I})(\text{R})$ hydrogenations, indicate that bulkier alkyl groups may have weaker hafnium carbon bonds.¹¹ Halpern has noted similar trends for other transition metal alkyls.¹² This factor could contribute to the increased rate of oxygen insertion observed for $\text{Cp}^*_2\text{Hf}(\text{CH}_2\text{CHMe}_2)(\text{OOCMe}_3)$.

Although the range of solvent polarities is severely limited by the high reactivity of these compounds, no significant difference was noted for the rate of rearrangement of $\text{Cp}^*_2\text{Hf}(\text{CH}_2\text{CH}_3)(\text{OOCMe}_3)$ in more polar solvents, suggesting little polar character for the transition state of step k_2 .

The higher stability of the phenyl derivatives can also be accommodated with this mechanism, since the planar phenyl ring is constrained to lie in the equatorial plane of the bent sandwich structure. Although the crystal structure was disordered, a partial X-ray structure determination for $\text{Cp}^*_2\text{Hf}(\text{C}_6\text{H}_5)(\text{OOCMe}_3)$ revealed this arrangement for the phenyl group. The barrier to rotation is sufficiently large that nmr spectra indicate a static structure in solution at ambient temperature. The crowded wedge presumably inhibits the formation of the $\eta^2\text{-OOCMe}_3$ intermediate, forcing the complex to find an alternative path for decomposition (O-O bond homolysis). An additional factor may be the hafnium phenyl bond strength. The hafnium phenyl bond in $\text{Cp}^*_2\text{Hf}(\text{Ph})(\text{H})$ is on the order of 20 kcal/mol stronger than the hafnium carbon bond in $\text{Cp}^*(\eta^5, \eta^1\text{-C}_5(\text{CH}_3)_4\text{CH}_2\text{CH}_2\text{CH}_2)\text{HfH}$.¹¹ No clear conclusions can be drawn concerning the chloride, methyl and neohexenyl decompositions.

A alternative mechanism to initial η^2 -*t*-butylperoxide coordination is suggested by the homolytic O-O bond cleavage observed for $\text{Cp}^*_2\text{Hf}(\text{C}_6\text{H}_5)(\text{OOCMe}_3)$. In the phenyl case, cleavage of the O-O bond is followed by escape of $\cdot\text{OCMe}_3$. When the alkyl group is not

phenyl, cleavage of the O-O bond to form a caged radical pair is followed by migration of the alkyl group to Hf-O· to yield Cp*₂Hf(III)OR. Cp*₂Hf(III)OR recombines with the *t*-butoxide radical to yield the bis(alkoxide) product (Scheme I).



Scheme I

Conclusions: We have synthesized the first series of group IV metal alkylperoxide complexes and have studied two of the decomposition modes. The success of the synthetic strategy for these reactive complexes rests, in part, on the very fast reaction of the hydride derivatives and moderately fast reaction of the metallacycles with TBHP. With slower reactions, most of these species could never be isolated. Both decomposition pathways involve O-O bond cleavage. In the case of the phenyl derivatives, the process appears to involve homolytic cleavage of the O-O bond. The O-O bond strength for these complexes is estimated to be 22 kcal/mol. The hydride, ethyl, propyl, butyl, isobutyl and propyl bridged tuck-in derivatives decompose by insertion of an oxygen of the *t*-butylperoxide ligand into a hafnium carbon bond in a process which has a barrier of approximately 20 kcal/mol. Kinetic data for these reactions is consistent with a multistep decomposition process.

The crowded ligand environment surrounding a less reactive, third-row transition metal is very likely responsible for the thermal stability exhibited by members of this series of complexes. These same features seem to dictate the mechanism(s) for rearrangement to the very stable bis(alkoxide) derivatives.

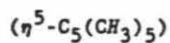
Table I. NMR, IR, and Analytical Data.

Compound ^a	Assignment	δ (ppm) ^b	J (Hz) ^c
$\text{Cp}^*_2\text{Hf}(\text{OOCMe}_3)\text{Cl}$	$(\eta^5\text{-C}_5(\text{CH}_3)_5)$	1.96 s	
	$\text{C}(\text{CH}_3)_3$	1.26 s	
	¹³ C $(\eta^5\text{-C}_5(\text{CH}_3)_5)$	119.9	
	$(\eta^5\text{-C}_5(\text{CH}_3)_5)$	80.3	
C 50.36 (50.25)	$\text{C}(\text{CH}_3)_3$	26.8	
H 6.97 (6.87)	$\text{C}(\text{CH}_3)_3$	11.9	
$\nu_{(\text{O}-\text{O})} = 835 \text{ cm}^{-1}$	$\text{C}(\text{CH}_3)_3$		
$\text{Cp}^*_2\text{Hf}(\text{OOCMe}_3)\text{H}$	Hf-H	10.28 s	
	$(\eta^5\text{-C}_5(\text{CH}_3)_5)$	2.00 s	
	$\text{C}(\text{CH}_3)_3$	1.23 s	
$\text{C}_7\text{D}_8, -50^\circ\text{C}$			
$\text{Cp}^*_2\text{Hf}(\text{OCMe}_3)\text{OH}$	Hf-OH	3.00 s	
	$(\eta^5\text{-C}_5(\text{CH}_3)_5)$	1.88 s	
	$\text{C}(\text{CH}_3)_3$	1.30 s	
$\text{C}_7\text{D}_8, -50^\circ\text{C}$			
$\text{Cp}^*_2\text{Hf}(\text{OOCMe}_3)\text{CH}_3$	$(\eta^5\text{-C}_5(\text{CH}_3)_5)$	1.93 s	
	$\text{C}(\text{CH}_3)_3$	1.19 s	
	CH_3	-0.25 s	
C 53.82 (54.29)			
H 7.45 (7.65)			
$\nu_{(\text{O}-\text{O})} = 838 \text{ cm}^{-1}$			



C 54.83 (55.06)
H 7.72 (7.82)

$\nu_{(\text{O}-\text{O})} = 845 \text{ cm}^{-1}$

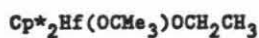


1.92 s

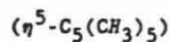
1.64 t $J_{\text{HH}}=7.8$

1.20 s

0.45 q $J_{\text{HH}}=7.8$



C 54.75 (55.06)
H 7.75 (7.82)

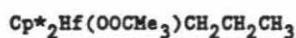


4.26 q $J_{\text{HH}}=7.2$

1.98 s

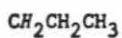
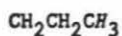
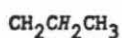
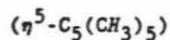
1.38 s

1.30 t $J_{\text{HH}}=7.2$



C 55.68 (55.80)
H 7.92 (7.97)

$\nu_{(\text{O}-\text{O})} = 838 \text{ cm}^{-1}$



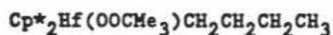
1.90 s

1.63 m

1.33 t $J_{\text{HH}}=7.1$

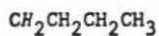
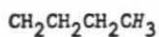
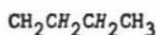
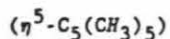
1.19 s

0.39 m



C 56.25 (56.50)
H 8.01 (8.13)

$\nu_{(\text{O}-\text{O})} = 842 \text{ cm}^{-1}$



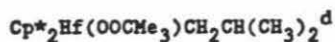
1.91 s

1.60 m

1.21 s

1.17 m

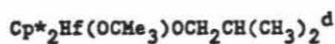
0.38 m



C 56.20 (56.51)
H 7.85 (8.12)

$\nu_{(\text{O}-\text{O})} = 842 \text{ cm}^{-1}$

$(\eta^5\text{-C}_5(\text{CH}_3)_5)$	1.95 s
$\text{CH}_2\text{CH}(\text{CH}_3)_2$	1.27 d $J_{\text{HH}}=6$
$\text{C}(\text{CH}_3)_3$	1.23 s
$\text{CH}_2\text{CH}(\text{CH}_3)_2$	0.27 d $J_{\text{HH}}=6$



$\text{CH}_2\text{CH}(\text{CH}_3)_2$	3.97 d $J_{\text{HH}}=6.8$
$(\eta^5\text{-C}_5(\text{CH}_3)_5)$	1.99 s
$\text{C}(\text{CH}_3)_3$	1.40 s
$\text{CH}_2\text{CH}(\text{CH}_3)_2$	1.03 d $J_{\text{HH}}=6.6$



C 57.82 (58.00)
H 7.88 (8.11)

$\nu_{(\text{O}-\text{O})} = 843 \text{ cm}^{-1}$

$\text{CH}=\text{CHC}(\text{CH}_3)_3$	6.02 d $J_{\text{HH}}=19.5$
$\text{CH}=\text{CHC}(\text{CH}_3)_3$	5.63 d $J_{\text{HH}}=19.5$
$(\eta^5\text{-C}_5(\text{CH}_3)_5)$	1.88 s
$\text{C}(\text{CH}_3)_3, \text{CHCHC}(\text{CH}_3)_3$	1.24 s



C 58.75 (58.77)
H 7.13 (7.13)

$\nu_{(\text{O}-\text{O})} = 848 \text{ cm}^{-1}$

C_6H_5	7.75 m
	7.42 m
	7.36 m
	7.18 m
	7.04 m
$(\eta^5\text{-C}_5(\text{CH}_3)_5)$	1.79 s
$\text{C}(\text{CH}_3)_3$	1.30 s

$\text{Cp}^*_2\text{Hf}(\text{OOCMe}_3)_m\text{-C}_6\text{H}_3\text{Me}_2$

C 60.20 (59.75)	$\text{C}_6\text{H}_3(\text{CH}_3)_2$	7.40 s
H 7.35 (7.52)		6.80 s
		6.68 s
	$\text{C}_6\text{H}_3(\text{CH}_3)_2$	2.43 s
		2.42 s
	$(\eta^5\text{-C}_5(\text{CH}_3)_5)$	1.82 s
$\nu(\text{O-O}) = 838 \text{ cm}^{-1}$	$\text{C}(\text{CH}_3)_3$	1.35 s

 $\text{Cp}^*(\eta^5\text{-C}_5(\text{CH}_3)_4\text{CH}_2\text{CH}_2\text{CH}_2)\text{Hf}(\text{OOCMe}_3)^e$

C 55.25 (55.26)	$(\eta^5\text{-C}_5(\text{CH}_3)_4\text{CH}_2\text{CH}_2\text{CH}_2)$	3.08 m
H 7.49 (7.49)		2.69 m
	$(\eta^5\text{-C}_5(\text{CH}_3)_4\text{CH}_2\text{CH}_2\text{CH}_2)$	2.13 s
		1.91 s
		1.80 s
		1.65 s
	$(\eta^5\text{-C}_5(\text{CH}_3)_5)$	1.91 s
	$\text{C}(\text{CH}_3)_3$	1.21 s
	$(\eta^5\text{-C}_5(\text{CH}_3)_4\text{CH}_2\text{CH}_2\text{CH}_2)$	0.93 m
$\nu(\text{O-O}) = 843 \text{ cm}^{-1}$	$(\eta^5\text{-C}_5(\text{CH}_3)_4\text{CH}_2\text{CH}_2\text{CH}_2)$	0.13 m

 $\text{Cp}^*(\eta^5\text{-C}_5(\text{CH}_3)_4\text{CH}_2\text{CH}_2\text{CH}_2\text{O})\text{Hf}(\text{OCMe}_3)^e$

	$(\eta^5\text{-C}_5(\text{CH}_3)_4\text{CH}_2\text{CH}_2\text{CH}_2\text{O})$	4.18 m
		4.03 m
	$(\eta^5\text{-C}_5(\text{CH}_3)_4\text{CH}_2\text{CH}_2\text{CH}_2\text{O})$	2.41 m
	$(\eta^5\text{-C}_5(\text{CH}_3)_4\text{CH}_2\text{CH}_2\text{CH}_2\text{O})$	2.10 s
		2.00 s
		1.86 s
		1.84 s
	$(\eta^5\text{-C}_5(\text{CH}_3)_5)$	2.00 s
	$(\eta^5\text{-C}_5(\text{CH}_3)_4\text{CH}_2\text{CH}_2\text{CH}_2\text{O})$	1.78 m
	$\text{C}(\text{CH}_3)_3$	1.37 s

a) Analyses are recorded with the calculated values in parantheses and were performed by the CIT analytical laboratory. IR spectra were recorded on a Beckman 4240 spectrometer b) All nmr spectra were recorded on Varian EM390, JEOL FX90Q, or JEOL GX400 spectrometers in C_6D_6 unless otherwise noted. Chemical shifts are reported in ppm relative to TMS. c) Coupling constants are reported in Hertz. d) Isolated and analyzed as a mixture with the inserted product. ca. 75% $\text{Cp}^*_2\text{Hf}(\text{OOCMe}_3)\text{CH}_2\text{CH}(\text{CH}_3)_2$. e) Isolated and analyzed as a mixture with the inserted product. ca. 80% $\text{Cp}^*(\eta^5\text{-C}_5(\text{CH}_3)_4\text{CH}_2\text{CH}_2\text{CH}_2)\text{Hf}(\text{OOCMe}_3)$. These are tentative assignments of the aliphatic protons in the propyl bridge.

Experimental Section

General Considerations: All manipulations were carried out using glove box or high vacuum line techniques unless otherwise noted. Solvents were dried by standard techniques and further purified by vacuum transfer from "titanocene"¹³ or benzophenone ketyl. Hydrogen was purified by passage over MnO on vermiculite¹⁴ and activated 4 Å sieves. Ethylene, isobutylene, and CO were used directly from the cylinder. Other reagents were degassed and vacuum transferred from 4 Å sieves or used directly as received.

tert-Butylhydroperoxide was dried by azeotrope distillation and stored cold over 4 Å sieves.¹⁵ In a typical example 10 mls of 90% *t*-butylhydroperoxide (5% H₂O, 5% *t*-BuOH) were mixed in a 50 ml flask with 30 mls of benzene. Boiling chips were added and the H₂O, *t*-BuOH, C₆H₆ azeotrope was distilled off at 67° C until the temperature rose to the boiling point of benzene. Approximately 10 mls of benzene were distilled off of the solution to give 4 M *t*-butylhydroperoxide in benzene. The concentration of the *t*-butylhydroperoxide / benzene solution can be increased by allowing more benzene to distill off. Approximate concentration can be determined effectively by nmr integration.

¹H nmr spectra were recorded with Varian EM-390, JEOL FX90Q, and JEOL GX400 spectrometers. ¹³C spectra were recorded with a JEOL FX90Q spectrometer. Infrared spectra were measured on a Beckman 4240 spectrometer as nujol mulls. Elemental analyses were performed by C.I.T. Analytical Laboratories. Molecular weights were determined using a Signer molecular weight apparatus.¹⁶

Procedures: Kinetic data were collected by monitoring the reactions in flame sealed nmr tubes with ferrocene as the internal standard. In a typical experiment 25 mg of compound were placed in an nmr tube with 8 mg of ferrocene, solvent was added and the reaction

was followed by nmr spectroscopy. Survey reactions were generally carried out in nmr tubes with rubber septa wrapped with parafilm. TBHP solution was added via syringe.

The starting hafnium complexes not reported elsewhere were prepared as follows.

Cp*₂Hf(X)(H) (X = Cl, I): An improvement over the reported method² for synthesizing these materials has been developed by A. R. Bulls. 5.594 g (7.97 mmol) of Cp*₂HfI₂ were stirred with 0.780 g (10 mmol) of LiCH₂CMe₃ for 24 hours in benzene. The benzene solution was filtered and the benzene was removed *in vacuo*. 4.34 g (6.71 mmol, 85% yield) of Cp*₂Hf(CH₂C(Me)₃)(I) were isolated at -78°C from petroleum ether. 3.3 g (5.11 mmol) of Cp*₂Hf(CH₂CMe₃)(I) were dissolved in 30 mls of benzene in a appr. 250 ml glass bomb. 1 atmosphere of H₂ was admitted at -198° C (3.8 atm at room temperature) and the bomb was heated at 80° C overnight. 2.67 g (4.81 mmol, 94% yield) of Cp*₂Hf(I)(H) were isolated from petroleum ether.

Cp*₂Hf(C₆H₃(Me)₂)(H): 500 mg (0.87 mmol) of Cp*₂Hf(I)(H) and 205 mg (1.83 mmol) of LiC₆H₃(Me)₂ were stirred together in toluene for 12 hours. Toluene was removed *in vacuo* and the 310 mg (0.56 mmol, yield 64%) of Cp*₂Hf(C₆H₃(Me)₂)(H) were isolated from petroleum ether.

Cp*₂Hf(R)(OOCMe₃) derivatives: The compounds synthesized from hafnium hydride complexes are prepared by addition of a slight excess of dried *tert*-butylhydroperoxide solution to a petroleum ether solution of the appropriate starting material. The metallacycle ring opening reactions require an excess of TBHP (4 - 10 equivalents) in order to insure product formation before decomposition can take place. The additions are carried out at 0°C or room temperature depending on the stability of the product and the solutions are stirred for 5 to 10 minutes and then filtered at that temperature. Although the products can be isolated by condensing and cooling the petroleum ether solutions to -78°C, better

yields are obtained if the petroleum ether is vacuum transferred off and acetone is used to isolate the solid. Yields can also be improved by insuring that excess TBHP and benzene are removed from the solution by two or three cycles of adding and removing *in vacuo* petroleum ether before adding acetone. Yields are generally in the range of 50 to 75%. The solids were stored in a glove box refrigerator.

Cp*₂Hf(Cl)(OOCMe₃): 400 mg (0.824 mmol) of Cp*₂Hf(Cl)(H) were placed in a 25 ml round bottom with septum capped side arm. 7 mls of petroleum ether were vacuum transferred onto the solid at -78° C. 163 μls of 4.8 M TBHP solution were added *via* syringe. After H₂ evolution was complete, the solution was filtered at -78° C, condensed and 275 mg (0.480 mmol, 58% yield) of Cp*₂Hf(Cl)(OOCMe₃) were isolated from petroleum ether at -78° C.

Cp*₂Hf(CH₃)(OOCMe₃): Cp*₂Hf(CH₃)(H) (222 mg, 0.48 mmol) was dissolved in 12 mls of petroleum ether and TBHP solution (0.072 mls, 9.3 M) was added. After filtering, petroleum ether was removed *in vacuo* and 126 mg (0.22 mmol, 48% yield) of Cp*₂Hf(CH₃)(OOCMe₃) were isolated from acetone.

Cp*₂Hf(CH₂CH₃)(OOCMe₃): 800 mg (1.67 mmol) of Cp*₂Hf(CH₂CH₃)(H) were placed in a 25 r.b. with septum capped side arm and dissolved in 15 mls of petroleum ether. 1.0 mls of 1.83 M TBHP solution were added *via* syringe. After H₂ evolution the reaction mixture was filtered and petroleum ether was removed *in vacuo*. 530 mg (0.94 mmol, 56% yield) of Cp*₂Hf(CH₂CH₃)(OOCMe₃) were isolated from acetone.

Cp*₂Hf(CH₂CH₂CH₃)(OOCMe₃): 507 mg (1.03 mmol) of Cp*₂Hf(CH₂CH₂CH₃)(H) were dissolved in 12 mls of petroleum ether at 0° C and 0.274 mls of 4.5 M TBHP solution were added. The solution was filtered and petroleum ether was removed *in vacuo*. 113 mg

(0.19 mmol, 19% yield) of $\text{Cp}^*_2\text{Hf}(\text{CH}_2\text{CH}_2\text{CH}_3)(\text{OOCMe}_3)$ were isolated from acetone.

This product was very soluble and proved difficult to crystallize.

$\text{Cp}^*_2\text{Hf}(\text{CH}=\text{CHCMe}_3)(\text{OOCMe}_3)$: 355 mg (0.66 mmol) of $\text{Cp}^*_2\text{Hf}(\text{CH}=\text{CHCMe}_3)(\text{H})$ were dissolved in 12 mls of petroleum ether and 0.86 mls of 9.3 M TBHP solution were added and after H_2 evolution was complete the solution was filtered. Petroleum ether was removed *in vacuo* and 260 mg (0.42 mmol, 63% yield) of $\text{Cp}^*_2\text{Hf}(\text{CH}=\text{CHCMe}_3)(\text{OOCMe}_3)$ were isolated from acetone.

$\text{Cp}^*_2\text{Hf}(\text{C}_6\text{H}_5)(\text{OOCMe}_3)$: 533 mg (1.01 mmol) of $\text{Cp}^*_2\text{Hf}(\text{C}_6\text{H}_5)(\text{H})$ were dissolved in 15 mls of petroleum ether in a 25 ml r.b with septum capped side arm. 0.9 mls (1.5 eq) of 1.83 M TBHP solution were added *via* syringe and the mixture was stirred for five minutes before filtering. 367 mg (0.59 mmol, 59% yield) of $\text{Cp}^*_2\text{Hf}(\text{C}_6\text{H}_5)(\text{OOCMe}_3)$ were isolated from petroleum ether.

$\text{Cp}^*_2\text{Hf}(\text{C}_6\text{H}_3(\text{Me})_2)(\text{OOCMe}_3)$: 0.095 mls of 9.3 M TBHP solution were added *via* syringe to a solution of 290 mg (0.52 mmol) of $\text{Cp}^*_2\text{Hf}(\text{C}_6\text{H}_3(\text{Me})_2)(\text{H})$ in 15 mls of petroleum ether. The solution was filtered and petroleum ether removed *in vacuo*. 224 mg (0.35 mmol, yield 67%) of $\text{Cp}^*_2\text{Hf}(\text{C}_6\text{H}_3(\text{Me})_2)(\text{OOCMe}_3)$ were isolated from acetone.

$\text{Cp}^*(\eta^5, \eta^1\text{-C}_5\text{Me}_4(\text{CH}_2)_3)\text{Hf}(\text{OOCMe}_3)$: 409 mg (0.86 mmol) of $\text{Cp}^*(\eta^5, \eta^1\text{-C}_5\text{Me}_4(\text{CH}_2)_3)\text{Hf}(\text{H})$ were dissolved in 12 mls of petroleum ether. The solution was cooled to 0°C and 0.111 mls of 9.3 M TBHP solution were added. After H_2 evolution was complete the petroleum ether solution was filtered at 0°C and petroleum ether was removed *in vacuo*. The products, 80% $\text{Cp}^*(\eta^5, \eta^1\text{-C}_5\text{Me}_4(\text{CH}_2)_3)\text{Hf}(\text{OOCMe}_3)$ and 20% $\text{Cp}^*(\eta^5, \eta^1\text{-C}_5\text{Me}_4(\text{CH}_2)_3\text{O})\text{Hf}(\text{OCMe}_3)$ were isolated in 26% yield (127 mg, 0.23 mmol) from acetone at 0°C .

Cp*₂Hf(CH₂CH(CH₃)₂)(OOCMe₃): 400 mg (0.79 mmol) of Cp*₂Hf(CH₂CH(CH₃)CH₂) were dissolved in 15 mls of petroleum ether and the solution was cooled to 0° C. 1.5 equivalents of TBHP solution (0.128 mls, 9.3 M) were added and an almost immediate loss of the yellow starting material color was observed. Petroleum ether was removed *in vacuo*, added, removed, and added again. The solution was then filtered and petroleum ether was again removed. Acetone at 0° C was used to precipitate 215 mg (0.36 mmol, 46% yield) of the products, 75% Cp*₂Hf(CH₂CH(CH₃)₂)(OOCMe₃) and 25% Cp*₂Hf(OCH₂CH(CH₃)₂)(OCMe₃). Care was taken remove as much solvent as possible from the solid isolated on the frit by passing argon through it, before warming the solid to room temperature. An earlier attempt at isolating this solid, inadequately dried, resulted in its rapid decomposition upon warming.

Cp*₂Hf(CH₂CH₂CH₂CH₃)(OOCMe₃): Cp*₂Hf(CH₂CH₂CH₂CH₂) (370 mg, 0.73 mmol) was slurried in 5 mls of petroleum ether and 10 equivalents of TBHP solution were added. Everything went into solution in two minutes and the mixture was stirred for fifty minutes at room temperature. After removing the petroleum ether, benzene and excess TBHP *in vacuo* petroleum ether was transferred onto the solid again and the solution was filtered. The petroleum ether solution was concentrated to almost an oil and NCCH₃ was added to precipitate the solid Cp*₂Hf(CH₂CH₂CH₂CH₃)(OOCMe₃) (264 mg, 0.44 mmol, 61% yield).

Crystal Structure Determination of Cp*₂Hf(CH₂CH₃)(OOCMe₃): A single crystal of dimensions 0.22 X .22 X 0.28 mm, bounded by the [101], [101] and [010] faces was cooled to 97.5 K on a locally modified Syntex p1 diffractometer equipped with cryocooler, graphite monochromator, and MoK α radiation. The preliminary photographic workup on other crystals indicated a unit cell of monoclinic symmetry, and space group P2₁/C with Z = 4. The least-squares refinement of the orientation matrix with the setting angles of twelve reflections generated the following cell parameters at 97.5 K: $a = 19.890(7) \text{ \AA}$, $b = 8.746(4)$

\AA , $c = 17.532(6) \text{\AA}$, $\beta = 124.987(24)^\circ$, $V = 2498(2) \text{\AA}^3$. Intensity data were collected by $\theta - 2\theta$ scans of width 2.00° (plus dispersion) at $6^\circ/\text{min}$. for the hemisphere $(\pm h, \pm k, l)$ to $2\theta = 40^\circ$. The three check reflections indicated no decomposition. The data were averaged over $2/m$ symmetry (average goodness-of-fit = 1.04 and $R = 0.078$ for paired reflections), and reduced to F_o^2 . The form factors were taken from the *International Tables for X-Ray Crystallography*, IV, Table 2.2B, pp. 99-101. The absorption correction appeared to be negligible and was not applied ($\mu = 41.46 \text{ cm}^{-1}$, range of transmission factor 0.3-0.5).

The coordinates of the hafnium atom were determined from the Patterson map, and the remainder of the structure from subsequent Fourier maps. The hydrogen atoms were placed at idealized positions with $B = 3.0 \text{\AA}^2$ and were not refined. The full-matrix least-squares refinement of atom coordinates and U_{ij} 's of the non-hydrogen atoms, the scale factor, and a term for isotropic secondary extinction ($g = 6.6(11) \times 10^{-8}$) minimizing $\sum \omega [(kF_o)^2 - F_c^2]^2$ yielded a goodness-of-fit = $\{\sum \omega [(kF_o)^2 - F_c^2]^2 / (n - p)\}^{1/2} = 1.37$ (2349 reflections, 263 parameters), $R_F = \sum |F_o - F_c| / \sum F_o = 0.054$ (2222 reflections, $I > 0$), and $R'_F = 0.037$ (1721 reflections, $I > 3\sigma$); the largest peak in the $\Delta\rho$ map was approximately 4 e/\AA^3 . The atom coordinates and U_{eq} 's for non-hydrogen atoms are given in Table X1. Table X2 contains the U_{ij} 's for non-hydrogen atoms, Table X3 the atom coordinates for hydrogen atoms and Table X4 the bond lengths and angles, torsion angles, and least-squares plane information.

Table X1. Atom Coordinates and U_{eq} 's ($\times 10^4$) for $Cp_2Hf(C_2H_5)(OOC_4H_9)$.

Atom	x	y	z	U_{eq}
Hf	2340.2(3)	747.4(6)	2723.3(3)	129(2)
C11	1720(7)	-1076(16)	1329(8)	215(112)
C12	1108(6)	-823(17)	1482(7)	177(42)
C13	853(6)	737(17)	1273(7)	171(146)
C14	1356(8)	1459(15)	1011(8)	299(93)
C15	1893(7)	250(17)	1056(8)	257(65)
C11M	2007(7)	-2652(16)	1280(8)	363(46)
C12M	695(8)	-2082(16)	1660(9)	365(43)
C13M	79(8)	1366(15)	1078(9)	396(45)
C14M	1297(8)	3046(18)	727(10)	529(56)
C15M	2421(7)	516(19)	726(8)	468(88)
C21	2512(8)	430(14)	4281(7)	201(64)
C22	1710(7)	998(15)	3641(7)	171(87)
C23	1783(7)	2503(15)	3382(8)	205(51)
C24	2638(7)	2874(14)	3877(8)	192(50)
C25	3074(7)	1612(15)	4410(8)	215(35)
C21M	2712(7)	-1061(14)	4800(8)	308(39)
C22M	969(7)	229(15)	3466(8)	353(37)
C23M	1123(7)	3685(14)	2887(8)	298(41)
C24M	2950(7)	4409(16)	3878(8)	281(40)
C25M	4016(7)	1480(15)	5107(8)	335(62)
O1	3081(4)	1922(9)	2538(5)	244(35)
O2	3863(4)	2534(10)	3360(5)	237(31)
C31	4311(7)	3248(14)	3043(8)	219(34)
C32	5019(7)	4011(17)	3943(8)	407(47)
C33	3799(7)	4482(16)	2326(8)	339(38)
C34	4638(7)	2106(16)	2692(8)	328(35)
C41	3184(7)	-1326(14)	3331(8)	234(41)
C42	3836(7)	-1397(15)	3139(9)	299(43)

Table X2. Anisotropic U_{ij} 's ($\times 10^4$) for $\text{Cp}_2\text{Hf}(\text{C}_2\text{H}_5)(\text{OOC}_4\text{H}_9)$.

Atom	U_{11}	U_{22}	U_{33}	U_{12}	U_{13}	U_{23}
Hf	122(3)	163(3)	42(3)	-6(4)	12(2)	-9(4)
C11	201(79)	355(115)	22(68)	-52(74)	24(62)	-57(70)
C12	131(69)	256(92)	76(65)	-12(80)	19(58)	-35(75)
C13	12(63)	317(90)	91(67)	-26(77)	-25(56)	2(78)
C14	283(85)	90(82)	68(73)	-167(75)	-168(67)	21(64)
C15	184(81)	461(121)	64(74)	-75(81)	35(68)	-32(72)
C11M	346(85)	300(97)	227(84)	-31(78)	38(72)	-248(77)
C12M	410(90)	259(93)	306(89)	-118(78)	134(77)	-98(79)
C13M	317(87)	405(103)	285(85)	-131(76)	66(74)	-154(77)
C14M	440(101)	552(127)	294(95)	-291(90)	33(83)	-38(90)
C15M	411(87)	883(134)	70(71)	-208(99)	115(70)	-208(90)
C21	451(94)	163(95)	45(70)	-112(76)	174(74)	-91(66)
C22	165(77)	312(98)	22(65)	-86(72)	45(62)	-72(70)
C23	99(78)	274(95)	109(74)	-28(70)	-19(64)	-59(70)
C24	206(80)	161(86)	71(71)	68(72)	-1(65)	25(68)
C25	272(85)	193(86)	188(82)	-139(78)	137(74)	-200(75)
C21M	382(83)	273(103)	232(78)	-68(74)	154(70)	25(75)
C22M	348(87)	438(106)	315(85)	-83(76)	214(74)	-166(76)
C23M	231(78)	261(93)	263(81)	-1(68)	60(69)	-139(71)
C24M	339(78)	195(89)	215(76)	-10(76)	104(66)	-9(76)
C25M	288(85)	433(99)	88(73)	-1(73)	-8(68)	43(71)
O1	181(47)	348(60)	75(47)	-47(44)	-2(41)	-12(45)
O2	189(50)	314(60)	99(49)	-121(47)	18(45)	18(47)
C31	256(81)	206(86)	197(79)	61(70)	130(73)	73(70)
C32	227(75)	483(107)	277(82)	-98(81)	7(69)	-43(87)
C33	355(81)	304(97)	289(81)	-50(79)	143(71)	19(80)
C34	324(84)	372(96)	311(85)	74(77)	196(74)	75(79)
C41	274(78)	286(94)	106(71)	-97(66)	87(66)	-86(65)
C42	211(81)	288(95)	242(83)	133(68)	38(72)	1(71)

Table X3. Hydrogen Atom Coordinates ($\times 10^4$) and B's for $\text{Cp}_2\text{Hf}(\text{C}_2\text{H}_5)(\text{OOC}_4\text{H}_9)$.

Atom	<i>x</i>	<i>y</i>	<i>z</i>	<i>B</i>
H111	2008	-3359	1761	3.0
H112	2591	-2597	1443	3.0
H113	1650	-3094	636	3.0
H121	111	-2340	1037	3.0
H122	590	-1752	2146	3.0
H123	1027	-3047	1896	3.0
H131	99	2367	1178	3.0
H132	-62	877	1489	3.0
H133	-383	1195	413	3.0
H141	1596	3231	445	3.0
H142	1547	3788	1277	3.0
H143	716	3385	259	3.0
H151	2179	1187	207	3.0
H152	2530	-510	520	3.0
H153	2977	927	1236	3.0
H211	2312	-1830	4409	3.0
H212	2711	-940	5371	3.0
H213	3268	-1449	5002	3.0
H221	1021	-771	3503	3.0
H222	477	461	2810	3.0
H223	842	567	3913	3.0
H231	1184	4259	2460	3.0
H232	1137	4445	3331	3.0
H233	555	3214	2509	3.0
H241	2958	4502	3276	3.0
H242	3533	4569	4449	3.0
H243	2599	5237	3868	3.0
H251	4177	489	5376	3.0
H252	4224	2238	5635	3.0
H253	4302	1699	4798	3.0
H321	5474	4194	3920	3.0
H322	5208	3313	4498	3.0
H323	4842	5007	4063	3.0
H331	3489	5159	2581	3.0
H332	3360	4018	1696	3.0
H333	4139	5190	2220	3.0
H341	4997	1397	3173	3.0
H342	4946	2622	2468	3.0
H343	4172	1501	2153	3.0
H411	2841	-2293	3077	3.0
H412	3468	-1338	4032	3.0
H421	4081	-2528	3275	3.0
H422	4285	-636	3538	3.0
H423	3584	-1124	2464	3.0

Table X4. Bond lengths and angles and least-squares planes.

Atom	Atom	Dist.(Å)	Atom	Atom	Atom	Angle(°)
Hf	C11	2.568(14)	Hf	O1	O2	119.6(6)
Hf	C12	2.556(13)	R1	Hf	R2	135.0
Hf	C13	2.572(13)	O1	O2	C31	108.7(8)
Hf	C14	2.551(14)	O2	C31	C32	101.5(10)
Hf	C15	2.561(14)	O2	C31	C33	110.8(11)
Hf	C21	2.568(13)	O2	C31	C34	112.4(11)
Hf	C22	2.556(13)	Hf	C41	C42	115.1(9)
Hf	C23	2.528(13)	C11	C12	C13	108.7(12)
Hf	C24	2.555(13)	C12	C13	C14	106.6(11)
Hf	C25	2.552(14)	C13	C14	C15	106.3(12)
Hf	R1	2.218	C14	C15	C11	107.8(12)
Hf	R2	2.247	C15	C11	C12	110.6(12)
Hf	O1	1.970(8)	C21	C22	C23	107.6(11)
O1	O2	1.490(12)	C22	C23	C24	108.5(11)
O2	C31	1.437(16)	C23	C24	C25	107.3(12)
C31	C32	1.541(20)	C24	C25	C21	109.5(12)
C31	C33	1.522(20)	C25	C21	C22	107.1(12)
C31	C34	1.503(20)	C11M	C11	C15	124.9(13)
Hf	C41	2.280(13)	C11M	C11	C12	123.4(12)
C41	C42	1.518(19)	C12M	C12	C11	124.0(12)
C11	C12	1.407(19)	C12M	C12	C13	126.4(12)
C12	C13	1.429(19)	C13M	C13	C12	125.7(12)
C13	C14	1.463(19)	C13M	C13	C14	125.3(12)
C14	C15	1.473(20)	C14M	C14	C13	125.7(13)
C15	C11	1.372(20)	C14M	C14	C15	128.0(13)
C21	C22	1.416(19)	C15M	C15	C14	121.5(13)
C22	C23	1.426(19)	C15M	C15	C11	130.2(13)
C23	C24	1.436(19)	C21M	C21	C25	127.7(12)
C24	C25	1.385(19)	C21M	C21	C22	124.8(12)
C25	C21	1.444(19)	C22M	C22	C21	122.8(12)
C11	C11M	1.512(20)	C22M	C22	C23	128.5(12)
C12	C12M	1.510(20)	C23M	C23	C22	127.3(12)
C13	C13M	1.482(19)	C23M	C23	C24	122.5(12)
C14	C14M	1.456(21)	C24M	C24	C23	123.9(12)
C15	C15M	1.480(21)	C24M	C24	C25	128.4(12)
C21	C21M	1.508(19)	C25M	C25	C24	126.9(12)
C22	C22M	1.486(19)	C25M	C25	C21	123.4(12)
C23	C23M	1.498(19)				
C24	C24M	1.479(19)				
C25	C25M	1.549(20)				

Torsion Angles.

Atom	Atom	Atom	Atom	Torsion(°)
C42	C41	Hf	O1	-17.6(10)
C41	Hf	O1	O2	-70.9(7)
Hf	O1	O2	C31	176.1(7)
O1	O2	C31	C32	171.9(9)
O1	O2	C31	C33	56.1(12)
O1	O2	C31	C34	-70.1(12)

Deviations from Ring Least-squares planes*.

Atom	Dist.(Å)	Atom	Dist.(Å)
C11*	-.007	C21*	0.001
C12*	0.010	C22*	0.003
C13*	-.009	C23*	-.006
C14*	0.005	C24*	0.007
C15*	0.001	C25*	-.005
Hf	2.255	Hf	-2.247
C11M	-.287	C21M	0.144
C12M	-.182	C22M	0.259
C13M	-.388	C23M	0.280
C14M	-.029	C24M	0.175
C15M	-.151	C25M	0.078

*Atoms defining plane indicated by asterisk; unit weights used.

- 1) Moore, E.J.; Sullivan, J.M.; Norton, J.R. *J. Am. Chem. Soc.* 1986, 108, 2257.
- 2) Hillhouse, G.L.; Bercaw, J.E. *J. Am. Chem. Soc.* 1984, 106, 5472.
- 3) a) Manriquez, J.M.; McAlister, D.R.; Sanner, R.D.; Bercaw, J.E. *J. Am. Chem. Soc.* 1976, 98, 6733. b) Roddick, D.M.; Fryzuk, M.D.; Seidler, P.F.; Hillhouse, G.L.; Bercaw, J.E. *Organometallics* 1985, 4, 97, 1694. (c) Cp*₂Hf(CH₃)H is prepared cleanly by heating Cp*₂HfH₂ and (CH₃)₃PCH₂ at 80 °C for 1.5 hours in toluene. Eric J. Moore, Thesis, Caltech, 1984. (d) Cp*(η⁵,η¹-C₅(CH₃)₄CH₂CH₂CH₂)HfH is prepared by heating Cp*(η⁵-C₅(CH₃)₄CH₂CH₂CH₃)HfH₂ at 80 °C for 2 days. (A. Ray Bulls, unpublished results).
- 4) Sharpless, K.B.; Woodard, S.S.; Finn, M.G. *Pure Appl. Chem.* 1983, 55, 1823.
- 5) Roddick, D.M. Ph.D Thesis, California Institute of Technology, 1984.
- 6) Fronczek, F.R.; Baker, E.C.; Sharp, P.R.; Raymond, K.N.; Alt, H.G.; Rausch, M.D. *Inorg. Chem.* 1976, 15, 2284.
- 7) For information on the orbitals of bent metallocenes see Lauher, J.W.; Hoffmann, R. *J. Am. Chem. Soc.* 1976, 98, 1729.
- 8) a) Silverton, J.V.; Hoard, J.L. *Inorg. Chem.* 1963, 2, 243. b) Zr vs. Hf radii. Pauling, L. "The Nature of the Chemical Bond" Third Edition, Cornell University Press p.256, 1960.
- 9) Strukul, G.; Michelin, R.A.; Orbell, J.D.; Randaccio, L. *Inorg. Chem.* 1983, 22, 3706. b) Giannotti, C.; Fontaine, C.; Chiaroni, A.; Riche, C. *J. Organomet. Chem.* 1976, 113, 57. c) Mimoun, H.; Charpentier, R.; Mitschler, A.; Fischer, J.; Weiss, R. *J. Am. Chem. Soc.* 1980, 102, 1047. d) Mimoun, H.; Chaumette, P.; Mignard, M.; Saussine, L.; Fischer, J.; Weiss, R. *Nouv. J. Chim.* 1983, 7, 467.
- 10) Baldwin, A.C. in "The Chemistry of Functional Groups, Peroxides" (S. Patai, ed.) John Wiley & Sons Ltd, p. 97, 1983.
- 11) Bulls, A.R.; Bercaw, J.E. unpublished results.

- 12) Halpern, J. *Inorg. Chim. Acta* 1985, 100, 41.
- 13) Marvich, R.H.; Brintzinger, H.H. *J. Am. Chem. Soc.* 1971, 98, 2046.
- 14) Brown, T.L.; Dickerhof, D.W.; Bafus, D.A.; Morgan, G.L. *Rev. Sci. Instrum.* 1962, 33, 491.
- 15) Sharpless, K.B.; Verhoeven, T.R. *Aldrichimica Acta* 1979, 12, 63.
- 16) Clark, E.P. *Ind. Eng. Chem., Anal. Ed.* 1941, 13, 820.

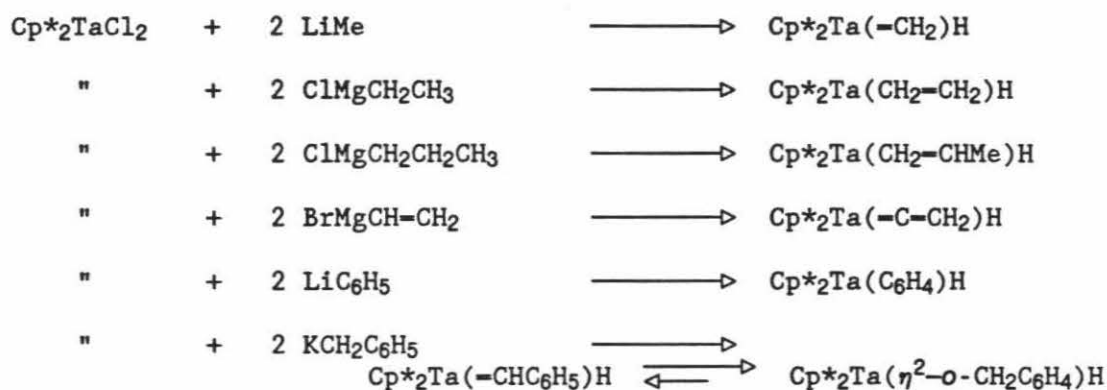
CHAPTER 3

Oxygen Derivatives of Permethyltantalocene

Abstract: $\text{Cp}^*_2\text{Ta}(\text{CH}_2)\text{H}$, $\text{Cp}^*_2\text{Ta}(\text{CHC}_6\text{H}_5)\text{H}$, $\text{Cp}^*_2\text{Ta}(\text{C}_6\text{H}_4)\text{H}$, $\text{Cp}^*_2\text{Ta}(\text{CH}_2=\text{CH}_2)\text{H}$ and $\text{Cp}^*_2\text{Ta}(\text{CH}_2=\text{CHMe})\text{H}$ react, presumably through $\text{Cp}^*_2\text{Ta-R}$ intermediates, with H_2O to give $\text{Cp}^*_2\text{Ta}(\text{O})\text{H}$ and alkane. $\text{Cp}^*_2\text{Ta}(\text{O})\text{H}$ was structurally characterized: space group $\text{P}2_1/\text{n}$, $a = 13.073(3)\text{\AA}$, $b = 19.337(4)\text{\AA}$, $c = 16.002(3)\text{\AA}$, $\beta = 108.66(2)^\circ$, $V = 3832(1)\text{\AA}^3$, $Z = 8$ and $R_F = 0.0672$ (6730 reflections). Reaction of *tert*-butylhydroperoxide with these same starting materials ultimately yields $\text{Cp}^*_2\text{Ta}(\text{O})\text{R}$ and HOCMe_3 . $\text{Cp}^*_2\text{Ta}(\text{CH}_2=\text{CHR})\text{OH}$ species are proposed as intermediates in the olefin hydride reactions. $\text{Cp}^*_2\text{Ta}(\text{O}_2)\text{R}$ species can be generated from the reaction of the same starting materials and O_2 . Lewis acids have been shown to promote oxygen insertion in these complexes.

Introduction

Gibson's reagent, $\text{Cp}^*_2\text{TaCl}_2$, reacts cleanly with two equivalents of alkyl lithium, potassium and Grignard reagents (M-R) to afford olefin hydride and alkylidene hydride complexes.¹ The tentative mechanism for the formation of these species involves initial generation of $\text{Cp}^*_2\text{Ta(III)-R}$, which rearranges by α or β -H elimination to give product. $\text{Cp}^*_2\text{TaH}_3$ is easily prepared from the reaction of $\text{Cp}^*_2\text{TaCl}_2$ and excess LiAlH_4 .^{1a}



Key to much of the reactivity of these complexes is the presence of the Ta(III) alkyl species ($\text{Cp}^*_2\text{Ta-R}$), which in solution is in equilibrium with the ground state structures. These equilibria have been probed by magnetization transfer and chemical trapping studies.²

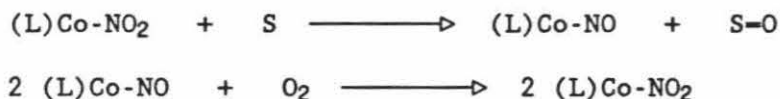


The reactions of $\text{Cp}^*_2\text{TaCl}_2$, $\text{Cp}^*_2\text{TaH}_3$ and the olefin and alkylidene hydride complexes with H_2O , HOOCMe_3 and O_2 are the subject of this chapter. We have isolated and/or observed tantalum oxo hydride, oxo chloride, oxo alkyl, peroxy chloride, peroxy alkyl, and

oxo alkoxide complexes. Preliminary results on the reactions of several of these complexes with Lewis acids will also be discussed.

Lewis acids have proven useful or essential for a number of transition metal centered transformations, e.g., olefin polymerization,³ olefin metathesis,⁴ and insertion of CO into metal alkyl bonds.⁵ Lewis acids have been shown to bind to coordinated olefin, carbonyl, halide and hydride ligands as well as to the metal center directly. Recent research on surface catalyzed oxidations suggests that Lewis acid sites next to surface oxo sites may play a key role in the activation of substrate molecules.⁶

Lewis acid interactions with transition metal based oxidation systems have been surprisingly little explored. The best examples come from the studies of (L)Co-NO₂ (L = tetradentate ligand).⁷

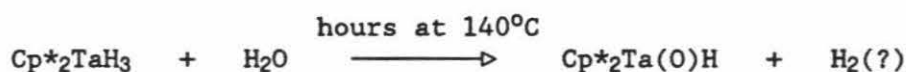
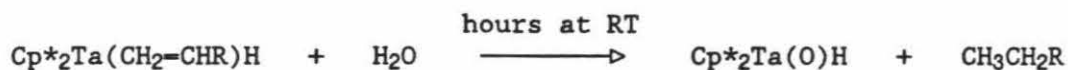
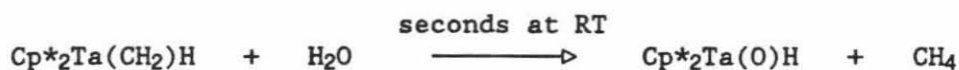


Lewis acids Li⁺ and BF₃·OEt₂ significantly increase the oxidizing ability of Co-NO₂ complexes. In the absence of Lewis acids (L)Co-NO₂ plus O₂ will catalyze only the oxidation of phosphines to phosphine oxides and isonitriles to isocyanates, presumably reactions driven by the formation of strong P=O and RNC=O bonds.^{7b} By the addition of Lewis acids, alcohols, organic sulfides, and cyclohexadiene can be catalytically oxidized. By selecting metal complexes, Pd^{7c} and Ti^{7d}, which serve as Lewis acids in the sense that they coordinate olefins, one can extend the reactivity of this system to produce ketones or epoxides. The Co-NO₂ oxidations are illustrative of at least two roles Lewis acids can play in oxidation reactions. In the first case, Lewis acids BF₃·OEt₂ and Li⁺ apparently activate the cobalt complex by complexation to the NO₂ ligand, increasing its susceptibility to nucleophilic attack by the added reagents (alcohol, sulfides,

cyclohexadiene). Alternatively, Lewis acids activate olefins, by coordination, towards nucleophilic attack by the NO₂ ligand.

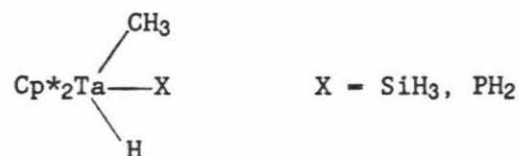
Results and Discussion

Reactions with Water: The olefin and alkylidene hydride complexes react cleanly with H₂O at room temperature to yield Cp*₂Ta(O)H and alkane. Cp*₂TaH₃ reacts with water slowly at 140°C to also yield Cp*₂Ta(O)H.⁸

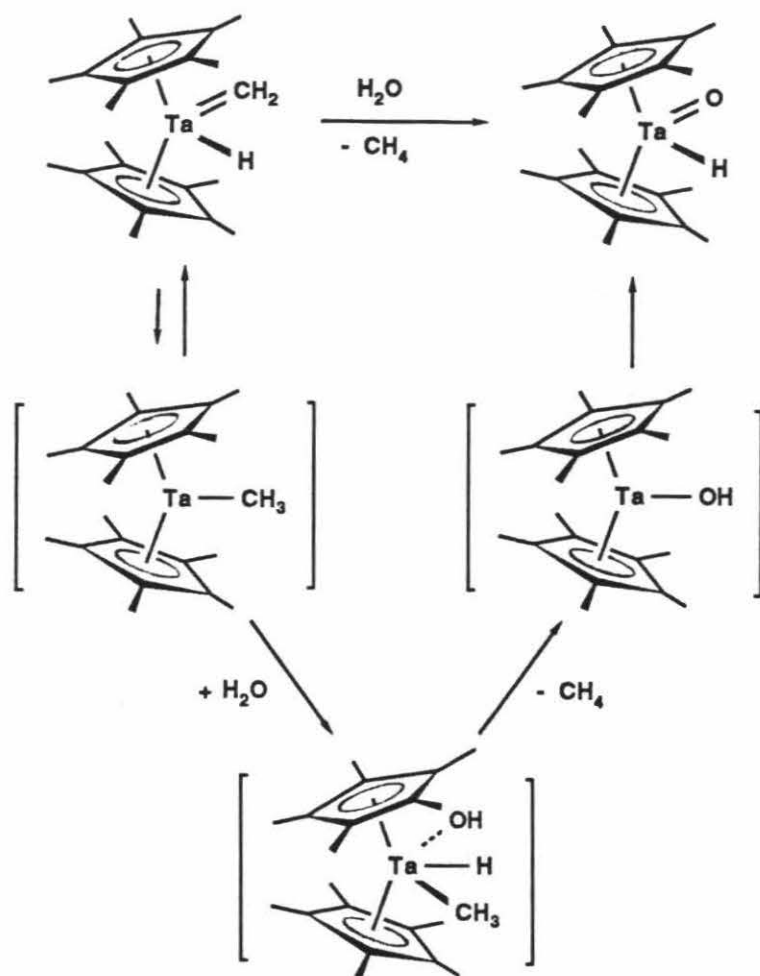


Cp*₂Ta(O)H is the first reported example of a transition metal oxo hydride complex with a terminal oxo ligand. Examples with bridging oxo ligands have been reported.⁹ In the ¹H nmr spectrum, the hydride resonance is found relatively far downfield at 7.43 ppm. The Ta-H stretch in the infrared spectrum comes at 1808 cm⁻¹ and upon deuteration moves to 1295 cm⁻¹. The Ta=¹⁶O stretch is observed at 850 cm⁻¹ and moves to 807 cm⁻¹ with ¹⁸O.

The relative rates of reaction with H₂O correspond, at least qualitatively, with the relative rates of Ta(III) alkyl formation. A possible mechanism is suggested by the reactions of SiH₄ and PH₃ with Cp*₂Ta(CH₂)H to give Cp*₂Ta(CH₃)(SiH₃)H and Cp*₂Ta(CH₃)(PH₂)H. SiH₄ and PH₃ apparently add to the metal center in a manner which precludes reductive elimination of methane.

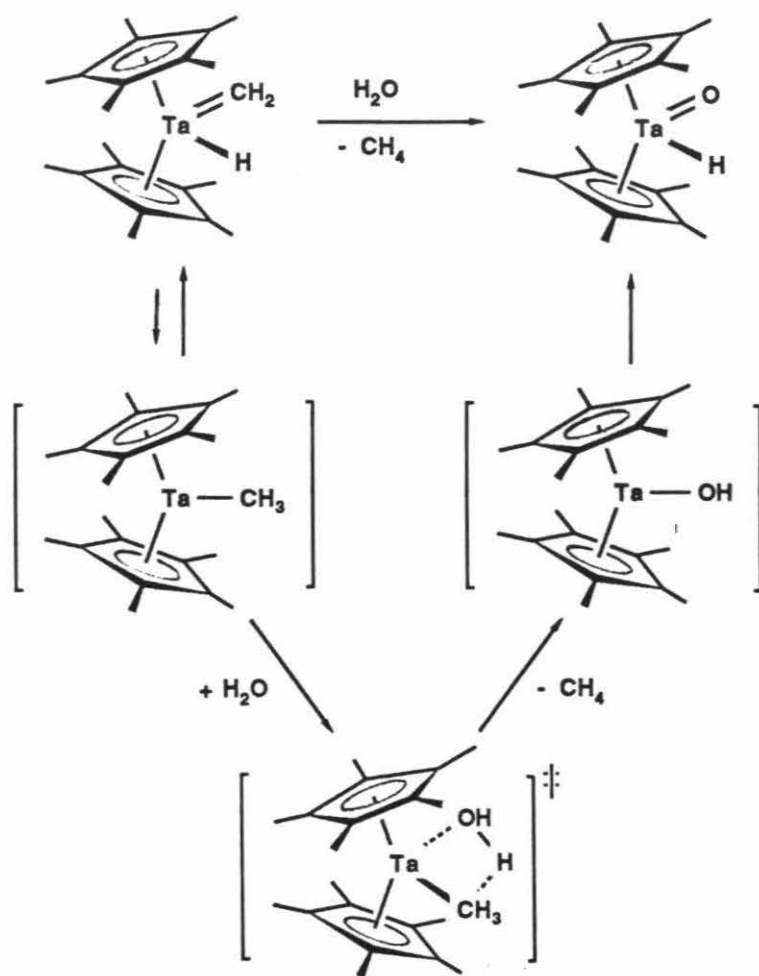


In this mechanism (Scheme I) $\text{Cp}^*_2\text{Ta(III)-R}$ is trapped by H_2O followed by oxidative addition of an O-H bond. Reductive elimination of methane leaves $\text{Cp}^*_2\text{Ta(OH)}$, which proceeds by $\alpha\text{-H}$ elimination to give $\text{Cp}^*_2\text{Ta(O)H}$.



Scheme I

Another possibility is that rather than adding the OH bond, the H_2O protonates the Ta-R bond directly, to again give $\text{Cp}^*_2\text{Ta(OH)}$ and finally product (Scheme II). This mechanism is consistent with one never observing a complex similar to $\text{Cp}^*_2\text{Ta}(\text{CH}_3)(\text{X})\text{H}$ when the OH bond adds in such a way as to preclude reductive elimination of methane.



Scheme II

Consistent with both of these mechanisms, the addition of D₂O to Cp*₂Ta(CH₂)H gives CH₃D and Cp*₂Ta(O)D. Attempts to generate Cp*₂Ta(OH) from Cp*₂Ta(O)H have proven unsuccessful. Upon heating at 110°C under CO for several hours one observes slow loss of Cp*H and starting material. The metal containing products of this reaction have not been identified. No reactions were observed with Me₃P=CH₂ and Me₃P=O.

It is interesting to note that the reaction of Cp*₂Ta(=CH₂)CH₃ with H₂O leads to immediate (seconds) decomposition with loss of Cp*H. This decomposition is not well understood.

Crystallographic Results: From an attempt to grow crystals of $\text{Cp}^*_2\text{Ta}(\text{CHC}_6\text{H}_5)\text{H}$ in petroleum ether, a crystal of $\text{Cp}^*_2\text{Ta}(\text{O})\text{H}$ (present as an impurity from the reaction of H_2O with $\text{Cp}^*_2\text{Ta}(\text{CHC}_6\text{H}_5)\text{H}$) was isolated by LeRoy Whinnery. Nhi Hua and Richard E. Marsh determined the structure by x-ray diffraction methods.¹⁰ The unit cell contains two distinct forms of the molecule. Figure 1 shows the orientations of the two forms of the molecule. Figure 2 shows the pseudotetrahedral orientation of the ligands about Ta(1) and Figure 3 the unit cell. The primary structural difference between the two forms is found in the H-Ta-O angles: H1-Ta1-O1, $71.1(4)^\circ$; H2-Ta2-O2, $75.5(3)^\circ$. The Ta1=O1 and Ta2=O2 bond lengths are the same, 1.76 Å. The tantalum Cp* carbon bonds average 2.486(9) Å and the ring C-C bonds average 1.411(12) Å, with the ring angles averaging $107.96(73)^\circ$. The C-CH₃ bonds of the two Cp* rings average 1.503(13) Å, with the C-C-CH₃ angles averaging $125.75(77)^\circ$. The Cp* centroid-Ta-centroid angles are R1-Ta1-R2, $137.9(2)^\circ$ and R3-Ta2-R4, $138.6(2)^\circ$.

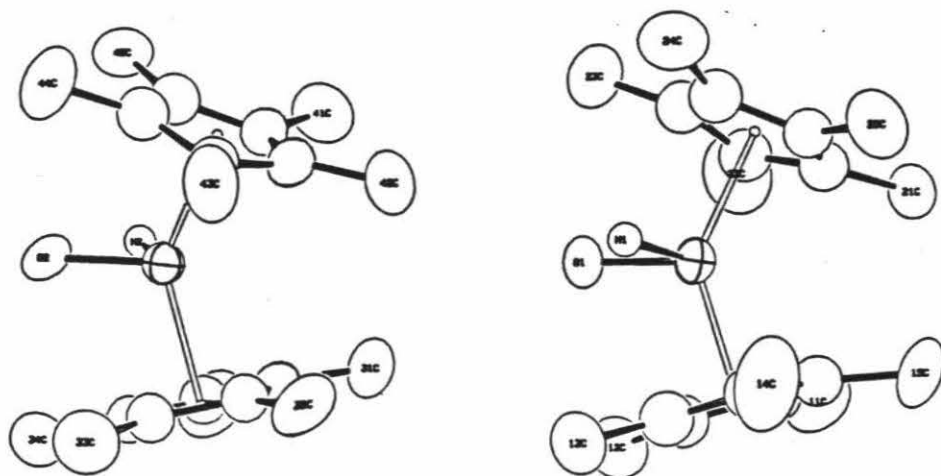


Figure 1. The two forms of $\text{Cp}^*_2\text{Ta}(\text{O})\text{H}$ and their relative orientations.

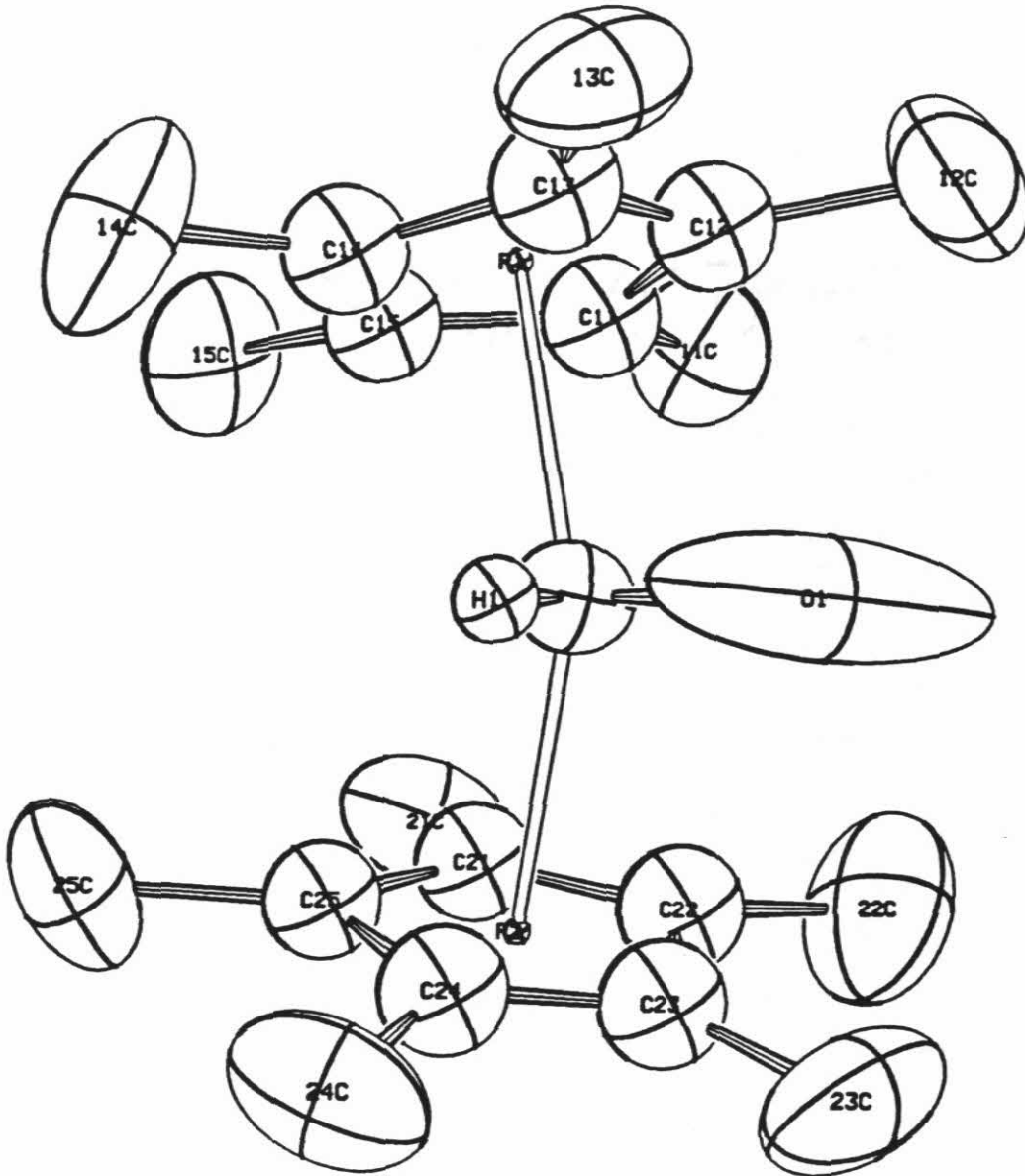


Figure 2. A view of Cp*₂Ta(O)H (Ta(1)).

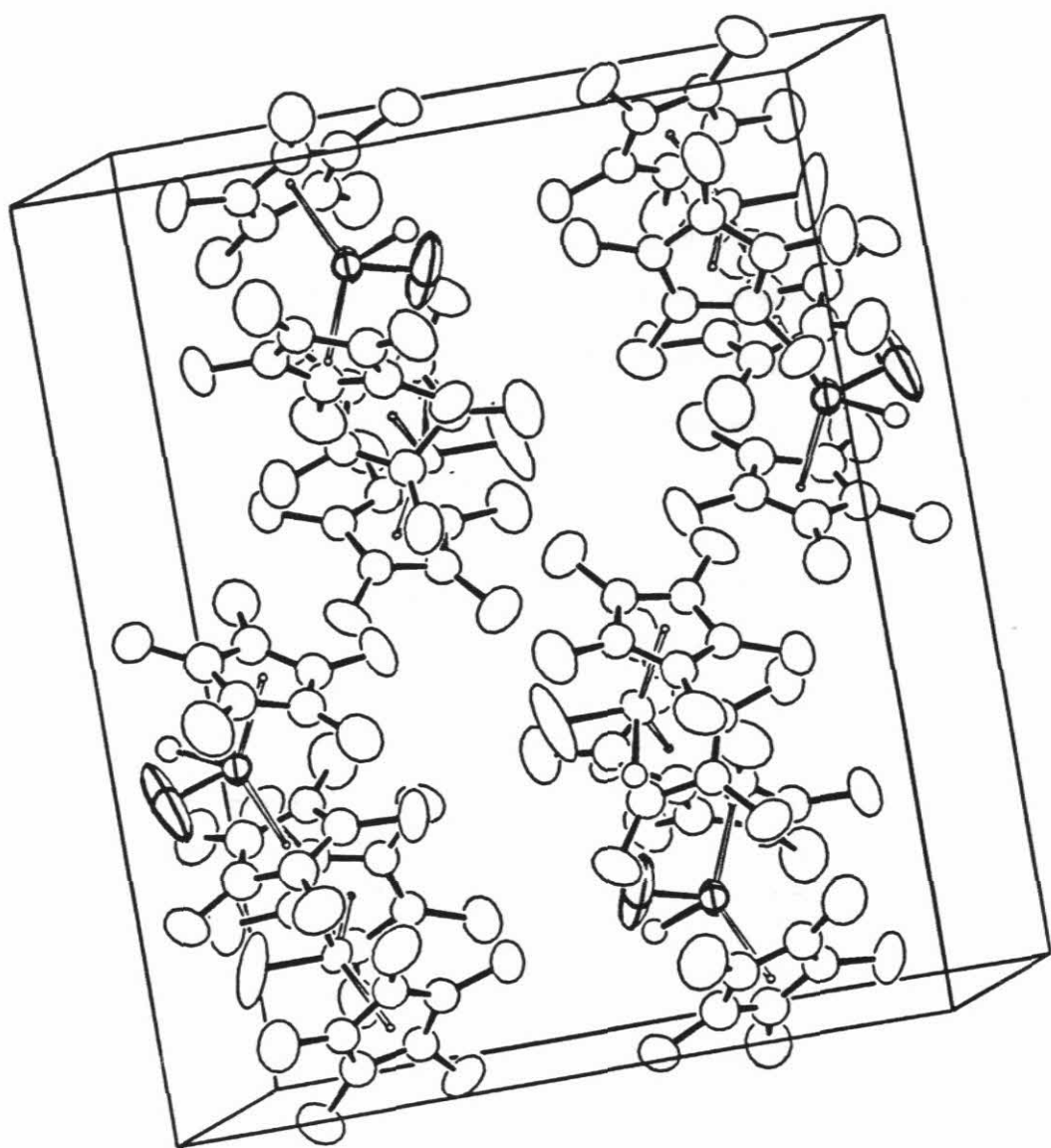
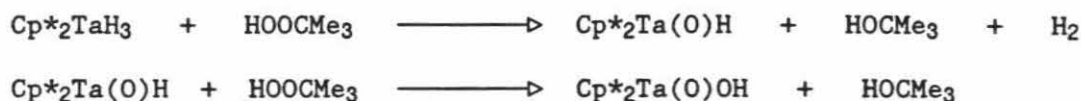


Figure 3. The unit cell of $\text{Cp}^*\text{Ta}(\text{O})\text{H}$

Oxo Alkyl Complexes: The reactions of *tert*-butylhydroperoxide (TBHP) with permethyltantalocene d^0 hydrides appear to be quite different from the reactions observed for permethylhafnocene hydrides (Chapter 2). Instead of metathesis to give H_2 and an alkylperoxide complex, *tert*-butylhydroperoxide serves ultimately as a source of the metal oxo functionality.

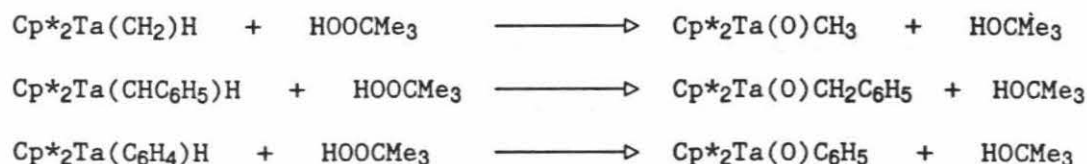
Accompanied by vigorous H_2 evolution, $Cp^*_2TaH_3$ reacts quickly (the reaction is over in seconds) with greater than one equivalent of TBHP to give $Cp^*_2Ta(O)H$. The addition of $HOOCMe_3$ to $Cp^*_2TaD_3$ gives only $Cp^*_2Ta(O)D$ (by nmr). $Cp^*_2Ta(O)H$ undergoes a second much slower (hours) reaction with TBHP to generate $Cp^*_2Ta(O)OH$. The Ta=O infrared stretch for $Cp^*_2Ta(O)OH$ is found at 845 cm^{-1} . The O-H region contains two resonances, a sharp, weak signal at 3660 cm^{-1} and a broad signal at 3380 cm^{-1} . Upon deuteration the broad signal moves to 1264 cm^{-1} .



$Cp^*_2Ta(\eta^2-OCH_2)H$ also reacts cleanly with TBHP, trapping $Cp^*_2Ta(OCH_3)$, to yield $Cp^*_2Ta(O)OCH_3$ and *t*-butanol.

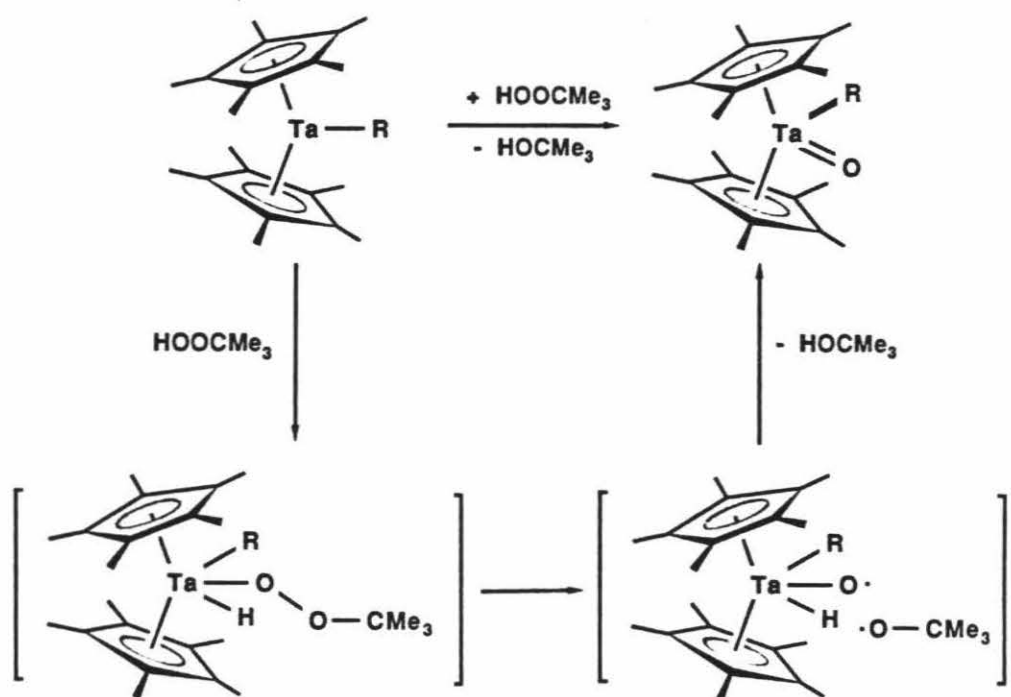


The addition of one equivalent of TBHP to solutions of $Cp^*_2Ta(CH_2)H$, $Cp^*_2Ta(CHC_6H_5)H$ or $Cp^*_2Ta(C_6H_4)H$ results in the immediate formation of the corresponding tantalum oxo alkyl complex.



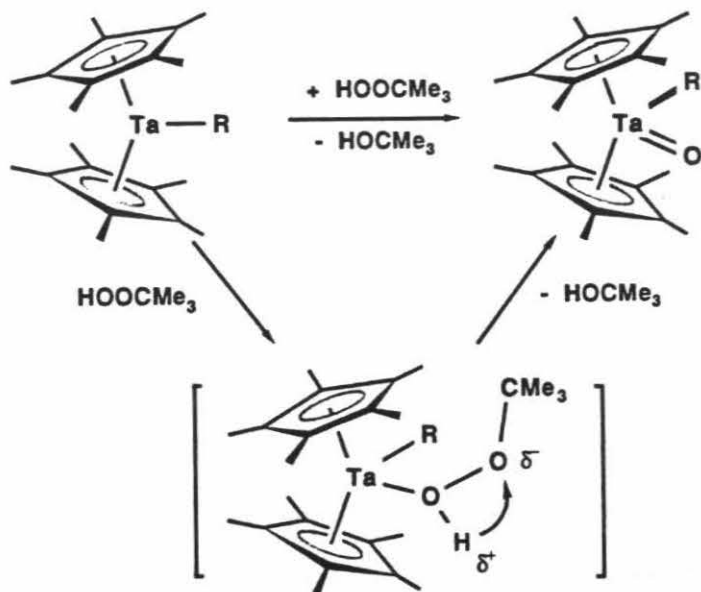
^1H nmr spectra are consistent with the above formulations, and the Ta=O infrared stretches are found in the region from 850 to 860 cm^{-1} . Heating these complexes at 80°C in the presence of TBHP has no further effect.

A reasonable mechanism for the formation of these species begins with the trapping of $\text{Cp}^*_2\text{Ta-R}$ with HOOCMe_3 (Scheme III). Oxidative addition of the OH bond would result in an alkylperoxide complex which must decompose to $\text{Cp}^*_2\text{Ta(O)(R)}$, possibly by O-O bond homolysis and radical abstraction of the tantalum hydride, before reductive elimination of alkane takes place.



Scheme III

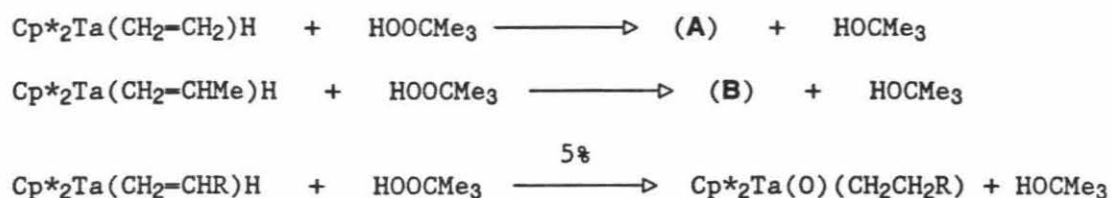
An alternative is to consider the trapping step a nucleophilic attack of the d^2 metal complex on the O-O bond of the peroxide with concerted transfer of H^+ to O-CMe_3 and oxo to metal (Scheme IV). This type of reaction has been invoked to explain the reactions of alkylperoxides with cytochrome P-450 model complexes.¹¹



Scheme IV

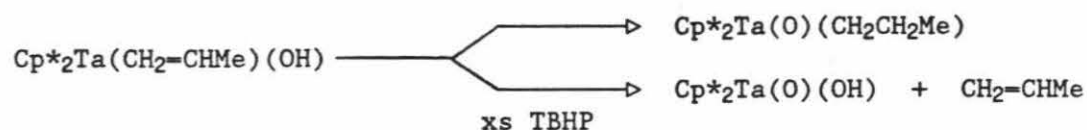
It was mentioned in the introductory chapter that $\text{Cp}^*_2\text{Ta}(\text{O})(\text{CH}_3)$ can also be obtained from the decomposition of $\text{Cp}^*_2\text{Ta}(\eta^2\text{-OCH}_2)\text{H}$.^{1b} Attempts to regenerate and trap the proposed intermediate $\text{Cp}^*_2\text{Ta}(\text{OCH}_3)$ from $\text{Cp}^*_2\text{Ta}(\text{O})(\text{CH}_3)$ have proven unsuccessful. One observes no reaction upon heating $\text{Cp}^*_2\text{Ta}(\text{O})(\text{CH}_3)$ with CNMe at 140°C for days. This is in contrast to $\text{Cp}^*_2\text{Ta}(\text{CH}_2)(\text{CH}_3)$ which rearranges cleanly upon heating to give $\text{Cp}^*_2\text{Ta}(\text{CH}_2=\text{CH}_2)\text{H}$, presumably through $\text{Cp}^*_2\text{TaCH}_2\text{CH}_3$.² Photolysis of $\text{Cp}^*_2\text{Ta}(\text{O})(\text{CH}_3)$ also does not regenerate $\text{Cp}^*_2\text{Ta}(\eta^2\text{-OCH}_2)\text{H}$. Light induced rearrangement has been observed in the conversion of $\text{Cp}^*_2\text{Ta}(\text{S})\text{CH}_3$ to $\text{Cp}^*_2\text{Ta}(\eta^2\text{-SCH}_2)\text{H}$.¹²

The reactions of TBHP with $\text{Cp}^*_2\text{Ta}(\text{CH}_2=\text{CH}_2)\text{H}$ and $\text{Cp}^*_2\text{Ta}(\text{CH}_2=\text{CHMe})\text{H}$ are more complicated than those of the complexes above. The addition of excess TBHP to the yellow olefin hydride complexes results, over a period of several minutes, in the formation of yellow-orange intermediates (A) and (B) which still contain olefin bound to the metal. One also observes the immediate formation of approximately 5% $\text{Cp}^*_2\text{Ta}(\text{O})(\text{R})$ (colorless), which may form through $\text{Cp}^*_2\text{Ta-R}$ by a pathway similar to that outlined above for $\text{Cp}^*_2\text{Ta}(\text{CH}_2)\text{H}$, $\text{Cp}^*_2\text{Ta}(\text{CHC}_6\text{H}_5)\text{H}$ and $\text{Cp}^*_2\text{Ta}(\text{C}_6\text{H}_4)\text{H}$.



Although as yet it has proven impossible to cleanly isolate (A) or (B), on the basis of subsequent reactivity, color, and nmr spectra, reasonable candidates for these species are (A) = $\text{Cp}^*_2\text{Ta}(\text{CH}_2=\text{CH}_2)(\text{OH})$ and (B) = $\text{Cp}^*_2\text{Ta}(\text{CH}_2=\text{CHMe})(\text{OH})$. (A) and (B) have been isolated as mixtures with $\text{Cp}^*_2\text{Ta}(\text{O})(\text{R})$ and TBHP. Even in the presence of excess TBHP, these complexes are stable for weeks if stored at low temperature in the solid state. The nmr spectra for these complexes show Cp^* resonances farther upfield than those observed for any of the other permethyltantalocene complexes. Compare 1.55 ppm for (A) with 1.79 ppm for $\text{Cp}^*_2\text{Ta}(\text{O})(\text{Et})$ and 1.70 for $\text{Cp}^*_2\text{Ta}(\text{CH}_2=\text{CH}_2)\text{H}$. Because of the coordinated propene, (B) has inequivalent Cp^* 's at 1.65 and 1.53 ppm. Figures 1 and 2 show representative ^1H nmr spectra for (A) and (B) and their decomposition products.

(A) and (B) both decompose by at least two pathways to give two products, $\text{Cp}^*_2\text{Ta}(\text{O})\text{R}$ and $\text{Cp}^*_2\text{Ta}(\text{O})(\text{H})$ and olefin. When the reactions were carried out in the presence of excess TBHP, $\text{Cp}^*_2\text{Ta}(\text{O})(\text{H})$ was converted to $\text{Cp}^*_2\text{Ta}(\text{O})(\text{OH})$.



Although the rate of decomposition of (A) varies depending on conditions, the product ratios are relatively constant: 80% $\text{Cp}^*_2\text{Ta}(\text{O})(\text{CH}_2\text{CH}_3)$ and 20% $\text{Cp}^*_2\text{Ta}(\text{O})(\text{OH})$. Polar solvents considerably increase the rate of decomposition and the percentage of $\text{Cp}^*_2\text{Ta}(\text{O})(\text{CH}_2\text{CH}_3)$.

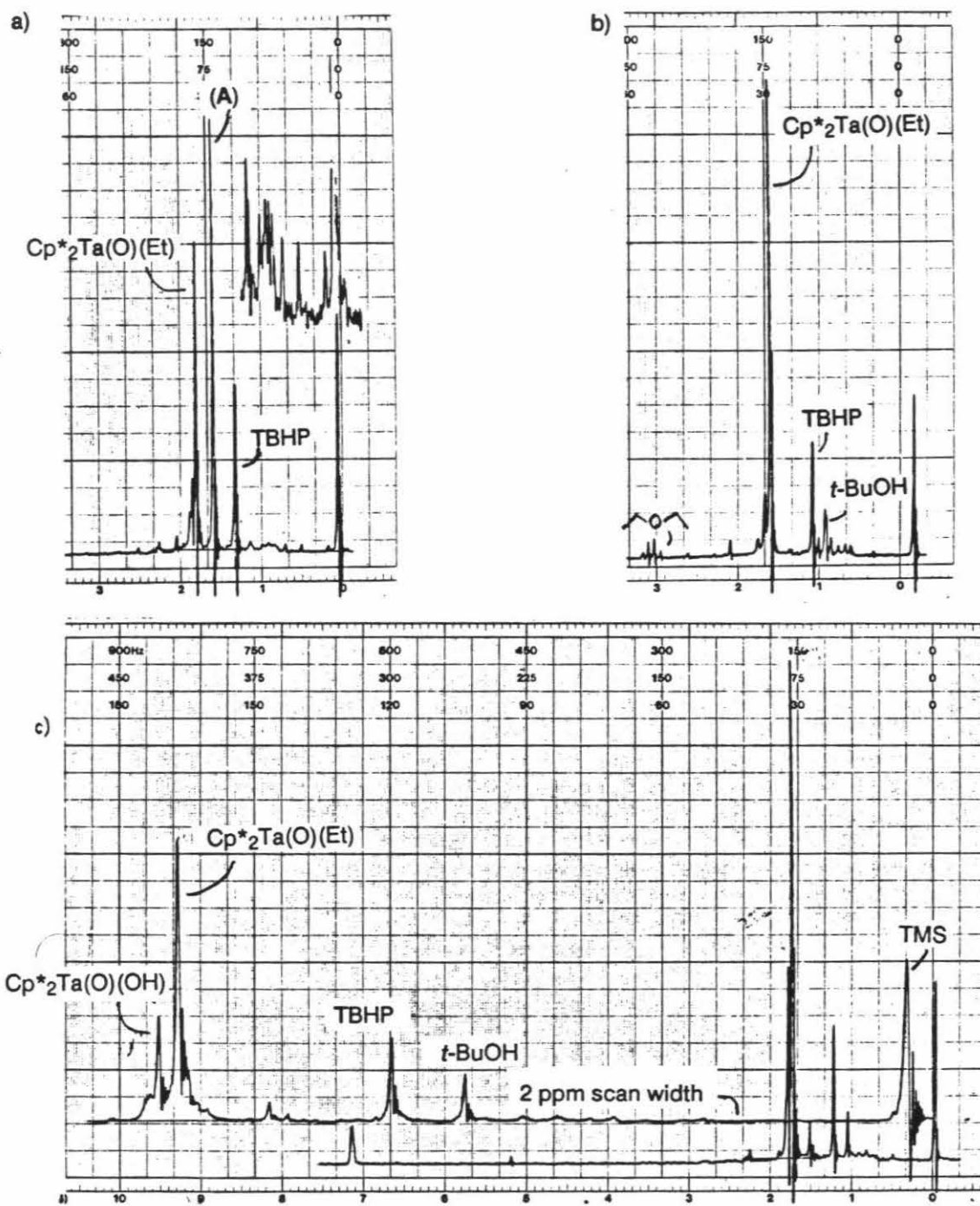


Figure 1. a) Isolated sample of (A), Cp*₂Ta(O)(Et), and TBHP. b) Decomposition products upon addition of 0.002 M EtMgCl in ether to (A). The decomposition is accelerated and yields almost entirely Cp*₂Ta(O)(Et). c) Decomposition of (A) without added Grignard. The products are Cp*₂Ta(O)(Et) and Cp*₂Ta(O)(OH). Expanded spectrum of the region from 0 to 2 ppm.

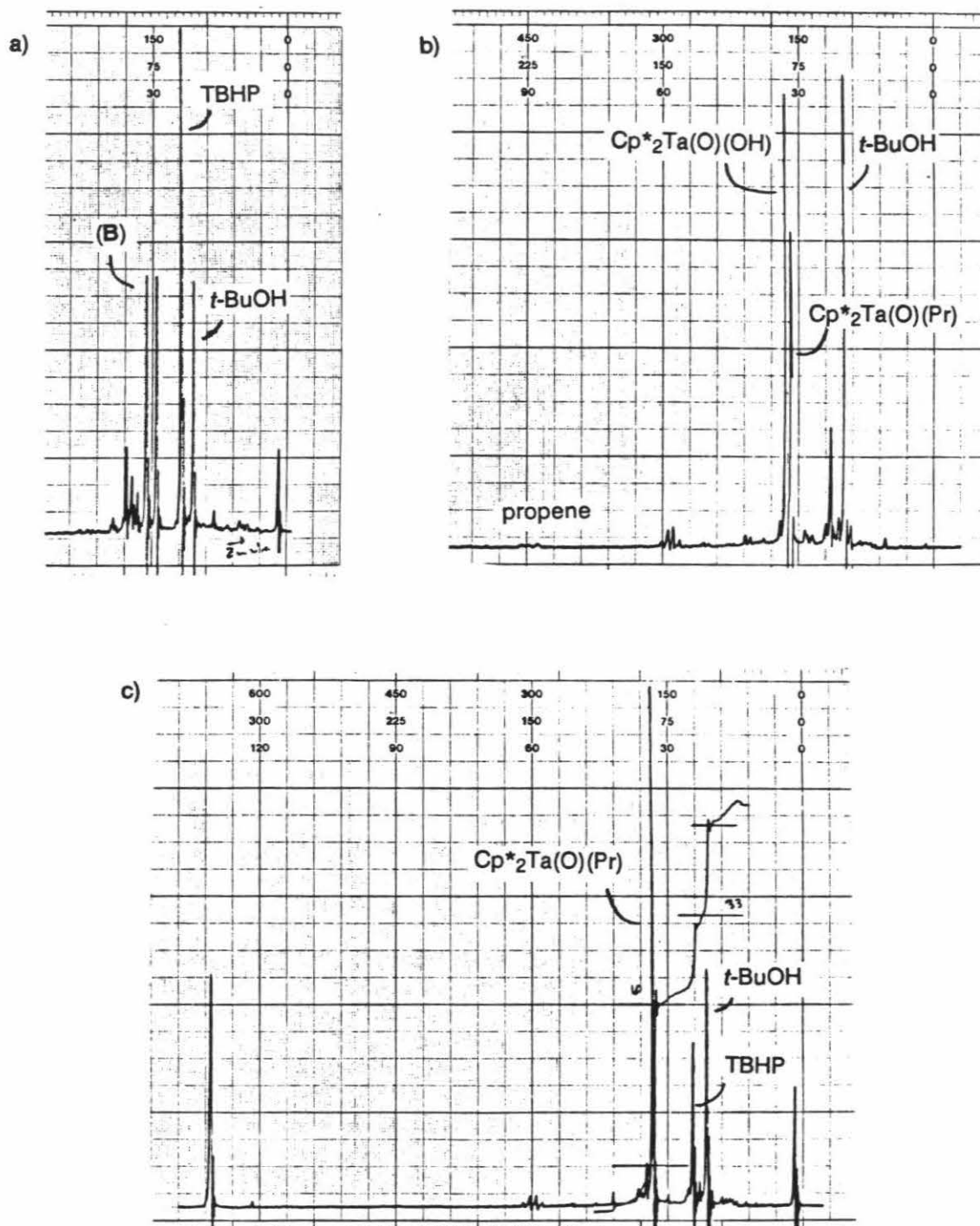


Figure 2. a) Spectrum of (B) generated *in situ* from $\text{Cp}^*_2\text{Ta}(\text{CH}_2=\text{CHMe})\text{H}$ and excess TBHP. b) Products from the decomposition of (B) without added Grignard, $\text{Cp}^*_2\text{Ta}(\text{O})(\text{OH})$, propene and $\text{Cp}^*_2\text{Ta}(\text{O})(\text{Pr})$. c) $\text{Cp}^*_2\text{Ta}(\text{O})(\text{Pr})$, from the decomposition of (B) in the presence of PrMgCl .

For (B), both the rate of decomposition and the product ratios are variable. In fact, different batches of $\text{Cp}^*_2\text{Ta}(\text{CH}_2=\text{CHMe})\text{H}$ (identical by nmr) gave different final product ratios, all after initially forming (B). The cleanest batches of starting material give greater amounts of $\text{Cp}^*_2\text{Ta}(\text{O})(\text{OH})$ and propene than $\text{Cp}^*_2\text{Ta}(\text{O})(\text{CH}_2\text{CH}_2\text{CH}_3)$. Decomposition of (B) under one atmosphere of propene did not change the product ratios.

After wading through numerous nmr experiments to sort out the above reactions, it became clear that the decompositions of (A) and (B) to $\text{Cp}^*_2\text{Ta}(\text{O})(\text{R})$ were probably catalyzed by impurities in the starting materials (*vide infra*).

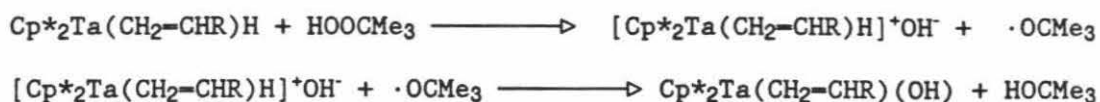
Approximate relative rates, $k(50^\circ\text{C})$, for $\text{Cp}^*_2\text{Ta}-\text{R}$ formation in the olefin hydride and alkylidene hydride complexes are listed below.

$\text{Cp}^*_2\text{Ta}(\text{CHC}_6\text{H}_5)\text{H}$	10^4	sec^{-1}
$\text{Cp}^*_2\text{Ta}(=\text{CH}_2)\text{H}$	10^2	sec^{-1}
$\text{Cp}^*_2\text{Ta}(\text{C}_6\text{H}_4)\text{H}$	10^1	sec^{-1}
$\text{Cp}^*_2\text{Ta}(\text{CH}_2=\text{CHMe})\text{H}$	10^0	sec^{-1}
$\text{Cp}^*_2\text{Ta}(\text{CH}_2=\text{CH}_2)\text{H}$	10^{-1}	sec^{-1}

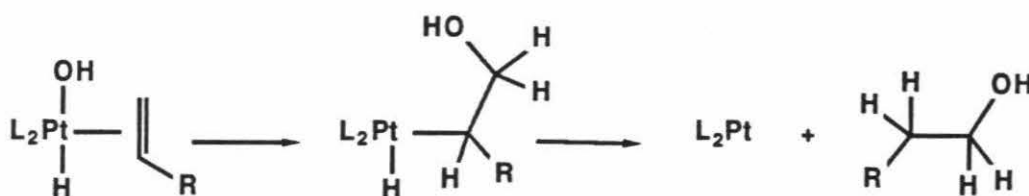
If the equilibrium concentrations of the tantalum(III) alkyl species follow the same trends, these rates offer a fairly straightforward explanation for the difference in reactivity between $\text{Cp}^*_2\text{Ta}(\text{CH}_2)\text{H}$, $\text{Cp}^*_2\text{Ta}(\text{CHC}_6\text{H}_5)\text{H}$, $\text{Cp}^*_2\text{Ta}(\text{C}_6\text{H}_4)\text{H}$ and $\text{Cp}^*_2\text{Ta}(\text{CH}_2=\text{CH}_2)\text{H}$, $\text{Cp}^*_2\text{Ta}(\text{CH}_2=\text{CHMe})\text{H}$. For the latter two complexes, the concentration of $\text{Cp}^*_2\text{Ta}-\text{R}$ is too low for trapping to be the predominant mechanism and a second reaction pathway takes over. Consistent with this, the reaction of $\text{Cp}^*_2\text{Ta}(\text{CH}_2=\text{CH}_2)\text{H}$ and $\text{Cp}^*_2\text{Ta}(\text{CH}_2=\text{CHMe})\text{H}$ with TBHP is much faster (minutes) than reaction with H_2O (hours). For the other complexes reactions with both H_2O and TBHP seem to be complete within a minute of addition.

Working on the assumption (A) and (B) are the species suggested above, a possible mechanism for their formation involves oxidation of $\text{Cp}^*_2\text{Ta}(\text{CH}_2=\text{CHR})\text{H}$ by TBHP to give

$[\text{Cp}^*_2\text{Ta}(\text{CH}_2=\text{CHR})\text{H}]^+\text{OH}^-$ and $\cdot\text{OCMe}_3$. The *t*-butoxy radical then abstracts the tantalum hydride hydrogen from $[\text{Cp}^*_2\text{Ta}(\text{CH}_2=\text{CHR})\text{H}]^+\text{OH}^-$ or escapes and generates other radicals by catalyzing the decomposition of TBHP.¹³ One always observes greater than one equivalent of TBHP consumed in these reactions.



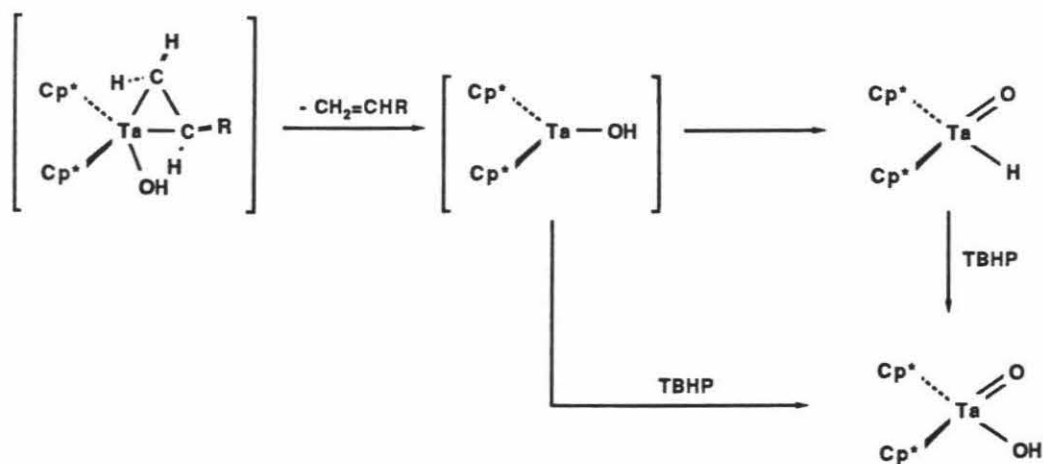
To the best of our knowledge, no examples of olefin hydroxide complexes have been reported, although they have been invoked as possible intermediates for Wacker-type oxidations¹⁴ and recently, by Trogler and Jensen for platinum catalyzed olefin hydrations.¹⁵ For these late transition metal examples, formation of the olefin hydroxide complex is followed by olefin insertion into the metal oxygen bond.



The decomposition of $\text{Cp}^*_2\text{Ta}(\text{CH}_2=\text{CHR})(\text{OH})$ to $\text{Cp}^*_2\text{Ta}(\text{O})(\text{CH}_2\text{CH}_2\text{R})$ is an unprecedented rearrangement. On the basis of the limited experimental evidence one can only speculate as to mechanism.

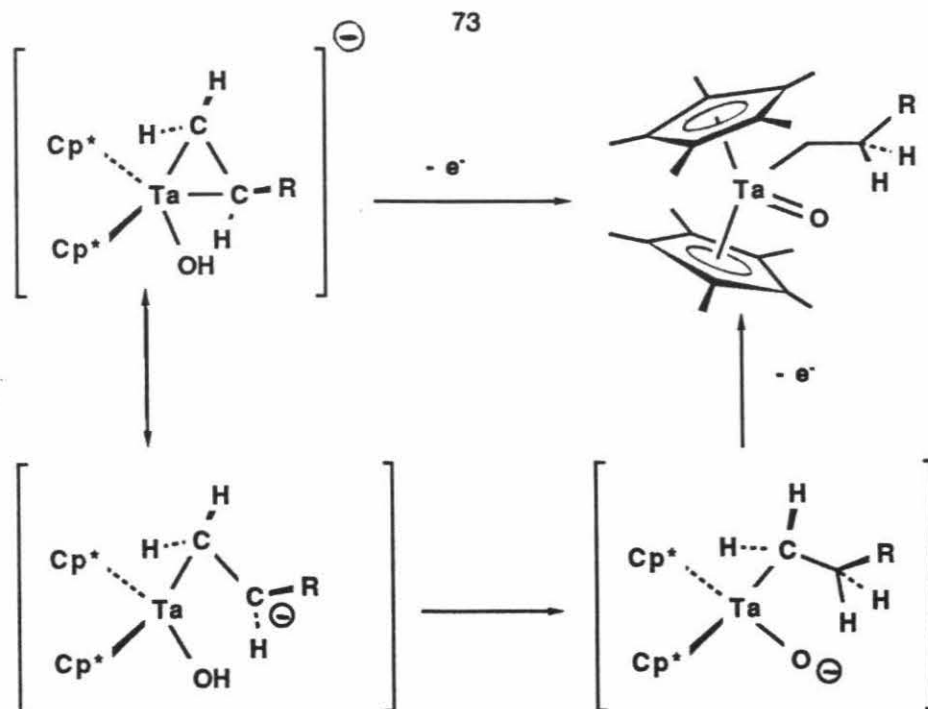
$\text{Cp}^*_2\text{Ta}(\text{CH}_2=\text{CHR})(\text{OH})$ decomposition can be explained by invoking two mechanistic pathways. The first pathway involves loss of olefin to leave $\text{Cp}^*_2\text{Ta}(\text{OH})$ (Scheme V). $\text{Cp}^*_2\text{Ta}(\text{OH})$ converts rapidly to $\text{Cp}^*_2\text{Ta}(\text{O})\text{H}$ or is trapped by *t*-butylhydroperoxide to give $\text{Cp}^*_2\text{Ta}(\text{O})(\text{OH})$. Consistent with this being a sterically driven process, the propene derivative loses olefin much more readily than the ethylene complex. The rate of olefin loss from $\text{Cp}^*_2\text{Ta}(\text{CH}_2=\text{CHR})(\text{OH})$ seems to be constant under different reaction

conditions. The percentage of final product derived from this pathway is therefore dependent on the rearrangement rate of $\text{Cp}^*_2\text{Ta}(\text{CH}_2=\text{CHR})(\text{OH})$ to $\text{Cp}^*_2\text{Ta}(\text{O})(\text{CH}_2\text{CH}_2\text{R})$, which can vary considerably.



Scheme V

The variable nature of the second decomposition pathway, $\text{Cp}^*_2\text{Ta}(\text{CH}_2=\text{CHR})(\text{OH})$ to $\text{Cp}^*_2\text{Ta}(\text{O})(\text{CH}_2\text{CH}_2\text{R})$, is difficult to explain. One possibility is that impurity left in the starting material (XMgR) initiates the transformation by electron transfer to $\text{Cp}^*_2\text{Ta}(\text{CH}_2=\text{CHR})(\text{OH})$. $[\text{Cp}^*_2\text{Ta}(\text{II})(\text{CH}_2=\text{CHR})(\text{OH})]^-$ rearranges quickly to $[\text{Cp}^*_2\text{Ta}(\text{IV})(\text{O})(\text{CH}_2\text{CH}_2\text{R})]^-$ which then continues the process by transferring an electron to another molecule of $\text{Cp}^*_2\text{Ta}(\text{CH}_2=\text{CHR})(\text{OH})$. This leads to speculation as to why the tantalum (II) intermediate $[\text{Cp}^*_2\text{Ta}(\text{II})(\text{CH}_2=\text{CHR})(\text{OH})]^-$ would undergo this rearrangement. The driving force for this proposed rearrangement comes from localizing the negative charge on oxygen. A conceptualization of this process is shown below (Scheme VI): Initially the added electron is localized on the olefin/alkyl ligand. This carbanion pulls the proton off of $\text{Ta}-\text{OH}$ and leaves the negative charge on oxygen.

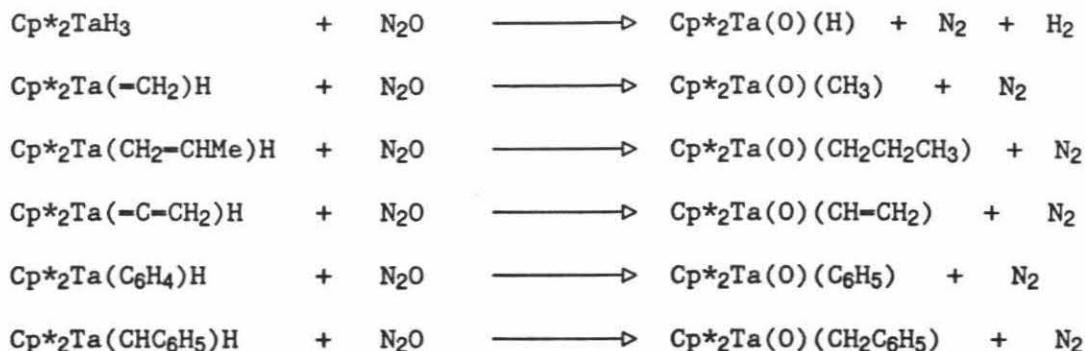


To test the above mechanism, several experiments were carried out. It was found that stirring the starting olefin complex with $\text{HO}(\text{CMe}_3)$ for several hours,¹⁶ to remove residual alkyl grignards, did not influence the rates of (A) and (B) formation, but did significantly slow the rates of decomposition. Conversely, addition of 0.002M of C1MgEt to 0.025 M of (A) resulted in much faster (approximately 30X)¹⁷ decomposition to $\text{Cp}^*_2\text{Ta}(\text{O})\text{CH}_2\text{CH}_3$. (B) not only decomposes more quickly with C1MgPr , the only product formed is $\text{Cp}^*_2\text{Ta}(\text{O})\text{CH}_2\text{CH}_2\text{CH}_3$. The addition of both potassium and potassium naphthalide increased the rate of decomposition of (A), but the reactions were less clean.

$\text{Cp}^*_2\text{Ta}(\text{C}=\text{CH}_2)\text{H}$ does not react cleanly with TBHP, although some $\text{Cp}^*_2\text{Ta}(\text{O})(\text{CH}=\text{CH}_2)$ is formed.

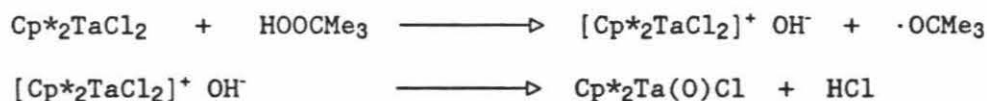
It is possible to generate oxo alkyl complexes using other reagents. Preliminary results with N_2O indicate this reagent can also be used to cleanly generate tantalum oxo alkyl species.

For $\text{Cp}^*_2\text{Ta}(\text{CH}_2=\text{CHMe})\text{H}$ and $\text{Cp}^*_2\text{Ta}(\text{C}=\text{CH}_2)\text{H}$ this reaction is much cleaner than the reactions with TBHP.

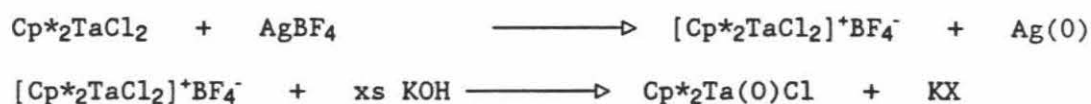


$\text{Me}_3\text{P}=\text{O}$ does not react with $\text{Cp}^*_2\text{Ta}(\text{CH}_2)\text{H}$ before decomposition of the tantalum complex to the metalated Cp^* species.

$\text{Cp}^*_2\text{TaCl}_2$ reacts with greater than one equivalent of TBHP and H_2O_2 to give $\text{Cp}^*_2\text{Ta}(\text{O})\text{Cl}$. During the reaction with TBHP one can observe the green color of $\text{Cp}^*_2\text{TaCl}_2$ in solution transform to an orange-red color. The orange color fades to give a colorless solution. An intermediate, probably responsible for the orange-red color, is observed in the nmr with a Cp^* resonance at 2.2 ppm, the correct region for a cationic species. This suggests a mechanism for the formation of $\text{Cp}^*_2\text{Ta}(\text{O})\text{Cl}$: oxidation of $\text{Cp}^*_2\text{TaCl}_2$ to $[\text{Cp}^*_2\text{TaCl}_2]^+ \text{OH}^-$ followed by loss of HCl .



To test this mechanism, $\text{Cp}^*_2\text{Ta}(\text{O})\text{Cl}$ was synthesized from $[\text{Cp}^*_2\text{TaCl}_2]^+\text{BF}_4^-$ (orange)¹⁸ and excess KOH . In fact, this is a better method of synthesis for $\text{Cp}^*_2\text{Ta}(\text{O})\text{Cl}$ than the TBHP or H_2O_2 reactions.



Lewis Acid Reactions: Initial indications are that Lewis acids (AlR'_3) react with $\text{Cp}^*_2\text{Ta}(\text{O})(\text{R})$ ($\text{R} = \text{Alkyl}, \text{H}$) to form adducts.



$\text{Cp}^*_2\text{Ta}(\text{O})\text{H}$ has two potential sites to bind Lewis acids; the hydride and oxo ligands. Gerard Parkin has isolated $\text{Cp}^*_2\text{Ta}(\text{O})\text{H} \cdot \text{AlEt}_3$ and spectroscopic evidence indicates that AlEt_3 is bound to the oxo ligand.¹⁹ The hydride resonance in the nmr shifts downfield almost 2 ppm, from 7.43 ppm to 9.10 ppm upon Lewis acid coordination. The Ta-H infrared band shifts from 1808 to 1861 cm^{-1} and the oxo stretch changes from 850 to 837 cm^{-1} and becomes broader. Similar observations were made for $\text{Cp}^*_2\text{Ta}(\text{CH}_2=\text{CH}_2)\text{H} \cdot \text{AlEt}_3$.²⁰ A crystal structure of this complex confirmed Lewis acid coordination to the olefin ligand rather than the hydride. Adduct formation is the only reaction with Lewis acids yet observed for the oxo alkyl complexes.

$\text{Cp}^*_2\text{Ta}(\text{O})\text{Cl}$ undergoes ligand rearrangement with AlMe_3 to yield $\text{Cp}^*_2\text{Ta}(\text{O})\text{Me} \cdot \text{AlMe}_2\text{Cl}$.

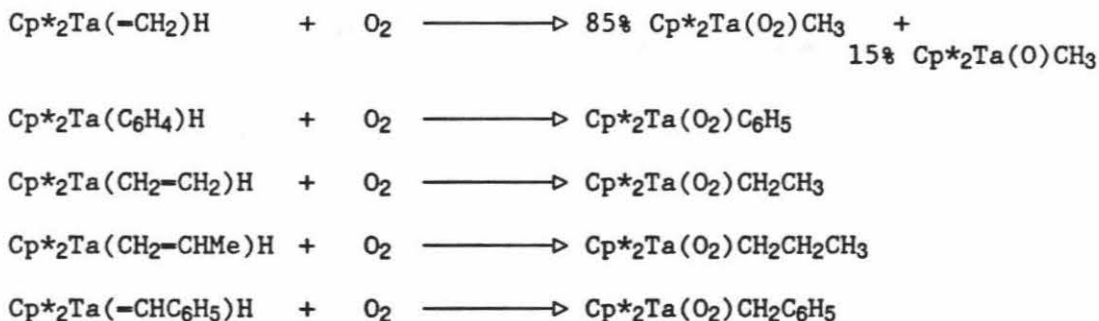


$\text{Cp}^*_2\text{Ta}(\text{O})\text{Me}$ can be recovered by adding H_2O to the reaction to precipitate the aluminum reagents. AlEt_3 simply forms an adduct with $\text{Cp}^*_2\text{Ta}(\text{O})\text{Cl}$ and does not appear to alkylate the tantalum.

Peroxo Complexes: $\text{Cp}^*_2\text{Ta}(\text{O})\text{Cl}$ reacts with H_2O_2 to generate $\text{Cp}^*_2\text{Ta}(\text{O}_2)\text{Cl}$. This reaction is precedented for $\text{Cp}_2\text{Nb}(\text{O})\text{Cl}$.²¹ Upon heating with PPh_3 , $\text{Cp}^*_2\text{Ta}(\text{O}_2)\text{Cl}$ cleanly transfers oxygen to give $\text{Cp}^*_2\text{Ta}(\text{O})\text{Cl}$ and OPPh_3 . No other substrates have been successfully oxygenated. $\text{Cp}^*_2\text{Ta}(\text{O})\text{Me}$ does not react with H_2O_2 . The other oxo alkyl complexes have not been tested for this reaction.

It was mentioned in the introductory chapter that no transition metal peroxo alkyl complexes have been reported. Organometallic intermediates have, however, been suggested for metal peroxide oxidations.²²

The reactions of $\text{Cp}^*_2\text{Ta}(\text{CH}_2)\text{H}$, $\text{Cp}^*_2\text{Ta}(\text{CHC}_6\text{H}_5)\text{H}$, $\text{Cp}^*_2\text{Ta}(\text{C}_6\text{H}_4)\text{H}$,¹⁸ $\text{Cp}^*_2\text{Ta}(\text{CH}_2=\text{CH}_2)\text{H}$ and $\text{Cp}^*_2\text{Ta}(\text{CH}_2=\text{CHMe})\text{H}$ with O_2 give the first examples of this type of complex.



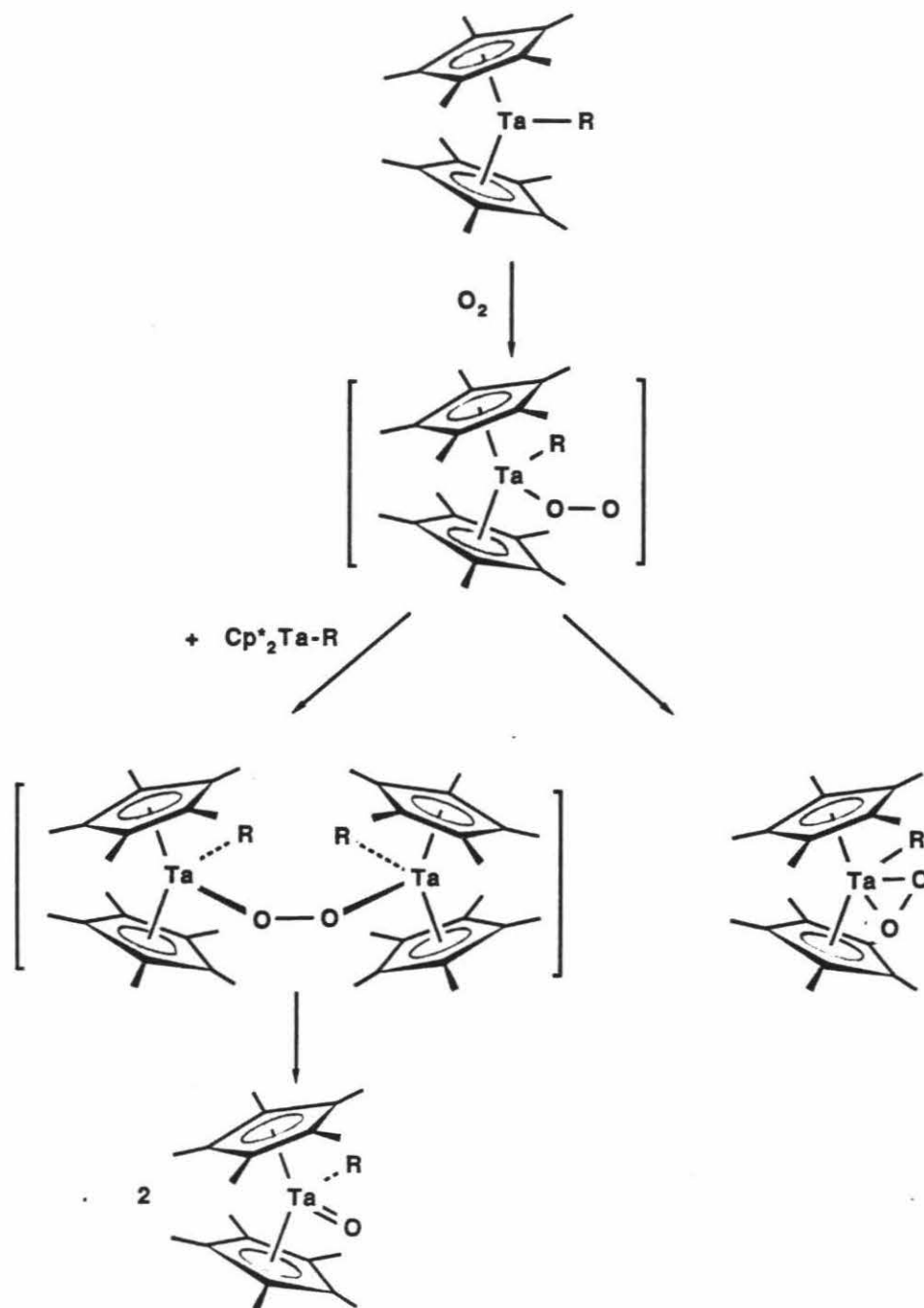
These reactions were carried out by dissolving the starting materials in petroleum ether, placing one atmosphere of dry O_2 over the solution at -78°C and allowing the reaction to warm to room temperature. During warming, the solution color changes and white solid precipitates. In general, these compounds are almost insoluble in petroleum ether, moderately soluble in diethyl ether and soluble in aromatic solvents. Molecular weight measurement indicates $\text{Cp}^*_2\text{Ta}(\text{O}_2)\text{CH}_3$ is a monomer. ^1H nmr spectra show Cp^* resonances for these complexes always upfield of the corresponding oxo alkyl complexes. The infrared spectra show bands for the O-O stretch in the region $860\text{-}865\text{ cm}^{-1}$.

The reaction of $\text{Cp}^*_2\text{Ta}(\text{CH}_2)\text{H}$ is the least clean of the above reactions. One always observes the formation of at least 10% $\text{Cp}^*_2\text{Ta}(\text{O})\text{CH}_3$ and occasionally 5 to 10% of an unidentified species. Approximately 3% of $\text{Cp}^*_2\text{Ta}(\text{O})\text{R}$ is formed in the $\text{Cp}^*_2\text{Ta}(\text{CH}_2=\text{CHR}')\text{H}$ reactions. At the other extreme, the reaction of $\text{Cp}^*_2\text{Ta}(\text{=CHC}_6\text{H}_5)\text{H}$ with O_2 is very clean, even when carried out by shaking an open nmr tube in the air.

$\text{Cp}^*_2\text{Ta}(\text{=C=CH}_2)\text{H}$ and $\text{Cp}^*_2\text{TaH}_3$ do not react cleanly with oxygen under the conditions employed. In the latter case one observes the formation of $\text{Cp}^*_2\text{Ta}(\text{O})\text{H}$ and $\text{Cp}^*_2\text{Ta}(\text{O})\text{OH}$. One of the major products in the former reaction is likely $\text{Cp}^*_2\text{Ta}(\text{O}_2)\text{CH=CH}_2$. Why $\text{Cp}^*_2\text{Ta}(\text{=C=CH}_2)\text{H}$ reacts differently than the other complexes with both TBHP and O_2 is not understood.

Trapping of $\text{Cp}^*_2\text{Ta-R}$ by O_2 is a reasonable first step in the formation of $\text{Cp}^*_2\text{Ta}(\text{O}_2)\text{R}$ (Scheme VII). High spin $\text{Cp}^*_2\text{Ta-R}$ would be a biradical with one electron in each of the two non-bonding orbitals.²³ A biradical metal center should have no spin imposed barrier for reacting with triplet O_2 . The proposed initial step involves end on binding of the O_2 to give Ta(IV) super oxide species. This complex can then either close to form $\text{Cp}^*_2\text{Ta}(\text{O}_2)\text{R}$ or react with a second equivalent of $\text{Cp}^*_2\text{Ta-R}$ to form $\text{Cp}^*_2\text{Ta}(\text{R})\text{-OO-Cp}^*_2\text{Ta}(\text{R})$. $\text{Cp}^*_2\text{Ta}(\text{R})\text{-OO-Cp}^*_2\text{Ta}(\text{R})$ decomposes rapidly to $\text{Cp}^*_2\text{Ta}(\text{O})\text{R}$. The percentage of $\text{Cp}^*_2\text{Ta}(\text{O})\text{R}$ formed would then depend on the sterics of the R ligand and the concentration of $\text{Cp}^*_2\text{Ta-R}$. A similar mechanism has been proposed to explain Mo=O formation from O_2 , MoCl_5 and KCN.²⁴

A second possibility, formation of $\text{Cp}^*_2\text{Ta}(\text{O})\text{R}$ by oxygen transfer from $\text{Cp}^*_2\text{Ta}(\text{O}_2)\text{R}$ to $\text{Cp}^*_2\text{Ta-R}$ was eliminated by the observation that $\text{Cp}^*_2\text{Ta}(\text{O}_2)\text{CH}_3$ does not react with $\text{Cp}^*_2\text{Ta}(\text{CH}_2)\text{H}$.

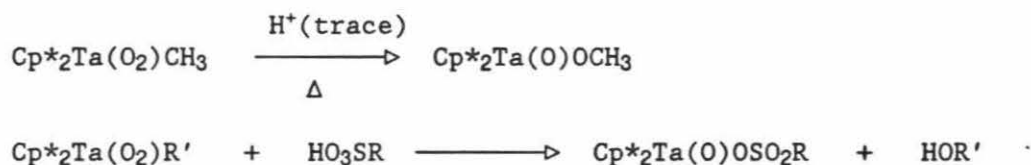


Scheme VII

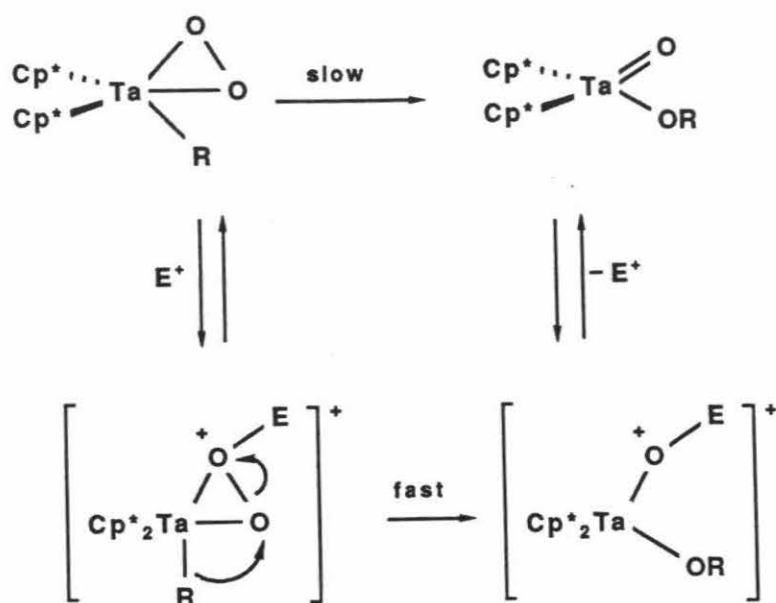
All of the complexes are stable in the solid state if stored at low temperature.

$\text{Cp}^*_2\text{Ta}(\text{O}_2)\text{CH}_3$ is stable at room temperature in benzene for weeks. $\text{Cp}^*_2\text{Ta}(\text{O}_2)\text{CH}_2\text{CH}_3$, $\text{Cp}^*_2\text{Ta}(\text{O}_2)\text{CH}_2\text{CH}_2\text{CH}_3$ and $\text{Cp}^*_2\text{Ta}(\text{O}_2)\text{CH}_2\text{C}_6\text{H}_5$ are less stable. One observes 10-15% decomposition after one week in solution. At 80°C $\text{Cp}^*_2\text{Ta}(\text{O}_2)\text{CH}_3$ will cleanly oxidize PPh_3 to OPPh_3 , leaving $\text{Cp}^*_2\text{Ta}(\text{O})\text{CH}_3$. The other complexes decompose before transferring oxygen.

An attempt to oxidize styrene at 80°C resulted in the very clean transformation of $\text{Cp}^*_2\text{Ta}(\text{O}_2)\text{CH}_3$ to $\text{Cp}^*_2\text{Ta}(\text{O})\text{OCH}_3$. Curiously, when $\text{Cp}^*_2\text{Ta}(\text{O}_2)\text{CH}_3$ is heated in the presence of NEt_3 , one observes neither oxidation of the amine nor rearrangement to $\text{Cp}^*_2\text{Ta}(\text{O})\text{OCH}_3$ before decomposition. When heated alone, one occasionally observes the same transformation as a non-first order process. It seemed unreasonable that styrene was responsible for the observed reactivity. Aldrich styrene, however, contains 10-15 ppm 4 *tert*-butylcatechol as stabilizer and the catechol could serve as an acid catalyst for the rearrangement. To test this possibility both phenol²⁵ and MeSO_3H were successfully used to catalyze the rearrangement. Heating to 80°C is required to drive the rearrangement at a reasonable rate when trace amounts of acid are used. Heating $\text{Cp}^*_2\text{Ta}(\text{O}_2)\text{CH}_3$ with H_2O results in the formation of both $\text{Cp}^*_2\text{Ta}(\text{O})\text{OCH}_3$ and $\text{Cp}^*_2\text{Ta}(\text{O})\text{CH}_3$.²⁶ If one equivalent of RSO_3H ($\text{R} = \text{CH}_3, \text{C}_6\text{H}_4\text{CH}_3$) is added to $\text{Cp}^*_2\text{Ta}(\text{O}_2)\text{R}'$ ($\text{R}' = \text{CH}_3, \text{CH}_2\text{CH}_3, \text{CH}_2\text{CH}_2\text{CH}_3, \text{CH}_2\text{C}_6\text{H}_5$) at room temperature, one observes a slow conversion over a period of three days to $\text{R}'\text{OH}$ and $\text{Cp}^*_2\text{Ta}(\text{O})\text{OSO}_2\text{R}$.



A possible mechanism for the acid catalyzed rearrangement is shown below (Scheme VIII).



Scheme VIII

These results suggested it might be of interest to test the reactivity of Lewis acids with these complexes. Preliminary results indicate that aluminum alkyls work well to instigate oxygen transfer. AlEt_3 reacts immediately and stoichiometrically with $\text{Cp}^*_2\text{Ta}(\text{O}_2)\text{CH}_2\text{CH}_3$, $\text{Cp}^*_2\text{Ta}(\text{O}_2)\text{CH}_2\text{CH}_2\text{CH}_3$ and $\text{Cp}^*_2\text{Ta}(\text{O}_2)\text{CH}_2\text{C}_6\text{H}_5$ to give $\text{Cp}^*_2\text{Ta}(\text{O})(\text{OR}) \cdot \text{AlEt}_3$.

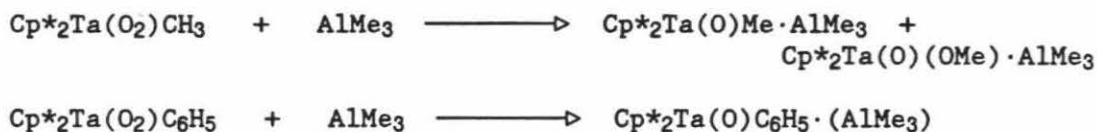


Over a period of several days at room temperature these adducts convert to $\text{Cp}^*_2\text{Ta}(\text{O})\text{Et}$ and presumably AlEt_2OR (bound to the oxo complex).



$\text{Cp}^*_2\text{Ta}(\text{O}_2)\text{CH}_3$ reacts much more slowly than the above compounds with AlEt_3 and AlMe_3 . Even in these slower reactions, one never observes a Lewis acid adduct of the peroxo species. Approximately two equivalents of AlMe_3 are required to complete the reaction. In

the final product mixture one observes $\text{AlMe}_x\text{OMe}_{3-x}$ and only 10% of $\text{Cp}^*_2\text{Ta}(\text{O})(\text{OCH}_3) \cdot \text{AlMe}_3$, the rest is $\text{Cp}^*_2\text{Ta}(\text{O})\text{CH}_3 \cdot \text{AlMe}_3$.²⁷ Initially one might suspect this reaction takes place in a manner similar to the reactions above, *i.e.*, formation of $\text{Cp}^*_2\text{Ta}(\text{O})(\text{OCH}_3) \cdot \text{AlMe}_3$ followed by ligand redistribution between aluminum and tantalum. $\text{Cp}^*_2\text{Ta}(\text{O})(\text{OCH}_3) \cdot \text{AlMe}_3$, however, does not appear to undergo ligand redistribution on the time scale of the reaction. In addition, $\text{Cp}^*_2\text{Ta}(\text{O}_2)\text{C}_6\text{H}_5$ reacts with AlMe_3 in a similar manner to produce $\text{Cp}^*_2\text{Ta}(\text{O})\text{C}_6\text{H}_5 \cdot \text{AlMe}_3$. One does not observe $\text{Cp}^*_2\text{Ta}(\text{O})\text{CH}_3$ in this reaction.



AlMe_3 is a dimer in solution with only a small amount of monomer in equilibrium with the dimer. If one considers attack of the dimer $(\text{AlMe}_3)_2$ on $\text{Cp}^*_2\text{Ta}(\text{O}_2)\text{R}$ ($\text{R} = \text{CH}_3, \text{C}_6\text{H}_5$) as the initial step of the above reaction, the coordination of the first AlMe_3 activates the peroxy moiety for insertion into the $\text{Al}-\text{CH}_3$ of the second AlMe_3 . The difference in reactivity for $\text{Cp}^*_2\text{Ta}(\text{O}_2)\text{R}$ ($\text{R} = \text{CH}_3, \text{C}_6\text{H}_5$) vs. ($\text{R} = \text{CH}_2\text{CH}_3, \text{CH}_2\text{CH}_2\text{CH}_3, \text{CH}_2\text{C}_6\text{H}_5$) may be due to the difference in metal alkyl bond strengths. Metal methyl and metal phenyl bonds tend to be stronger than normal alkyl bonds.²⁸ A recent report by Bryndza, Fong, Paciello, Tam and Bercaw, correlating $\text{H}-\text{X}$ with $\text{M}-\text{X}$ bond strengths, would suggest $\text{R} = \text{CH}_3, \text{C}_6\text{H}_5$ bonds are on the order of 6 kcal/mol stronger than $\text{R} = \text{CH}_2\text{CH}_3, \text{CH}_2\text{CH}_2\text{CH}_3$ and as much as 18 kcal/mol stronger than $\text{R} = \text{CH}_2\text{C}_6\text{H}_5$.²⁹

Conclusion

Permethyltantalocene alkylidene and olefin hydride complexes have served as starting materials to generate a number of complexes relevant to metal based oxidation systems. The first example of a metal oxo hydride complex was generated by several different

routes. New examples have been added to the relatively sparse literature on metal oxo alkyl complexes. If correctly assigned, the proposed intermediates in the reaction of TBHP with $\text{Cp}^*_2\text{Ta}(\text{CH}_2=\text{CHR})\text{H}$ are the first observed metal olefin hydroxide complexes. The first organometallic metal peroxo complexes have been isolated from clean reactions with O_2 . And Lewis acid promotion of oxygen transfer has been shown to take place quite readily.

Unifying themes emerge from both the hafnium alkylperoxide (Chapter 2) and tantalum peroxo alkyl studies. Heterolytic transfer of oxygen to a nucleophile (in this case, R^-) is greatly facilitated by stabilization of the negative charge built up during nucleophilic attack on the O-O bond. One can accomplish this in the case of the hafnium alkylperoxide complexes by donating electron density from the alkoxide oxygen into an empty orbital on the metal. The tantalum peroxo alkyl complexes demonstrate this principle without the ambiguity surrounding the question of η^2 -alkylperoxide coordination. When the metal no longer contains an accessible empty orbital, as is the case with the tantalum complexes, the addition of an external Lewis acid can perform the same function. All of this is consistent with observations made for peracid oxidations of nucleophiles; the greater the electron withdrawing ability of the acid group, the more the oxidation process is facilitated.³⁰ When the metal does not have the internal capacity or an external reagent for accepting electron density, one observes reactions consistent with homolytic bond cleavage. Relative metal carbon bond strengths also seem to influence the course of reaction. In both the hafnium and tantalum studies, we have observed that the complexes with stronger metal carbon bonds (methyl, phenyl) react more slowly, and often find alternate reaction pathways.

It is obvious from the foregoing material that work in the tantalum system is not yet complete. Work is continuing in an attempt to study alkyl to oxo migrations. The Lewis acid promoted alkyl to peroxo migrations are also under study.

TABLE I. NMR, IR AND ANALYTICAL DATA

Compound	Assignment	δ (ppm)	J (Hz)
$\text{Cp}^*_2\text{Ta}(\text{=CH}_2)\text{H}$			
	Ta-CH ₂	10.17 (s)	
	($\eta^5\text{-C}_5(\text{CH}_3)_5$)	1.95 (s)	
	Ta-H	1.75 (s, bd)	
C 54.30 (54.08)			
H 7.11 (7.08)			
	¹³ C ($\eta^5\text{-C}_5(\text{CH}_3)_5$)	12.00 (q)	126.5
1792 ν (Ta-H)	($\eta^5\text{-C}_5(\text{CH}_3)_5$)	107.45 (s)	
	CH ₂	239.47 (t)	127.0
$\text{Cp}^*_2\text{Ta}(\text{=CHC}_6\text{H}_5)\text{H}$ (I) \rightleftharpoons $\text{Cp}^*_2\text{Ta}(\text{CH}_2\text{-o-C}_6\text{H}_4)\text{H}$ (II)			
(I)	CHC ₆ H ₅	10.67 (s)	
	CHC ₆ H ₅	7.5-6.5 (m)	
	Ta-H	2.81 (s)	
	($\eta^5\text{-C}_5(\text{CH}_3)_5$)	1.90 (s)	
C 59.76 (59.76)			
H 6.83 (6.89)			
(II)	CH ₂ C ₆ H ₄	7.5-6.5 (m)	
	Ta-H	3.79 (s)	
	($\eta^5\text{-C}_5(\text{CH}_3)_5$)	1.60 (s)	
	CH ₂ C ₆ H ₄	0.58 (s)	

Cp*₂Ta(=CH₂)CH₃

		CH ₂	9.46(s)	
		(η ⁵ -C ₅ (CH ₃) ₅)	1.77(s)	
		CH ₃	-0.49(s)	
C 55.92 (55.99)				
H 7.54 (7.34)				
	¹³ C	CH ₃	9.30(q)	120.8
		(η ⁵ -C ₅ (CH ₃) ₅)	11.59(q)	125.7
		(η ⁵ -C ₅ (CH ₃) ₅)	108.93(s)	
		CH ₂	230.45(t)	129.4

Cp*₂Ta(O)H

		Ta-H	7.43(s)	
		(η ⁵ -C ₅ (CH ₃) ₅)	1.93(s)	
C 51.00 (51.28)				
H 6.59 (6.67)				
1808 ν(Ta-H)				
1295 ν(Ta-D)				
850 ν(Ta- ¹⁶ O)				
807 ν(Ta- ¹⁸ O)				
	¹³ C	(η ⁵ -C ₅ (CH ₃) ₅)	11.43(q)	127.0
		(η ⁵ -C ₅ (CH ₃) ₅)	114.20(s)	

Cp*₂Ta(O)H · AlEt₃

		Ta-H	9.10(s)	
1861 ν(Ta-H)				
837 ν(Ta=O)		(η ⁵ -C ₅ (CH ₃) ₅)	1.77(s)	
		Al(CH ₂ CH ₃) ₃	1.69(t)	8.0
		Al(CH ₂ CH ₃) ₃	0.41(q)	8.0

Cp*₂Ta(O)OH

3660 $\nu(\text{O-H})$	$(\eta^5\text{-C}_5(\text{CH}_3)_5)$	1.85(s)
3380 $\nu(\text{O-H})$		
1264 $\nu(\text{O-D})$		
845 $\nu(\text{Ta=O})$		

Cp*₂Ta(O)CH₃

	$(\eta^5\text{-C}_5(\text{CH}_3)_5)$	1.77(s)	
	CH_3	0.25(s)	
C 51.89 (52.28)			
H 6.73 (6.89)			
	¹³ C $(\eta^5\text{-C}_5(\text{CH}_3)_5)$	11.65(q)	126.0
855 $\nu(\text{Ta=O})$	CH_3	20.34(q)	122.0
	$(\eta^5\text{-C}_5(\text{CH}_3)_5)$	115.26(s)	

Cp*₂Ta(O)Cl

850 $\nu(\text{Ta=O})$	$(\eta^5\text{-C}_5(\text{CH}_3)_5)$	1.88(s)
------------------------	--------------------------------------	---------

Cp*₂Ta(O₂)Cl

858 $\nu(\text{O-O})$	$(\eta^5\text{-C}_5(\text{CH}_3)_5)$	1.77(s)
-----------------------	--------------------------------------	---------

Cp*₂Ta(O₂)CH₃

	$(\eta^5\text{-C}_5(\text{CH}_3)_5)$	1.68(s)
C 50.99 (50.60)		
H 6.78 (6.69)	CH_3	0.15(s)
858 $\nu(\text{O-O})$		

Cp*₂Ta(O₂)CH₂CH₃

863 ν (O-O)	(η^5 -C ₅ (CH ₃) ₅)	1.65(s)	
	CH ₂ CH ₃	under Cp*	
	CH ₂ CH ₃	0.80(q)	7.3

Cp*₂Ta(O₂)CH₂CH₂CH₃

C 52.83 (52.47)	(η^5 -C ₅ (CH ₃) ₅)	1.64(s)	
H 7.00 (7.08)	CH ₂ CH ₂ CH ₃	under Cp*	
861 ν (O-O)	CH ₂ CH ₂ CH ₃	1.35(t)	7.2
	CH ₂ CH ₂ CH ₃	0.70(m)	

Cp*₂Ta(O₂)CH₂C₆H₅

C 56.34 (56.44)	CH ₂ C ₆ H ₅	7.75-6.95(m)	
H 6.46 (6.49)	CH ₂ C ₆ H ₅	2.10(s)	
863 ν (O-O)	(η^5 -C ₅ (CH ₃) ₅)	1.67(s)	

Compounds not isolated**Cp*₂Ta(O)CH₂CH₃**

860 ν (Ta=O)	CH ₂ CH ₃	1.88(t)	7.6
	(η^5 -C ₅ (CH ₃) ₅)	1.79(s)	
	CH ₂ CH ₃	0.94(q)	7.6

Cp*₂Ta(O)CH₂CH₂CH₃

(η^5 -C ₅ (CH ₃) ₅)	1.78(s)
CH ₂ CH ₂ CH ₃	under Cp*
CH ₂ CH ₂ CH ₃	1.28(t) 7.1
CH ₂ CH ₂ CH ₃	0.84(m)

Cp*₂Ta(O)CH₂C₆H₅

CH ₂ C ₆ H ₅	7.67-7.02(m)
CH ₂ C ₆ H ₅	2.29(s)
(η^5 -C ₅ (CH ₃) ₅)	1.78(s)

Cp*₂Ta(O)C₆H₅

C ₆ H ₅	7.93-6.68(m)
(η^5 -C ₅ (CH ₃) ₅)	1.73(s)

Cp*₂Ta(O)CH₃·AlMe₃

(η^5 -C ₅ (CH ₃) ₅)	1.66(s)
CH ₃	0.38
Al(CH ₃) ₃	-0.27

Cp*₂Ta(O)C₆H₅·AlMe₃

C ₆ H ₅	7.92-6.45(m)
(η^5 -C ₅ (CH ₃) ₅)	1.63(s)
Al(CH ₃) ₃	-0.09(s)

$\text{Cp}^*_2\text{Ta}(\text{O})\text{OCH}_3$ OCH_3 4.18(s) $(\eta^5\text{-C}_5(\text{CH}_3)_5)$ 1.92(s)

Experimental Section

General Considerations: See experimental section, Chapter 2.

Oxygen was dried by passage through a trap at -78°C or used directly from the lecture bottle. N_2O was freeze-pump-thawed before use. 90% hydrogen peroxide was obtained from FMC Corporation and used as received.

Procedures: Many of the reactions reported in this chapter were carried out in septa capped nmr tubes. In a typical experiment, 15 mg of starting material were placed in an nmr tube and dissolved in 0.4 mls of benzene- d_6 . TBHP was added as a benzene solution *via* syringe. The reactions were then followed by nmr.

$\text{Cp}^*_2\text{Ta}(\text{=CH}_2)\text{H}$: 1.114 g (2.14 mmol) of $\text{Cp}^*_2\text{TaCl}_2$ were stirred in 20 mls of ether for 20 hours with 4 ml of 1.5M LiMe solution. (The end of the reaction is indicated by a lightening of the reaction mixture and loss of the green color of $\text{Cp}^*_2\text{TaCl}_2$. The final ether solution is often red.) Ether was removed *in vacuo* and petroleum ether was added. To remove residual ether and ensure complete precipitation of LiCl, three cycles of adding and removing petroleum ether were performed. After filtering, 800 mg (1.72 mmol, 80% yield) of $\text{Cp}^*_2\text{Ta}(\text{CH}_2)\text{H}$ were isolated from petroleum ether at -78°C . One usually observes $\text{Cp}^*_2\text{Ta}(\text{CH}_2=\text{CH}_2)\text{H}$ and $\text{Cp}^*_2\text{Ta}(\text{CH}_2)\text{CH}_3$ as minor impurities in this reaction.

$\text{Cp}^*_2\text{Ta}(\text{CD}_2)\text{D}$ was successfully synthesized from LiCD_3 generated from CD_3Br and Li in ether. LiCD_3 generated from CD_3I did not work as well.

$\text{Cp}^*_2\text{Ta}(\text{=CHC}_6\text{H}_5)\text{H}$: 1.028 g (1.97 mmol) of $\text{Cp}^*_2\text{TaCl}_2$ and 644 mg (4.95 mmol, 2.5 eq.) of $\text{KCH}_2\text{C}_6\text{H}_5$ were slurried in 30 ml of ether for 16 hours. Ether was removed *in vacuo*, petroleum ether was added and removed three times. Petroleum ether was added and the solution filtered. Two crops totaling 734 mg (1.35 mmol, 69% yield) of $\text{Cp}^*_2\text{Ta}(\text{=CHC}_6\text{H}_5)\text{H}$

were isolated from petroleum ether at -78°C . $(\text{C}_6\text{H}_5\text{CH}_2)_2$ was sublimed from the solid before isolation. $\text{Cp}^*_2\text{Ta}(\text{=CHC}_6\text{H}_5)\text{H}$ is in equilibrium in solution with the metallacycle obtained by ortho metallation of the benzyl group.

$\text{Cp}^*_2\text{Ta}(\text{CH}_2)\text{CH}_3$: 350 mg (0.75 mmol) of $\text{Cp}^*_2\text{Ta}(\text{CH}_2)\text{H}$ and 98 mg (1.09 mmol) of $\text{Me}_3\text{P}=\text{CH}_2$ were stirred for 20 hours in 15 ml of petroleum ether. Petroleum ether and PMe_3 were removed *in vacuo*. Petroleum ether was added, the solution was filtered and 313 mg (0.65 mmol, 87% yield) of $\text{Cp}^*_2\text{Ta}(\text{CH}_2)\text{CH}_3$ were isolated at -78°C .

$\text{Cp}^*_2\text{Ta}(\text{O})\text{H}$: 450 mg (0.91 mmol) of $\text{Cp}^*_2\text{Ta}(\text{CH}_2=\text{CHCH}_3)\text{H}$ were dissolved in 15 ml of benzene. 0.036 ml ($> 2\text{eq}$) of H_2O were added to the solution *via* syringe. The solution was stirred for 18 hours at room temperature until the color had faded to light yellow (the reaction can be heated with a warm water bath to drive it to completion). The benzene solution was filtered and benzene was pulled off *in vacuo*. Petroleum ether was added, removed, and added again. 265 mg (0.57 mmol, 62% yield) of $\text{Cp}^*_2\text{Ta}(\text{O})\text{H}$ were isolated at -78°C from petroleum ether.

$\text{Cp}^*_2\text{Ta}(\text{O})\text{OH}$: 500 mg (1.1 mmol) of $\text{Cp}^*_2\text{TaH}_3$ were dissolved in petroleum ether. 0.7 ml of 9.3 M TBHP were added with the petroleum ether solution at -78°C . The solution was stirred for 32 hours at room temperature. Cycles of pulling off and adding petroleum ether were performed six times to remove excess TBHP and *t*-butanol. After filtering the petroleum ether solution 365 mg (0.75 mmol, 68% yield) of $\text{Cp}^*_2\text{Ta}(\text{O})\text{OH}$ were isolated at -78°C . The solid was pumped on overnight.

$\text{Cp}^*_2\text{Ta}(\text{O})\text{CH}_3$: 475 mg (1.02 mmol) of $\text{Cp}^*_2\text{Ta}(\text{CH}_2)\text{H}$ were dissolved in 15 ml of petroleum ether. 0.250 ml of 4 M TBHP solution were added *via* syringe. The solution was stirred for 10 minutes and filtered. Two crops, 354 mg (0.73 mmol, 72% yield), of $\text{Cp}^*_2\text{Ta}(\text{O})\text{CH}_3$ were isolated from petroleum ether at -78°C .

(A) = Cp*₂Ta(CH₂=CH₂)OH (?): 250 mg (0.52 mmol) of Cp*₂Ta(CH₂=CH₂)H were dissolved in 10 ml of petroleum ether. 0.3 ml of 9.3 M TBHP solution were added and the solution was stirred for 25 minutes at room temperature. Petroleum ether was repeatedly pulled off *in vacuo*, added and pulled off until a solid instead of an oil remained in the flask. 135 mg of solid, containing Cp*₂Ta(O)CH₂CH₃, Cp*₂Ta(CH₂=CH₂)OH and TBHP was isolated from petroleum ether at -78°C.

Cp*₂Ta(O)Cl: 1.09 g (1.8 mmol) of [Cp*₂TaCl₂]⁺BF₄⁻ and 252 mg (2.5 eq) of KOH were slurried together in 15 ml of CH₂Cl₂ for 14 hours. The CH₂Cl₂ was removed *in vacuo* and toluene was added. After filtering, 363 mg (0.73 mmol, 40% yield) of Cp*₂Ta(O)Cl were isolated from toluene at -78°C.

Cp*₂Ta(O₂)Cl: 500 mg (0.99 mmol) of Cp*₂TaCl₂ were suspended in 15 ml of nitrogen purged toluene. 0.6 ml of 90% H₂O₂ were added against an argon flow. The solution immediately began to change color from dark green to orange. The orange color was located in the H₂O₂/H₂O phase. The solution became colorless after 4 hours of stirring. 0.200 ml of NEt₃ were added at the end of the reaction and the reaction mixture was stirred for an additional 20 minutes. The toluene layer was separated and washed with H₂O. The toluene was removed *in vacuo* and petroleum ether was used to isolate 186mg (0.36 mmol, 36% yield) of Cp*₂Ta(O₂)Cl.

Cp*₂Ta(O₂)CH₃: 474 mg (1.02 mmol) of Cp*₂Ta(CH₂)H were dissolved in 30 ml petroleum ether and the solution was cooled to -78°C. 1 atmosphere of dried O₂ was placed over the solution. The cold bath was removed and with vigorous stirring the solution was allowed to come to room temperature. Petroleum ether was removed and toluene added. The solution was filtered and concentrated. Petroleum ether was added to the toluene solution to precipitate the solid. Two crops totaling 206 mg (0.41 mmol, 40% yield) of

$\text{Cp}^*_2\text{Ta}(\text{O}_2)\text{CH}_3$ were isolated from toluene/petroleum ether at -78°C . The solid contained approximately 10% $\text{Cp}^*_2\text{Ta}(\text{O})\text{CH}_3$.

$\text{Cp}^*_2\text{Ta}(\text{O}_2)\text{CH}_2\text{CH}_3$: 460 mg (0.96 mmol) of $\text{Cp}^*_2\text{Ta}(\text{CH}_2=\text{CH}_2)\text{H}$ were dissolved in 25 ml of petroleum ether and the solution was cooled to -78°C . 1 atmosphere of O_2 was placed over the solution and the solution was allowed to warm to room temperature. The solution was stirred for an additional 25 minutes after reaching room temperature, filtered and 243 mg (0.47 mmol, 49% yield) were isolated at -78°C from petroleum ether.

$\text{Cp}^*_2\text{Ta}(\text{O}_2)\text{CH}_2\text{CH}_2\text{CH}_3$: 455 mg (0.92 mmol) of $\text{Cp}^*_2\text{Ta}(\text{CH}_2=\text{CHCH}_3)\text{H}$ were reacted with O_2 in similar manner to the above complexes. A benzene/petroleum ether solution was filtered and concentrated to almost an oil. 5 ml of petroleum ether were added and the solid, 290 mg (0.55 mmol, 60% yield) of $\text{Cp}^*_2\text{Ta}(\text{O}_2)\text{CH}_2\text{CH}_2\text{CH}_3$, was isolated at -78°C .

$\text{Cp}^*_2\text{Ta}(\text{O}_2)\text{CH}_2\text{C}_6\text{H}_5$: 1 atmosphere of O_2 was placed over a solution of 350 mg (0.65 mmol) of $\text{Cp}^*_2\text{Ta}(\text{CHC}_6\text{H}_5)\text{H}$ in petroleum ether/toluene at -78°C . After warming to room temperature the solvent was pulled off *in vacuo* and petroleum ether was added. After filtering, 278 mg (0.48 mmol, 75% yield) of $\text{Cp}^*_2\text{Ta}(\text{O}_2)\text{CH}_2\text{C}_6\text{H}_5$ were isolated at -78°C .

Lewis Acid Studies: The survey reactions with AlR_3 were carried out in nmr tubes. AlR_3 reagents were generally added as toluene solutions *via* syringe. The Lewis acid free rearrangement products could be generated by precipitating the aluminum reagents with H_2O .

Crystal Structure Determination of $\text{Cp}^*_2\text{Ta}(\text{O})\text{H}$: A single crystal was sealed in a thin-walled glass capillary. The crystal was optically centered on an Enraf Nonius CAD4 diffractometer equipped with $\text{MoK}\alpha$ radiation for intensity data collection. Space group $\text{P}2_1/n$, a special setting of #14, was chosen based on the systematic absences of $h0l$ where $h + l = 2n + 1$, and $0k0$ where $k = 2n + 1$ in the intensity data. A total of 11187

reflections were collected with $1 \leq \theta \leq 15$ in the quadrant $(\pm h, +k, +l)$. Crystal data are shown in Table II.

Crystal decay was monitored by 3 check reflections which were monitored after every 10000 seconds of exposure. The check reflection intensities decreased at an average rate of 3.0% over the 79.92 hours of exposure. The intensities were scaled accordingly. The data were also corrected for absorption with transmission factors varied from 0.061 to 0.286.

The position of the tantalum atoms were determined from a Patterson map. From Fourier and Difference Fourier maps, all the remaining atoms were located. The tantalum, oxygen and methyl carbon atoms were allowed to refine with Gaussian parameters. All other atoms were refined with isotropic B's. Several cycles of full-matrix least-squares refinement led to convergence with $R = 0.0672$ for 6730 reflections and $R = 0.042$ with $F_o > 3\sigma F_o^2$. The goodness-of-fit = $[\sum \omega(F_o^2 - F_c^2)^2 / (n - p)]^{1/2}$ is 1.80 for $n = 6730$ reflections and $p = 299$ parameters. Final parameters are contained in Table III. Table IV contains the hydrogen coordinates and Table V lists bond lengths.

TABLE II. CRYSTAL DATA

$a = 13.073(3) \text{ \AA}$	Crystal System	: Monoclinic
$b = 19.337(4) \text{ \AA}$	Space Group	: $P2_1/n$ (#14)
$c = 16.002(3) \text{ \AA}$	F(000)	: 464e
$\beta = 108.68(2)^\circ$	Radiation	: $\lambda \text{ MoK}\alpha = 0.71073 \text{ \AA}$
$V = 3832.35(1.46) \text{ cm}^3$	Temperature	: room
$\mu = 60.41 \text{ cm}^{-1}$		
Molecular Weight = 468.42 g/mol		
Density (calculated) = 1.62 g/cm ³		

TABLE III. ATOM COORDINATES AND U_{eq} 's OR B 's
Atom Coordinates ($\times 10^4$); U_{eq} ($\times 10^4$)

Atom	x	y	z	U_{eq} or B
TA1	2133(.3)	1278(.2)	6183(.2)	491(1)
TA2	2508(.3)	1392(.2)	1384(.2)	490(1)
11C	4467(7)	1109(5)	8123(6)	859(32)
12C	4695(8)	729(6)	6266(7)	1054(36)
13C	2670(9)	-224(5)	5242(6)	965(36)
14C	1201(10)	-375(6)	6429(6)	1149(39)
15C	2360(8)	343(5)	8270(5)	857(32)
21C	2275(8)	2106(5)	8323(5)	836(33)
22C	3341(10)	2864(6)	7065(7)	1201(42)
23C	1604(10)	2865(5)	5130(6)	1048(38)
24C	-416(7)	2031(6)	5179(6)	952(36)
25C	-12(7)	1474(6)	7116(6)	963(33)
31C	3891(8)	1068(5)	3694(5)	761(28)
32C	2232(8)	-121(5)	2672(6)	782(29)
33C	2562(8)	-328(6)	819(6)	963(36)
34C	4514(7)	637(6)	739(6)	892(30)
35C	5319(7)	1450(5)	2539(6)	916(32)
41C	2259(8)	2801(5)	2745(6)	823(31)
42C	1108(7)	1435(5)	3088(5)	744(26)
43C	-109(7)	754(6)	1206(5)	823(30)
44C	88(8)	1798(6)	-272(5)	981(37)
45C	1594(8)	3036(5)	658(6)	871(31)
O1	2602(12)	1497(6)	5300(6)	2640(63)
O2	2468(8)	1391(6)	290(5)	1778(46)
C11	3622(7)	734(4)	7404(5)	4.8(2)
C12	3748(7)	530(5)	6567(5)	5.0(2)
C13	2873(7)	117(5)	6119(5)	5.1(2)
C14	2209(7)	45(5)	6657(5)	4.9(2)
C15	2688(6)	414(4)	7448(5)	4.4(2)
C21	1829(6)	2099(4)	7326(5)	4.6(2)
C22	2285(7)	2456(5)	6764(5)	5.2(2)
C23	1491(7)	2490(5)	5903(5)	5.0(2)
C24	632(7)	2104(5)	5915(5)	5.0(2)
C25	818(6)	1851(4)	6809(5)	4.3(2)
C31	3692(6)	820(4)	2778(5)	3.9(2)
C32	2935(6)	323(4)	2310(5)	4.0(2)
C33	3133(6)	197(4)	1498(5)	4.3(2)
C34	4007(6)	607(4)	1485(5)	4.1(2)
C35	4350(6)	1005(4)	2244(5)	4.4(2)
C41	1650(6)	2288(4)	2057(5)	4.1(2)
C42	1186(6)	1685(4)	2208(5)	4.1(2)
C43	624(6)	1378(4)	1379(5)	4.4(2)
C44	687(7)	1868(5)	717(5)	4.8(2)
C45	1325(7)	2410(5)	1129(5)	4.7(2)

TABLE IV. HYDROGEN COORDINATES AND B's
Atom Coordinates ($\times 10^4$)

Atom	<i>x</i>	<i>y</i>	<i>z</i>	<i>B</i>
H1	1253	997	5250	2.0
H2	3339	2052	1315	2.0
H11a	5100	776	8394	7.7
H11b	4119	1247	8590	7.7
H11c	4731	1537	7893	7.7
H12a	5009	1221	6598	7.7
H12b	5289	375	6497	7.7
H12c	4468	813	5634	7.7
H13a	3365	-277	5118	7.7
H13b	2103	88	4762	7.7
H13c	2302	-698	5254	7.7
H14a	1404	-887	6522	7.7
H14b	743	-286	5763	7.7
H14c	740	-223	6807	7.7
H15a	2338	-173	8412	7.7
H15b	2852	615	8758	7.7
H15c	1552	575	8122	7.7
H21a	3083	2013	8486	7.9
H21b	1866	1771	8551	7.9
H21c	2175	2623	8523	7.9
H22a	3686	2848	7735	7.9
H22b	3893	2614	6746	7.9
H22c	3221	3338	6809	7.9
H23a	2137	3280	5336	7.9
H23b	1865	2547	4735	7.9
H23c	839	3088	4773	7.9
H24a	-289	2181	4581	7.9
H24b	-973	2341	5276	7.9
H24c	-649	1515	5115	7.9
H25a	-556	1249	6579	7.9
H25b	397	1113	7583	7.9
H25c	-407	1853	7396	7.9
H31a	4712	981	4036	7.4
H31b	3398	808	3947	7.4
H31c	3737	1613	3648	7.4
H32a	2725	-504	3091	7.4
H32b	1644	-349	2177	7.4
H32c	1908	200	3068	7.4
H33a	3074	-743	843	7.4
H33b	2344	-85	196	7.4
H33c	1887	-480	960	7.4
H34a	5341	777	1043	7.4
H34b	4121	1006	298	7.4
H34c	4488	138	495	7.4
H35a	5942	1167	2971	7.4
H35b	5136	1878	2828	7.4
H35c	5527	1578	1969	7.4
H41a	2677	2508	3338	7.2

TABLE IV. (Cont.)

Atom	<i>x</i>	<i>y</i>	<i>z</i>	<i>B</i>
H41b	2755	3069	2520	7.2
H41c	1687	3112	2905	7.2
H42a	1714	1631	3577	7.2
H42b	1150	891	3099	7.2
H42c	364	1587	3135	7.2
H43a	140	419	790	7.2
H43b	-30	516	1775	7.2
H43c	-870	909	860	7.2
H44a	318	2201	-605	7.2
H44b	300	1335	-480	7.2
H44c	-732	1814	-371	7.2
H45a	2073	2911	353	7.2
H45b	1915	3436	1165	7.2
H45c	892	3211	200	7.2

TABLE V. BOND LENGTHS

Distance(Å)	Distance(Å)	Distance(Å)	Distance(Å)
TA1 -C11	2.506(8)	TA2 -C31	2.527(8)
TA1 -C12	2.469(9)	TA2 -C32	2.500(8)
TA1 -C13	2.458(9)	TA2 -C33	2.439(8)
TA1 -C14	2.493(9)	TA2 -C34	2.442(8)
TA1 -C15	2.545(8)	TA2 -C35	2.476(8)
TA1 -C21	2.547(8)	TA2 -C41	2.488(8)
TA1 -C22	2.445(9)	TA2 -C42	2.552(8)
TA1 -C23	2.482(9)	TA2 -C43	2.461(8)
TA1 -C24	2.460(9)	TA2 -C44	2.456(9)
TA1 -C25	2.508(8)	TA2 -C45	2.456(9)
TA1 -O1	1.762(12)	TA2 -O2	1.735(10)
TA1 -H1	1.657(0)	TA2 -H2	1.701(0)
TA1 -R1	2.186(0)	TA2 -R3	2.167(0)
TA1 -R2	2.180(0)	TA2 -R4	2.176(0)
C11 -C12	1.456(12)	C31 -C32	1.410(11)
C11 -C15	1.390(12)	C31 -C35	1.438(11)
C11 -11C	1.502(13)	C31 -31C	1.483(12)
C12 -C13	1.390(12)	C32 -C33	1.425(11)
C12 -12C	1.516(14)	C32 -32C	1.505(12)
C13 -C14	1.411(12)	C33 -C34	1.396(11)
C13 -13C	1.497(14)	C33 -33C	1.500(13)
C14 -C15	1.412(12)	C34 -C35	1.386(11)
C14 -14C	1.492(14)	C34 -34C	1.540(13)
C15 -15C	1.515(13)	C35 -35C	1.478(13)
C21 -C22	1.410(12)	C41 -C42	1.371(11)
C21 -C25	1.401(12)	C41 -C45	1.428(12)
C21 -21C	1.513(12)	C41 -41C	1.507(13)
C22 -C23	1.437(13)	C42 -C43	1.425(11)
C22 -22C	1.526(15)	C42 -42C	1.522(12)
C23 -C24	1.353(12)	C43 -C44	1.444(12)
C23 -23C	1.482(14)	C43 -43C	1.511(12)
C24 -C25	1.456(12)	C44 -C45	1.370(12)
C24 -24C	1.501(13)	C44 -44C	1.531(13)
C25 -25C	1.515(13)	C45 -45C	1.524(13)

- 1) a) Gibson, V.C.; Bercaw, J.E.; Bruton, W.J.; Sanner, R.D. *Organometallics* 1986, 5, 976. b) van Asselt, A.; Burger, B.J.; Gibson, V.C.; Bercaw, J.E. *J. Am. Chem. Soc.* 1986, 108, 5347.
- 2) Parkin, G.; Bunel, E.; Burger, B.J.; Trimmer, M.S.; van Asselt, A.; Bercaw, J.E. *J. Mol. Cat.* 1987, in press.
- 3) Parshall, G.W. "Homogeneous Catalysis" John Wiley & Sons, New York, 1980.
- 4) Grubbs, R.H. in "Comprehensive Organometallic Chemistry" Vol. 8, p. 499 (ed. G. Wilkinson, F.G.A. Stone, E.W. Abel) Pergamon Press, Oxford, 1982.
- 5) a) Richmond, T.G.; Basolo, F.; Shriver, D.F. *Inorg. Chem.* 1982, 21, 1272 b) Butts, S.S.; Strauss, S.H.; Holt, E.H.; Stimson, R.E.; Alcock, M.W.; Shriver, D.F. *J. Am. Chem. Soc.* 1980, 102, 5093.
- 6) Madix, R.J. *Science* 1986, 1159.
- 7) a) Tovrog, B.S.; Diamond, S.E.; Mares, F.; Szalkiewicz, A. *J. Am. Chem. Soc.* 1981, 103, 3522. b) Tovrog, B.S.; Diamond, S.E.; Mares, F. *ibid.* 1980, 102, 270. c) Tovrog, B.S.; Mares, F.; Diamond, S.E. *ibid.* 1980, 102, 6616. d) Diamond, S.E.; Mares, F.; Szalkiewicz, A., Muccigrosso, D.A.; Solar, J.P. *ibid.* 1982, 104, 4266.
- 8) Olefins also react slowly at 140°C with Cp*₂TaH₃ to give the olefin hydride complexes. Ref. 1a.
- 9) Hillhouse, G.L.; Bercaw, J.E. *J. Am. Chem. Soc.* 1984, 106, 5472.
- 10) LeRoy L. Whinnery, Nhi G. Hua, Richard E. Marsh, Caltech.
- 11) Yaun, L.C.; Bruice, T.C. *J. Am. Chem. Soc.* 1986, 108, 1643 and references therein.
- 12) Parkin, G.; Bercaw, J.E. unpublished results.
- 13) Chapter 1.
- 14) Collman, J.P.; Hegedus, L.S. "Principles and Applications of Organotransition Metal Chemistry" University Science Books, Mill Valley, 1980.
- 15) Jensen, C.M.; Trogler, W.C. *J. Am. Chem. Soc.* 1986, 108, 723.

- 16) $\text{Cp}^*_2\text{Ta}(\text{CH}_2\text{CH}_2)\text{H}$ and HOCMe_3 can be heated to 80°C with no reaction.
 $\text{Cp}^*_2\text{Ta}(\text{CH}_2)\text{H}$ activates Cp^* ring methyl groups to give tuck-in complexes before reacting with HOME_3 .
- 17) Because (A) and (B) have not been isolated cleanly the rate comparisons are very approximate.
- 18) Trimmer, M.S.; Bercaw, J.E. unpublished results.
- 19) Parkin, G.; Bercaw, J.E. unpublished results.
- 20) McDade, C; Gibson, V.C.; Santarsiero, B.D.; Bercaw, J.E. *J. Am. Chem. Soc.* accepted for publication.
- 21) a) Sala-Pala, J.; Roue, J.; Guerchais, J.E. *J. Mol. Cat.* 1980, 7, 141. b) Bkouche-Waksman, I.; Bois, C.; Sala-Pala, J.; Guerchais, J.E. *J. Organomet. Chem.* 1980, 195, 307.
- 22) a) Mimoun, H.; Seree de Roch, I.; Sajus, L. *Tetrahedron* 1970, 26, 37. b) See Chapter 1.
- 23) Cp^*_2TaCl is probably a paramagnetic complex. Parkin, G. unpublished results. For a discussion of bent metallocene frontier orbitals see Lauher, J; Hoffmann, R. *J. Am. Chem. Soc.* 1976, 98, 1729.
- 24) Arzoumanian, H.; Alvarez, R.L.; Kowalak, A.D.; Metzger, J. *J. Am. Chem. Soc.* 1977, 99, 5175.
- 25) Phenol contains H_3PO_4 as stabilizer and this may be the actual catalyst.
- 26) This compound is probably formed by the reaction of H_2O with $\text{Cp}^*_2\text{Ta}(\text{O}_2)\text{CH}_3$ to give H_2O_2 and $\text{Cp}^*_2\text{Ta}(\text{O})\text{CH}_3$. It was mentioned earlier that the reverse reaction does not go.
- 27) The analysis of this reaction by nmr was complicated by the fact that the Cp^* resonances of $\text{Cp}^*_2\text{Ta}(\text{O}_2)\text{CH}_3$ and $\text{Cp}^*_2\text{Ta}(\text{O})\text{CH}_3 \cdot \text{AlMe}_3$ are degenerate at 90MHz.

- 28) Bruno, J.W.; Marks, T.J.; Morss, L.R. *J. Am. Chem. Soc.* **1983**, *105*, 6824.
- 29) a) Bryndza, H.E.; Fong, L.K.; Paciello, R.A.; Tam, W.; Bercaw, J.E. *J. Am. Chem. Soc.* **1987**, *109*, 1444. b) For relative R-H bonds strengths see Lowry, T.H.; Richardson, K.S. "Mechanism and Theory in Organic Chemistry" Harper & Row, New York, 1981.
- 30) Curci, R.; Edwards, J.O. in "Organic Peroxides" Vol. 1, 199, (Ed. Swern, D.) Wiley-Interscience, New York, 1970.